RESONANT PROPERTIES OF FLEXIBLE SPLIT RING RESONATOR METAMATERIAL STRUCTURES FOR DIFFERENT STRUCTURAL AND DIELECTRIC PARAMETERS

A THESIS

submitted to

MAHATMA GANDHI UNIVERSITY, KOTTAYAM

in partial fulfillment of the requirements

for the award of the degree of

DOCTOR OF PHILOSOPHY

in

PHYSICS (ELECTRONICS)

By

UMADEVI K S

Under the guidance of

Dr V P JOSEPH

DEPARTMENT OF PHYSICS

NEWMAN COLLEGE, THODUPUZHA

IDUKKI DISTRICT, KERALA- 685 585

FEBRUARY -2020

MAHATMA GANDHI UNIVERSITY

CERTIFICATE ON PLAGIARISM CHECK

1.	Name of the Research Scholar	**UMADEVI K. S**
2.	Title of the Thesis/Dissertation	Resonant Properties of Flexible Split Ring Resonator Metamaterial Structures for Different Structural and Dielectric Parameters
3.	Name of the Supervisor	Dr. V. P. JOSEPH
4.	Department/Institution/ Research Centre	Department of Physics New Man College, Thodupuzha
5.	Similar Content (%) identified	**3% (Three)**
6.	Acceptable Maximum Limit	25%
7.	Software Used	Urkund
8.	Date of Verification	07-02-2020

**Report on plagiarism check, items with % of similarity is attached*

Checked by (with Name, Designation & Signature) :

07/02/2020

Annu George
07.02.2020
ANNU GEORGE
Deputy Librarian in-charge
University Library
Mahatma Gandhi University
Kottayam - 686 560

Name & Signature of the Researcher : UMADEVI K. S

Name & Signature of the Supervisors : Dr. V. P. JOSEPH

DR. V.P.JOSEPH
ASSOCIATE PROFESSOR
HEAD OF THE POST GRADUATE & RESEARCH DEPT. OF PHYSICS
CHRIST COLLEGE, IRINJALAKUDA

Name & Signature of the HoD/HoI(Chairperson of the Doctoral Committee) :

Dr. THOMSON JOSEPH
PRINCIPAL
NEWMAN COLLEGE
THODUPUZHA

NEWMAN COLLEGE * THODUPUZHA, KERALA-685585 *

URKUND

Urkund Analysis Result

Analysed Document:	Umadevi K S - Resonant Properties of Flexible Split Ring Resonator Metamaterial Structures for Different Structural and Dielectric Parameters.pdf (D63567294)
Submitted:	2/7/2020 10:26:00 AM
Submitted By:	library@mgu.ac.in
Significance:	3 %

Sources included in the report:

https://www.osapublishing.org/oe/abstract.cfm?uri=oe-17-18-16046
https://corescholar.libraries.wright.edu/cgi/viewcontent.cgi?article=2780&context=etd_all
https://www.krishisanskriti.org/vol_image/06Jul201505071229%20%20%20%20%20%20%20%20%20Rakhi%20Rani%20%20%20%20%20%20%20%20%20%20%2044-47.pdf
https://www.researchgate.net/publication/313424119_Complex_permittivity_measurement_using_metamaterial_split_ring_resonators
https://www.researchgate.net/publication/237454207_Comparative_investigation_of_resonance_characteristics_and_electrical_size_of_the_double-sided_SRR_BC-SRR_and_conventional_SRR_type_metamaterials_for_varying_substrate_parameters
https://www.researchgate.net/figure/Refraction-spectrum-at-386-GHz-The-center-of-the-Gaussian-beam-is-shifted-to-the-left_fig5_213998213

Instances where selected sources appear:

28

07/02/2020

Annu George
07.02.2020
ANNU GEORGE
Deputy Librarian in-charge
University Library
Mahatma Gandhi University
Kottayam - 686 560

DECLARATION

I hereby declare that the thesis entitled "**Resonant Properties of Flexible Split Ring Resonator Metamaterial Structures for Different Structural and Dielectric Parameters"**, is an independent work carried out by me and it has not been submitted to any other institute or university for the award of any other degree.

Umadevi K S

Place:

Date:

CERTIFICATE

This is to certify that the thesis titled "**Resonant Properties of Flexible Split Ring Resonator Metamaterial Structures for Different Structural and Dielectric Parameters"**, submitted by UMADEVI K S, to the Mahatma Gandhi University for the award of the degree of **Doctor of Philosophy**, is a bona fide record of the research work done by her under my supervision. The contents of this thesis, in full or in parts, have not been submitted to any other institute or university for the award of any other degree.

Dr. V.P. Joseph
Research Guide
Associate Professor
Department of Physics
Christ College (Autonomous)
Irinjalakuda
Thrissur 680125

Place:
Date:

Dedicated to

My parents

My husband and children

My brother and Sisters

My teachers

My colleagues

ACKNOWLEDGEMENT

It is with immense gratitude I look upto God Almighty who had guided me and shown me the way throughout. I would like to specially thank Dr V P Joseph, Head and Associate Professor, Department of Physics, Christ College (Autonomous), Irinjalakuda for being my guide, mentor and motivator all these years. My years of toil and strain would not have manifested in the form of thesis without my greatest benefactor Dr V P Joseph. He often boosted my morale and rejuvenated my withered spirit. I'm sure, I cannot thank him enough.

I cannot forget Rev Dr Jolly Andrews, Asst Professor, Department of Physics, Christ College, Irinjalakuda for his valuable help during my paper publications and thesis writing. I express my heartfelt thanks and obligation to Dr Mathew Paul Ukken, Principal, Christ College, Irinjalakuda for selflessly offering the lab facilities. I had also been moved by the care and concern of all the teaching staff of the Department of Physics.

My thanks are due to Dr Thomson Joseph, Principal, Newman College, Thodupuzha and all the former principals of Newman College, who had provided all the facilities there as it's my research centre. I also express my gratitude to Dr Joe Jacob, Associate Professor, Department of Physics, Newman College, Thodupuzha for his academic help and kindness towards me.

It's only with gratitude I can remember my research colleagues, Ragi P Menon, Sreedevi P Chakyar, Nees Paul, Sikha K Simon, Jovia Jose, Bindhu C, Anju Sebastian, and Aswathy P V for their help and co-operation. Mr Joe Kizhakkoden deserves special mention for his whole-hearted support towards me.

I am deeply indebted to Rev Dr Harshajan Pazhayattil, Founder-Manager and Director of Prajyoti Niketan College, Pudukad for inculcating research fervour in my mind. I would also like to thank Dr Shaijan Paul, Principal for supporting me throughout in the course of

my research.

My Electronics family comprises HOD Mr Joseph P P, Dr Jibish Mathew, Ms Shinta G Nellai, Dr Shiji P V and Ms Susmy Johnson. I would not have completed my research without their selfless help and genuine love. Dr Dhanya Menon, Associate Professor, Department of English, Prajyoti Niketan College, Pudukad had been magnanimous to deliver academic guidance.

Brimming with love and gratitude , I look upto my beloved father Mr Sreekumaran Namboothiri who is now in his heavenly abode. I would like to dedicate my whole research work to my dearest mother Ms Aryadevi who had been with me during times of rain and shine. My husband Mr Manoj K P and my loving kids Devadath and Devanandha, had suffered much during my study. I owe them my life and love. My brother and sisters had been there instilling confidence and willpower. Ms Sreemathi Antharjanam, my mother-in-law had also been kind towards me and rendered necessary help during trying times.

Lastly, a word of thanks to all the teaching and non-teaching staff of Prajyoti Niketan College, Pudukad and all friends who had extended a helping hand towards me to undertake this challenging venture.

Umadevi K S

Contents

List of Tables

List of Figures

CHAPTER 1

Introduction and Literature Review

This chapter aims to provide the growth and evolution of the fascinating world of metamaterials, a special group of materials exhibiting negative values for permittivity (ϵ), permeability (μ) and refractive index (n). A general introduction to metamaterials, their history, classification and applications are included in this chapter. It also presents a brief review about the major research works done in this field and highlights the possibilities and potentialities of this artificially engineered material class. The aim and objectives of the study and the organization of thesis are also included.

1.1 General Introduction

Over the last few years, metamaterial has become one of the most interesting and highly focused areas of research in the field of microwave engineering. These artificially engineered materials exhibit some extraordinary electromagnetic properties at certain frequency bands ranging from microwave to optical spectrum, which arise due to the negative values of permittivity (ϵ), permeability (μ) and index of refraction (n). Generally the permittivity and permeability are both positive for ordinary materials. But for materials like metals and plasma, permittivity possesses negative values below their plasma frequencies. Natural materials with negative values of permeability are seldom seen.

During the early 40's, the metamaterial concept was known as 'Artificial Dielectrics' [1]. Later in 1968, Victor Vaselago predicted the possibility of existence of negative index materials and proposed a theoretical medium which were well matched with Maxwell's equations and demonstrated the unusual electromagnetic properties of the proposed medium [2]. However this concept was not materialized for around three decades due to the non-availability of negative permeability structures.

In 1999, John Pendry et al. introduced a negative permeability structure called Split Ring Resonator (SRR) [3]. He also investigated the possibility of using an array of thin wires through which negative permittivity can be achieved [4]. Combining thin wires and SRRs, Smith et al. materialized the first metamaterial in 2000 [5, 6]. This innovation made a revolutionary change in the field of material science and opened up a new door of metamaterials. These materials, which may be termed as the 'material of the millennium' are also referred to as Double Negative Media (DNG), backward wave media and Left Handed Materials (LHM).

1.2 History of Metamaterial

The promising field of metamaterial has today become a major research area in the field of science and engineering due to its exceptional properties and diverse applications. The Greek word 'meta' means 'beyond', indicates that the characteristics exhibited by these materials are beyond that of natural materials. The first step in the evolution of metamaterials is the concept of artificial dielectrics which was suggested by Lord Rayleigh in 1892 [7, 8]. He designed a continuous medium using metallic spherical shaped structures as the 'basis' having periodicity smaller than the interacting wavelength.

Based on this concept, Winston E. Kock made a replica of certain materials having similar characteristics as metamaterials in 1948 [1]. He used small metal spheres to realize light weight lenses at microwave frequencies based on Lorentz theory to illustrate artificial dielectrics. A detailed description of this phenomena is given by E. Collin [9]. Jagadish Chandra Bose and Kari Ferdinand Lindman investigated the chiral properties of certain materials in the early 19^{th} century by which a negative permeability behaviour was expected [10, 11]. In 1952, Schelkunoff and H. T. Friis proposed the first artificial magnetic structure SRR without using any magnetic components [12]. A. N. Lagarkov et al. investigated artificial magnetism using bi-helix inclusions [13]. In radio frequency region, the first magnetic material known as swiss roll was introduced by Witshire and Pendry in 2001 [14].

The term 'metamaterial' was first introduced by Rodger M. Walser in view of its exotic properties [15]. Metamaterials are constructed by the periodic arrangement of certain structures, similar to that of a crystalline structure. The structural parameters of the 'basis' unit and the 'lattice spacing' should be much less than the wavelength of the electromagnetic wave used. The basis of the metamaterial artificial medium may be

made by using a pairs of elements, in which one component produces a negative value for permittivity, and the other component produces a negative value for permeability. Natural materials with negative permeability are rarely known. Some materials show negative magnetic activity in the lower GHz region [16]. To attain this property at higher frequency ranges, artificially designed structures with smaller dimensions may be fabricated. The availability of modern engineering techniques for miniaturization made possible the fabrication of structures in micro or nano scale which may lead to the realization of a medium showing negative magnetic response.

In 1999, Pendry et al. fabricated an array of copper wires to produce negative permittivity and an array of SRRs to produce negative permeability [4, 3]. By combining these two arrays the first left-handed medium was constructed by Smith and his colleagues at the University of California at San Diago (UCSD) in 2000 [17]. Afterwards a wide variety of metamaterial structures are proposed for specific applications and also some modifications in its geometry are done to enhance its properties.

1.3 Classification of Materials

Materials can be classified according to the values of permittivity and permeability as shown by the μ - ϵ curve in Fig. 1.1. The four quadrants represent different types of materials. The first quadrant represents double positive materials whose permittivity and permeability are greater than zero. Ordinary materials like dielectrics are double positive and the wave propagation (phase velocity) and the energy flow (poynting vector) through them are in the same direction. The second quadrant symbolizes epsilon negative material (ENG), where the permittivity, ϵ is less than zero and permeability, μ is greater than zero. All metals and plasmas below their characteristic plasma frequency show this feature.

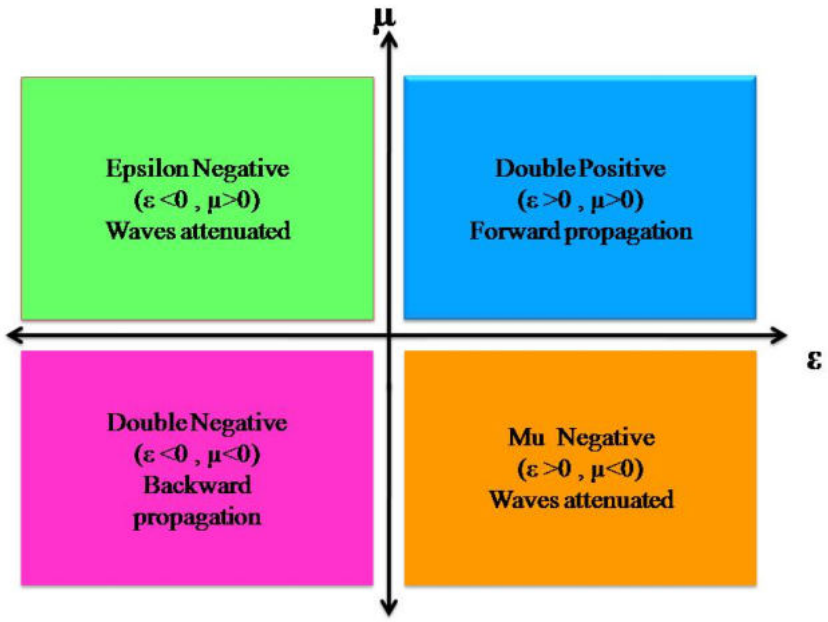

Figure 1.1: Classification of materials based on permeability and permittivity.

The third quadrant corresponds to double negative materials, those having negative values for both permittivity and permeability. No natural materials exist with DNG feature. Artificially fabricated materials or metamaterials exhibit DNG characteristics. The fourth quadrant stands for μ negative material (MNG), where the permittivity is greater than zero and permeability is less than zero. Certain magnetic materials having chiral structures show these characteristics at certain frequencies with narrow bandwidth.

If any one of the parameter is negative, the electromagnetic waves attenuate in that medium but when both the parameters are negative, waves propagate through the medium with its phase advancement opposite to the energy flow direction. A representation of classification of metamaterials by a simple flow diagram is given in Fig. 1.2.

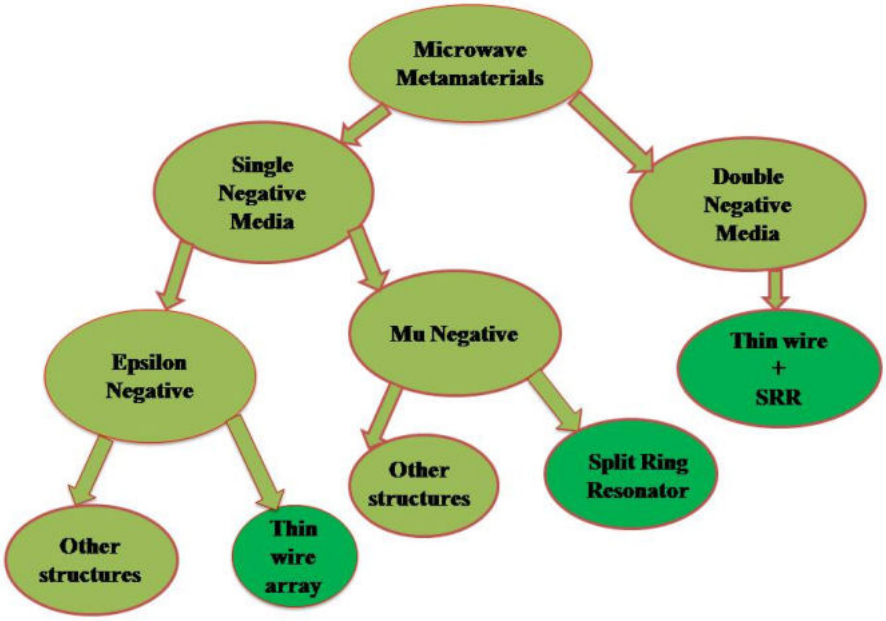

Figure 1.2: Chart showing the classification of different types of metamaterials.

1.3.1 Artificial negative permittivity structure at microwave frequencies using thin wire array

Permittivity is the measure of the electric polarization within the materials. Natural conducting materials like metals show negative values of permittivity below their plasma frequency which falls in the UV regime in most cases. Naturally occurring plasmas like ionosphere also exhibit this negative permittivity characteristics where the value of plasma frequency is lowered to regions of MHz frequencies because of its low electron density in comparison with that of metals. The materials having this negative permittivity characteristics can also be artificially engineered and the most commonly used structure is a wire medium made of thin conducting materials. In this case, the electron density may be lowered resulting in the favourable negative permit-

tivity properties at microwave frequencies. This thin wire medium is also referred to as artificial plasma. In 1962 Rotman et al. synthesized an artificial medium using an array of inductive wires [18].

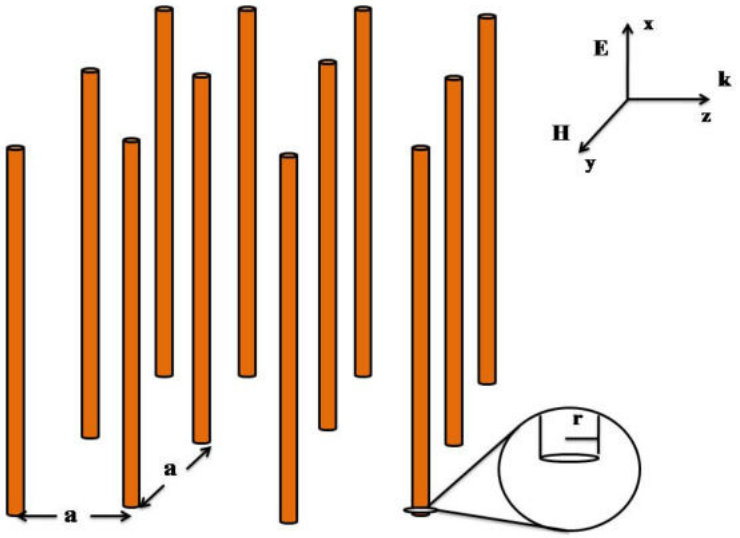

Figure 1.3: Negative permittivity artificial wire medium showing the periodicity a and radius r of the wire.

Later in 1999, Pendry et al. fabricated an array of conducting thin wires which behaves like plasma and possess negative permittivity over a wide range of microwave frequency spectrum [4, 19]. Negative permittivity is visible when these structures interact with an electromagnetic wave whereby the exciting structures act as electric field coupled resonators [20]. The relative permittivity of a medium depends on the frequency of the interacting electromagnetic wave. The expression for relative permittivity as a function of angular frequency ω is given by the expression

$$\epsilon_r(\omega) = 1 - \frac{{\omega_p}^2}{\omega^2}. \tag{1.1}$$

Here 'ω_p' is known as the plasma frequency of the medium and it is given by

$$\omega_p = \sqrt{\frac{Ne^2}{\epsilon_0 m}} \tag{1.2}$$

where N is the electron density of the medium, e is the charge of an electron and m is the mass of the electron. When $\omega < \omega_p$, the relative permittivity becomes negative and the corresponding material medium shows plasma behaviour.

Fig. 1.3 depicts an artificial plasma medium using an array of thin wires of radius r having lattice spacing a. The array is excited with an electromagnetic wave in such a way that the electric field vector is parallel to the wires. Then the movement of electrons are confined only inside the wires which leads to a reduced effective electron density N_{eff} and is given by [16]

$$N_{eff} = \frac{\pi r^2}{a^2} N. \tag{1.3}$$

Due to the high inductance and reduced effective electron density, the effective electron mass attains a large value and it is given by

$$m_{eff} = \frac{\mu_o r^2 N e^2}{2} \ln \frac{a}{r}. \tag{1.4}$$

Now the plasma frequency in (eqn 1.2) becomes ,

$$\omega_p = \sqrt{\frac{N_{eff} e^2}{m_{eff} \epsilon_0}} \tag{1.5}$$

such that the plasma frequency of thin wire array becomes

$$\omega_p{}^2 = \frac{2\pi c^2}{a^2 ln\frac{a}{r}} \tag{1.6}$$

where c is the velocity of light.

From eqn. 1.6, it can be seen that the plasma frequency of the thin wire structure only depends on its lattice spacing and the radius of wire. So it is easy to design plasma frequency of the wire medium in the lower frequency part of the microwave spectrum by simply adjusting the radius of the wire and lattice spacing. If the incoming electromagnetic wave has frequency less than the plasma frequency, then the thin wire structure acts as a negative permittivity medium according to eqn 1.1.

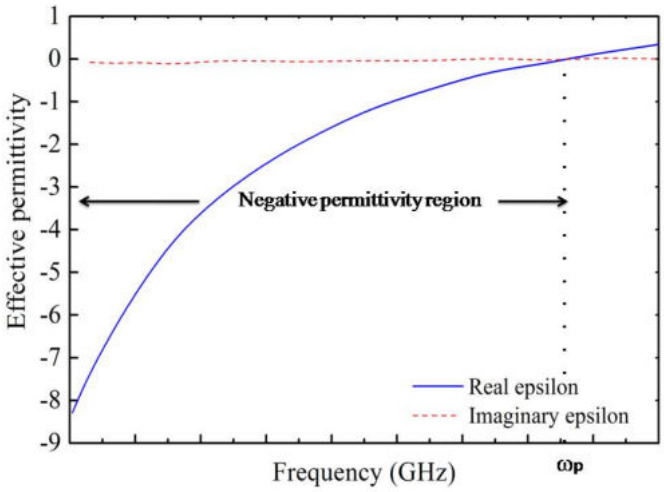

Figure 1.4: Dispersion diagram of thin wire structure showing the frequency dependent behaviour of relative permittivity. For frequencies less than ω_p, the relative permittivity becomes negative.

Fig. 1.4 depicts the frequency dependence behaviour of relative permittivity of a thin wire structure. Investigations on the electromagnetic response of some related

wire structures are also reported. The electromagnetic properties of 3D wire mesh are investigated by D. F. Sievenpiper et al [21]. S. I. Maslovski et al. proposed an analytical wire media with negative effective permittivity [22, 23]. The design of an isotropic negative permittivity medium using triple wires is presented by M. Hudlicka and J. Machac [24].

1.3.2 Artificial negative permeability structures at microwave frequencies using Split Ring Resonator

Permeability is a measure of the magnetization of the material when exposed to an external magnetic field. Naturally occurring materials having negative values of permeability are rarely seen. This forced the researchers to think about the development of negative permeability structures by artificial means. The most popular unit cell of microwave metamaterials for realizing negative permeability is SRR and this structure is proposed by Pendry et al [3]. It consists of two interleaved metallic rings that have splits on diametrically opposite sides and this structure is also called Edge Coupled SRR (ECSRR). Other variants of SRRs like complementary SRR (CSRR), Broadside Coupled SRR (BCSRR) and multi ring SRR are of much importance and are seen to have a wide variety of applications [25, 26, 27]. These structures are also fabricated in different shapes like square, circular and triangular geometries.

Other resonating structures like spiral resonator, omega shaped structure, S-shaped structure, hexagonal SRR [28] etc. also show negative permeability behaviour. More details of these structures are described in chapter 2. In presence of an external electromagnetic field, these structures show a resonance behaviour in terms of its effective inductance and capacitance resulting in a narrow band of negative magnetic response for frequencies just above the magnetic resonance frequency. Fig. 1.5 shows typical response curve of such a negative permeability structure demonstrating the negative

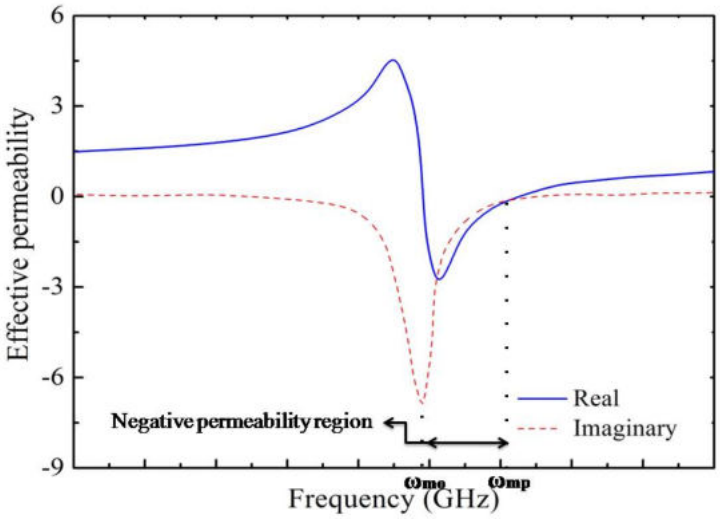

Figure 1.5: Dispersion diagram of a typical magnetic resonating structure showing the negative permeability region between ω_{mo} and ω_{mp}.

response between the resonance frequency ω_{mo} and the upper end of the resonance curve ω_{mp}.

1.3.3 Negative refractive index materials

By combining the negative permittivity thin wires and negative permeability SRRs, a double negative medium (DNG) or a medium with negative refractive index can be realized. A schematic diagram showing the metamaterial obtained by combining the thin wires and SRRs is shown in Fig. 1.6. This composite structure is proposed by Smith et al [17]. But the realization of the negative index medium with verification of negative refraction is performed by Shelby et al [29, 30]. Weiland et al. investigated the transmission and reflection properties of negative index materials [31]. A negative index metamaterial, which utilized co-planar waveguide is proposed by Anthony Grbic et al. and they realized backward radiation properties which may find applications in

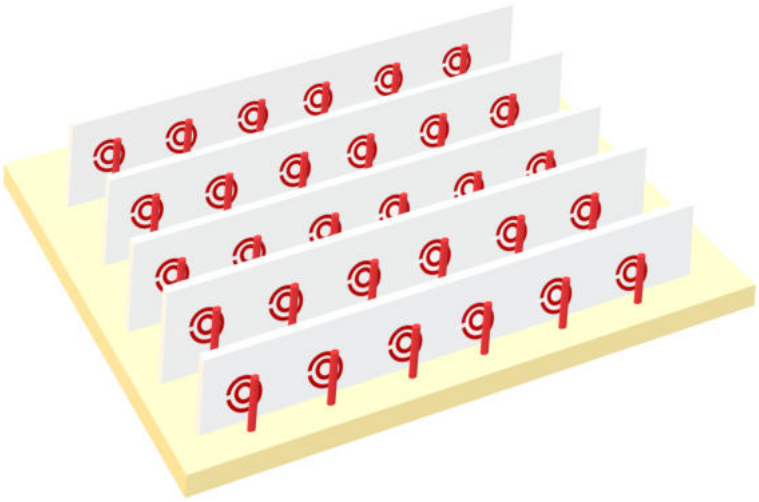

Figure 1.6: Schematic representation of artificial single layer composite metamaterial structure realized by combining thin wires and SRRs.

wireless communication and radar [32].

Several researchers have investigated the negative index metamaterial both theoretically and experimentally in microwave and optical frequencies [33, 34, 35]. Fig. 1.7 shows the dispersion diagram of a negative index composite medium. It is seen that in a small frequency region both the permittivity and the permeability exhibit negative values indicating the negative refractive index behaviour at the marked portion. Because of the negative values for ϵ, μ and n, metamaterials show some extraordinary properties other than natural materials.

1.4 Reversal of Snell's Law in Metamaterials

Metamaterials show several unusual electromagnetic properties which are different from the natural materials. The unique properties of these materials are due to the negative value of refractive index. In such materials, the direction of advancement of phase ($\overrightarrow{\mathbf{k}}$) and the direction of energy poynting vector ($\overrightarrow{\mathbf{S}}$) are in opposite directions

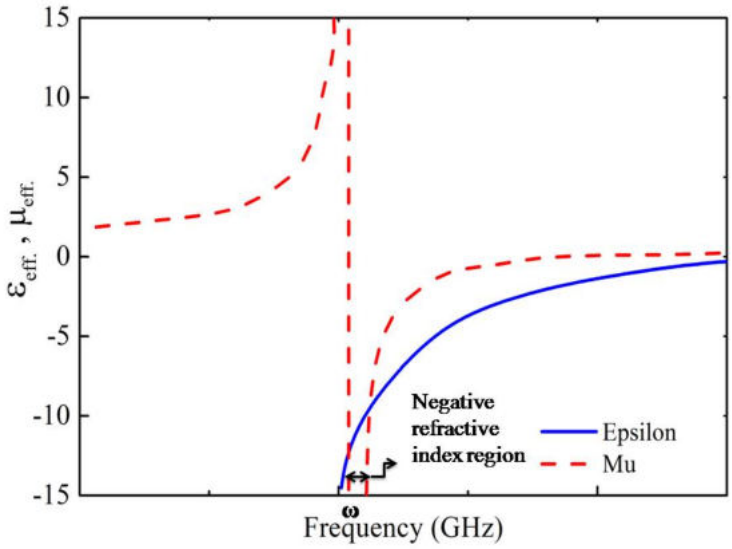

Figure 1.7: Dispersion diagram of both the negative permeability and negative permittivity resonances showing the negative index region where both the curves show negative values.

i.e. it shows a significant deviation from the propagation nature exhibited by natural materials, where both $\overrightarrow{\mathbf{k}}$ and $\overrightarrow{\mathbf{S}}$ are in the same direction. Fig. 1.8 depicts the propagation of electromagnetic wave in both right handed and left handed medium. Owing to this, the fundamental optical principle Snell's law also shows a reversed property.

The relation existing between angle of incidence, angle of refraction and refractive indices of two different material medium is given by Snell's law,

$$n_1 sin\theta_i = n_2 sin\theta_r \tag{1.7}$$

where n_1 and n_2 are the refractive indices of the two media, while θ_i and θ_r are the angle of incidence and angle of refraction. In positive index medium the refracted wave advances to the opposite side of the normal, while in negative index materials,

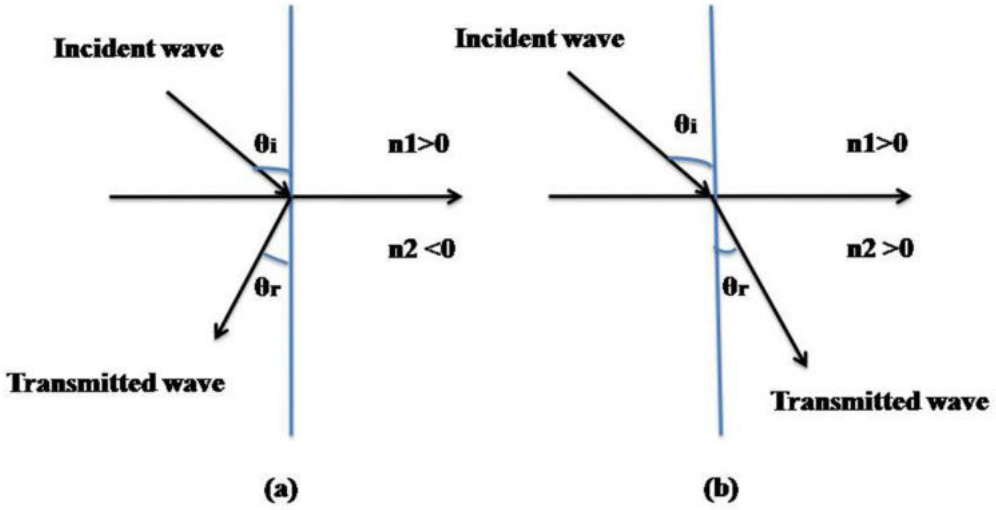

Figure 1.8: Refraction of waves in (a) double negative medium and (b) double positive medium.

the refracted wave advances in the same side of the normal and hence the angle of refraction becomes negative. This is the major unusual property that metamaterial exhibits and it is termed as negative refraction or reversal of Snell's law [36].

Shelby et al. verified the negative refraction using a composite medium obtained by thin wires and SRRs [29, 30]. Since the direction of energy poynting vector $\overrightarrow{\mathbf{S}}$ and the phase propagation direction are opposite in metamaterials as shown in Fig. 1.9, they may also show some associated effects like reverse Doppler effect and reverse Cerenkov radiation.

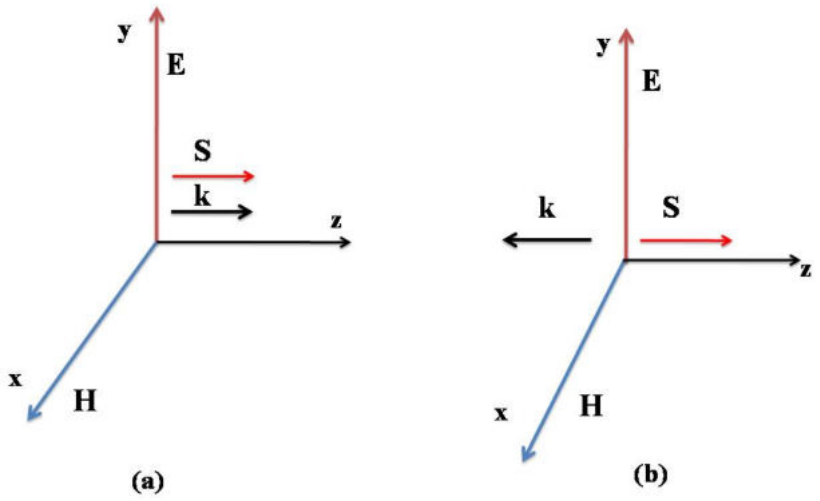

Figure 1.9: Propagation direction of energy poynting vector **S** in comparison with the propagation wave vector **k** in (a) right handed medium and (b) left handed medium.

1.5 Applications of Metamaterials

More and more researchers are attracted to the growing field of metamaterial because of its potential applications in amplification of the evanescent waves, frequency selective surfaces, miniaturized antennas, wireless communication, cloaking, sensing etc. Another interesting application of metamaterial is a super-lensing with high image quality, which can focus information smaller than the wavelength of electromagnetic wave used [36]. Some of the major applications of metamaterials are discussed in the following sections and are also pictorially represented in Fig. 1.10.

1.5.1 Cloaking

One of the interesting proposed applications of metamaterial is in cloaking, the bending of electromagnetic wave field around an object without reflection and absorp-

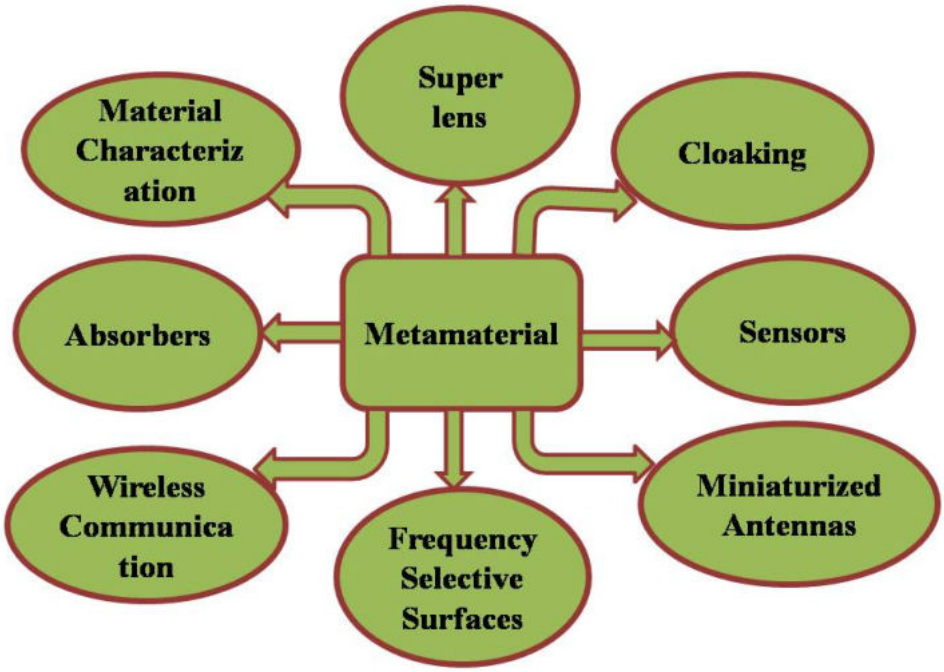

Figure 1.10: Chart showing various applications of metamaterials.

tion but making the object invisible. Transformation optics is used for the designing process of cloaking. The properties required to realize cloaking is that the material should be anisotropic, inhomogeneous and spatially invariant. Schurig et al. realized first microwave metamaterial cloak in 2006 [37]. The imperfection in the proposed cloak was reduced by conformal mapping technique introduced by F. Leonhardt et al [38]. At optical frequencies a non-magnetic cylindrical cloak was realized by removing undesired scattering using higher order transformation technique by Cai et al [39, 40, 41]. An inverse cloak was designed by Xu et al. which worked for all polarizations simultaneously [42]. Ribeiro and Paiva attempted some other types of invisibility cloaks designed by mathematical approach [43].

1.5.2 Superlens

Another major applications of metamaterial is the proposal of superlens. Dennis Gabbor in the early 20^{th} century used the term superlens to introduce a different lens array system [44]. The major limitation of conventional lens system is the diffraction limit, and hence the lens does not consider the near field objects during focusing. This limitation can be overcome with the metamaterial superlens. Pendry et al. introduced the first perfect lens system in 2000 using negative refraction that can focus the entire emitted spectrum [36]. Fig. 1.11 shows the double focusing effect of negative index medium which is utilized in superlens. Afterwards Smith et al. reported some possible limitations of the subwavelength imaging using a negative index slab [45]. Wiltshire et al. proposed near field imaging endoscope using swiss roll [46]. Liu. Z. et al. have introduced a super resolution diffraction-free lens [47]. Anthony Grib and George Eleftheriades investigated the process of beating the diffraction limit with the help of transmission line lens [48, 49].

Several researchers reported far field imaging system beyond and below the diffraction limit for improved resolution [50, 51, 52]. Igor I. Smolyaninov et al. reported super lens in the visible frequency range [53]. Wyatt Adams et al. reported a loss compensation method for Pendry's lens using plasmon injection scheme [54]. Xu Zhang et al. implemented high resolution hyperlens with loss compensation scheme [55]. W. S. Hart investigated ultra high resolution low loss superlens using semiconductor metamaterials [56].

1.5.3 Antennas

Antenna related researches are another important area of application of metamaterials. Irfan Bulu et al. reported a highly directive antenna using metamaterial medium

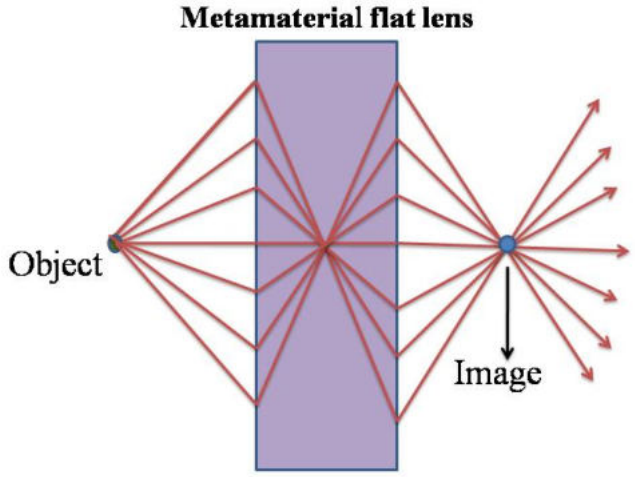

Figure 1.11: Demonstration of double focusing using negative refractive index metamaterial flat lens.

[57]. R. W. Ziolkowski introduced electrically small metamaterial antennas [58]. An impedance matching wideband antenna with tunability is proposed by Chunchen Lin [59]. Prathaban Mookiah and Kapil R. Dandekar proposed metamaterial substrate based antenna array having the properties of less mutual coupling, size reduction and improved channel capacity [60].

A. Sondas et al. proposed a micro strip patch antenna with SRR based substrate with tuning capability [61]. J. Kizhakooden et al. has realized a featherlight negative permittivity metamaterial inspired horn antenna which may find important applications in astronomy and satellite communication [62]. They have also proposed a negative permeability BCSRR loaded multiband microstrip patch antenna which can be used to radiate different frequencies simultaneously, which may be useful for

Wi-Max, Wi-Fi, Wi-LAN and Blue tooth applications [63].

1.5.4 Absorbers

Microwave absorbers are another important application area of metamaterials. Absorbers are particular materials which can be designed to control the transmission and reflection properties of the interacting wave. The choice of absorber for a particular application demands the frequency of absorption, designing pattern of the element and thickness. Winfield W. Salisbury developed an absorbant body for electromagnetic waves in early 1950's [64]. Filiberto Bilotti et al. proposed an absorber at microwave frequencies using split ring resonators in 2006 [65]. Another metamaterial absorber was proposed by N. I. Landy et al. in 2008 [66]. J. F. Wang et al. investigated 3-dimensional metamaterial absorbers [67]. Li Huang et al. introduced metamaterial absorbers at THz Frequencies in 2012 [68]. A special type thin light weight absorber with bandwidth wider than conventional frequency selective surface absorber used for stealth technology is proposed by Liang Kui Sun et al [69]. An absorber with flexibility is introduced by Y. J. Yoo et al. which can be used to suppress the mobile radiation [70].

Jinfeng Zhu et al. proposed a design using split square loops with varactor diode, acting as a microwave absorber with greater tunability [71]. A broadband absorber using circular split rings is designed and reported by Saptarshi Ghosh et al. which is ultra thin and can be used for applications like stealth technology [72]. Some research works are reported which dominates the absorption properties of sound waves using acoustic metamaterials. Hao Meng et al. investigated that an optimized metamaterial slab can absorb a wide band of underwater sound waves which may find application in the design of anechoic coating [73]. Tunable negative modulus acoustic materials with strong resonant characteristics using multi split hallow sphere is also reported [74]. A

detailed review of absorption of sound is written by Y. I. Bobrovnitskii in 2018 [75].

1.5.5 Sensors

Another major application of metamaterial is in sensor field. The essential parameters that influence the performance of a sensor are sensitivity and resolution. Robert W. Boyd and John E. Heebner reported a sensitive biosensor in 2001 [76]. Plasmon resonance microwave sensor, developed using negative index materials are reported by Ishimaru et al [77]. John F. O'Hara et al. investigated planar metamaterial thin film sensors in THz region [78]. Rohat Melik et al. introduced tape based wireless strain sensors using SRRs [79]. Sensing the dielectric samples using THz SRR are studied by Kenta Hattori et al [80]. Jordi Naqui et al. investigated novel sensors as position, angle and alignment sensors using the symmetry property of SRR [81, 82]. Pressure, humidity and temperature sensors using BCSRR are investigated by Evren Ekmecki et al [83]. M. S. Boybay et al. reported near field sensor for detecting biological tissues, location of buried objects etc. using metamaterial unit cells [84].

Sreedevi et al. developed a dielectric permittivity measurement sensor using SRR. They also carried out temperature dependent relative permittivity studies [85, 86] and humidity dependent studies of pulses and cereals using negative permeability SRR unit cells [87]. Sikha et al. made a vibration sensor using a specially designed BCSRR unit which may be used for detecting different types of natural and man made tremors [88]. They also reported a novel direct amplitude modulation technique using BCSRR as a sensor element [89]. Anju et al. realized sensors for precise determination of concentration of liquids [90] and a special type of rotation sensor using SRR units [91]. Hazel et al. reported a dielectric thickness sensor using a transmission line coupled SRR [92].

1.5.6 Frequency Selective Surfaces (FSS)

Frequency Selective Surface (FSS) is a panel used to select or reject a particular frequency band like filter and the filtering characteristics depend upon the shape and spacing of the different designs printed on the surface. Using asymmetric SRR, a FSS is designed to detect small frequency variations for biochemical sensing applications in the THz frequency range [93]. Farhad Bayatpur designed a loop-wire FSS and investigated the tuning possibilities of metamaterial based FSS using surface mount capacitors with sample dimensions less than the wavelength used [94, 95, 96]. Different multilayer metamaterial FSS structures using transmission line transfer matrix method are designed by H. Oraizi [97]. Another type of FSS consisting of rectangular SRR and T-shaped resonators as unit cells with stable incident angle and polarization is designed and proposed by Safiullah Khan which can be used in sensors and anti-reflection coating [98].

1.5.7 Material characterization

Another important application area of metamaterial is in material characterization. The characterization of dielectric properties of a material can be mainly carried out by resonant and non resonant methods. In non resonant method, the properties of the material are derived from the impedance and wave velocities over a wide frequency range. The resonant method, which is highly accurate and sensitive than non resonant method is used to measure the permittivity and permeability of low loss samples at a fixed frequency. Sreedevi et al. reported a direct and efficient method for determining the complex permittivity values of low loss materials using SRR units [86, 99, 85]. The permittivity measurements of liquids using SRR are presented by Erick Reyes Vera et al. which can be used in the bio-sensing applications and in food industry for quality

analyzing [100].

Kuiwen Xu et al. proposed a novel sensor using multi-layered coupled SRR for improving the Q-factor and measuring the complex permittivity of unknown samples [101]. A low loss high sensitivity sensor using symmetrical SRR is proposed by R. A. Alahnomi for material characterization of solid samples which can be found applications in bio-medical field and in quality control measurements [102]. A sensor with high sensitivity is proposed by M. S. Boybay et al. using SRR or CSRR units for the characterization of material properties. The method of fabrication of the sensor is quite simple and economical and it utilizes the microstrip technology [103]. Another sensor is presented by Chieh-Sen Lee et al. using square CSRR which can be incorporated in several microwave circuits [104]. They also reported a high resolution sensor for determining the relative permittivity and thickness at the same time using single and multi layered structural units [105, 106].

1.6 Objectives of the Study

The present study aims at the design and development of certain novel flexible metamaterial structures with variable structural and dielectric parameters at microwave frequency. They include SRR, BCSRR, Wire Split Ring Resonator (WSRR) and Wire Broadside Coupled Split Ring Resonator (WBCSRR). The resonant properties of the artificially fabricated structures mainly depend on the structural parameters like size, shape and spacing, and also on the dielectric properties of the substrate.

The main objective of the study is to develop different flexible resonators like SRR, BCSRR and WSRR and to analyze their variation of resonant frequency and bandwidth with respect to different structural parameters and substrate parameters. Based on the new designs proposed for flexible BCSRR, the thesis investigates the

possibility of realizing a wide band frequency selective metamaterial surface. Usually the SRR structures are fabricated on substrates using photochemical etching or printing methods. New ingeniously developed fabrication techniques other than those methods commonly employed are also detailed.

1.7 Glance at the Coming Chapters

Chapter 2 presents a detailed description of the negative permittivity and negative permeability structures. This chapter also mentions other mostly explored structures like BCSRR, Double sided SRR (DSRR), Omega (Ω) shaped structure and S-shaped structure. Negative permeability structures are very rarely seen in nature. Certain chiral materials show negative permeability at certain frequencies. But for specific applications, we have to design an artificial material for attaining negative permeability. SRRs are the most popular unit cells used for realizing negative permeability and the present work is mainly concentrating on this structure. Each unit cell of SRR acts as a LC oscillator in an external magnetic field and cause sharp absorption of microwave power corresponding to its resonant frequency. Tuning the resonant frequency of SRRs by various methods is also mentioned in this chapter. A detailed description of experimental set up using Vector Network Analyzer (VNA) to study transmission properties of SRR structure is also given.

Chapter 3 focuses on the development of a novel flexible SRR structure, its fabrication and study of its resonant characteristics. This novel SRR is the first flexible negative permeability structure in the microwave regime. This new design will pave a new way to the microwave industry for lot of applications like microwave absorbers and wearable microwave devices. A thin copper sheet coated with liquid photo-resist is fixed on a polymer film and it is exposed to ultraviolet light using suitable mask and

is subjected to chemical etching for materializing the structure.

Another novel method is also proposed for the fabrication of SRR using a printer. Instead of photo-masking, the SRR shapes are printed directly on the copper sheet and after that it is glued on a polymer film before doing chemical etching. The second method is simple and better. This novel flexible SRR fabricated on a thin inert substrate gives good resonant absorption of microwave power. Tuning the resonant frequency by varying the permittivity and thickness of the substrate is also presented. The result shows large shift in resonant frequency by using substrates of Polymethyl methacrylate (PMMA) and wax of different thicknesses.

In this chapter the structural parameter variation study of flexible SRR is also presented. By altering the inner radius, metal width, gap distance between rings and slit width of a flexible SRR, the resonant frequency can be tuned to desired values. A comparative study with SRR fabricated on rigid substrate is also included. The flexible SRR shows large frequency variation than SRR fabricated on rigid substrates. The absorption and scattering losses, which depend on the substrate parameters, are almost eliminated for this structure. The flexibility makes it usable in FSS of any shape. The experimental results are also verified by simulation.

Chapter 4 describes a modified version of SRR named as flexible BCSRR with its fabrication, resonant frequency characteristics and effect of dielectric substrate on the resonant frequency. BCSRR consists of two identical split rings located on two sides of the substrate with its splits in diametrically opposite ends. This structure also shows sharp resonant absorption. The effect of dielectric substrates on the resonant frequency of flexible BCSRR is also analyzed by using substrates of PMMA and wax. Another important advantage of this novel BCSRR structure is the possibility to vary resonant frequency by changing the spacing between the rings since the two rings are

fabricated on separate polymer films. The spacing between the rings is adjusted using pieces of papers or cloths of small dielectric constant. A remarkable shift in resonant frequency is observed for a small change in spacing between the rings.

The structural parameter variation can also affect the resonant frequency of flexible BCSRR. The experimental results are also verified by using simulation method. The application of this novel flexible BCSRR as microwave absorber is described in the next section. The negative index property of the bulk medium realized using BCSRR as metamaterial absorber is explained. The spacing between rings are progressively adjusted using layers of cotton fabric. A specific absorption band can be designed by properly modifying the structural parameters of the BCSRR structure. Along with the flexibility, the structure provides added advantage of wide band frequency tuning possibility. This BCSRR may find application in FSSs and in cloaking mechanism.

Chapter 5 comprises of the design, fabrication and resonant characteristics study of a new type of SRR fabricated using conducting wires. The fabrication method of this new WSRR is quite simple compared to other SRRs. No complex procedures like photo masking and chemical etching are involved. The WSRR unit cells are constructed using copper wires bent into the form of split rings using a cylindrical cavity shaped mold and by fixing them on a thin polymer film. The structure shows sharp absorption dip in the transmission spectra. The results of WSRR are compared with that of the conventional SRR of same dimension fabricated on a rigid substrate.

WSRR structure has sharp absorption and lower bandwidth compared to SRR. The experimental results are evaluated with the theoretical values and they are confirmed by simulation method. This chapter also discusses the realization of a bulk meta structure using WSRR which may find application in microwave wideband absorption realm. The structural parameter variations of WSRR and Wire BCSRR (WBCSRR)

are also carried out and they show higher structural dependent frequency tunability than conventional one. The other significant characteristics of WSRR are the enhanced Q-factor, high sensitivity and the avoidance of any rigid supporting substrate. The application of novel flexible WSRR structure may have potential applications in the field of sensors, material characterization studies etc.

The **last chapter** gives the summary of the results obtained in the present research work. It also describes the relevance of the work in microwave industry and discusses the scope of future work in this new field of research. The results of the study revealed that by suitably changing the dielectric substrate and structural parameters of the novel proposed types of SRR structures, the resonant frequency can be precisely tuned to any desired value. The proposed structures may also find applications in frequency selective surfaces, cloaking and various types of sensors and absorbers. It is also observed that the method of fabrication employed here can be extended to flexible and tunable negative index metamaterials.

CHAPTER 2

Negative Permeability Split Ring Resonator Structure

Materials generally show good response to electrical excitations at wide frequency range. But magnetic response is not observed in all frequencies particularly at higher frequencies. In ferromagnetic and ferrimagnetic substances, a limited or a narrow band magnetic response is observed in low frequency regions. A material with negative permeability, which can be used for different frequency regions are not available in nature. So artificial structures which show strong magnetic response for particular applications in specific frequency ranges have to be designed. Split Ring Resonator (SRR) is the most commonly used microwave component showing negative permeability. This chapter mainly deals with the SRR, its electromagnetic response, its different variants and also other resonators having different shapes. It provides a review of SRR structure, applications and different measurement methods to analyze its resonant characteristics.

2.1 Split Ring Resonator

Split Ring Resonator (SRR) is designed and proposed by Pendry et al [3]. For designing a negative permeability material, Pendry first considered an array of metallic cylinders with radius r. The magnetic resonance in relation to the effective permeability of the SRR structure may be written as [16]

$$\mu_{eff} = \frac{B_{eff}}{\mu_o H_{eff}} \tag{2.1}$$

where B_{eff} is the effective magnetic induction and H_{eff} is the effective magnetic field. They are given as

$$B_{eff} = \mu_o H_o \tag{2.2}$$

and

$$H_{eff} = H_o - \frac{\pi r^2}{a^2} j \tag{2.3}$$

where H_o is the applied magnetic field and j is the induced current per unit length of the cylinder. Now the effective relative magnetic permeability of the structure becomes

$$\mu_{eff} = 1 - \frac{\frac{\pi r^2}{a^2}}{1 + i\frac{2\rho}{\mu_o \omega r}} \tag{2.4}$$

where a is the periodicity, ρ is the resistance per unit length of the cylinder surface and ω is the angular frequency of the exciting electromagnetic wave. But the value of μ_{eff} observed is not negative for this system since the response is mainly due to inductance alone. To introduce a capacitive element, Pendry considered two cylindrical conductive shells with splits in diametrically opposite ends as shown in Fig. 2.1 (a). The split blocks the current through the rings and generate a capacitance across the splits.

The combined effect of capacitance and inductance results in a resonance. But the problem about this structure is anisotropy which arise due to the flow of current along the length of the cylinder. It produces a metal like response and causes a dominant electrical resonance activity. So Pendry modified the structure into a flat disk form of split rings which reduces the electrical activity and also eliminates the continuous conducting path considerably.

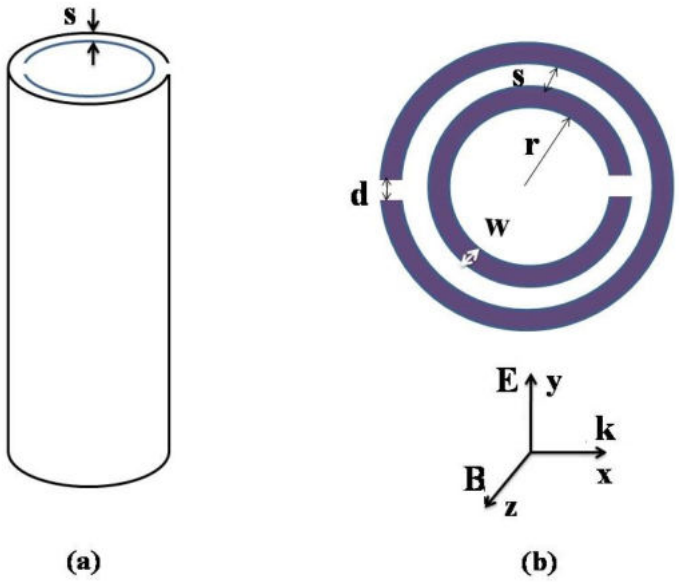

Figure 2.1: Schematic representation of (a) cylindrical shells with splits and (b) flat SRR unit with structural parameters.

For the new structure, the effective permeability equation takes the form as [107]

$$\mu_{eff} = 1 - \frac{\frac{\pi r^2}{a^2}}{1 + \frac{2i\rho}{\mu_0 \omega r} - \frac{3dc^2}{\pi^2 \omega^2 r^3}} \tag{2.5}$$

where d is the split width and c is the velocity of light.

This proposed structure is widely called as Split Ring Resonator (SRR) or Edge Coupled SRR (ECSRR). A schematic diagram of the ECSRR structure is shown in Fig. 2.1 (b). It consists of two concentric rings having different radii and splits at diametrically opposite ends. The splits on the rings and gap between the rings induce a capacitance which results magnetic resonance in SRR. The splits blocks the current flow through the rings but the current flow is maintained by the mutual inductance between the rings. The closed ring will not have magnetic resonance but will maintain electrical resonance.

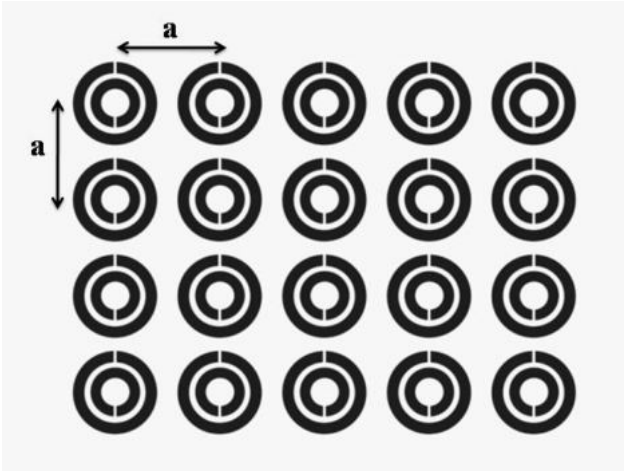

Figure 2.2: Schematic representation of two-dimensional array of SRRs with periodicity a.

When an external magnetic field is applied perpendicular to the plane of SRR as shown in Fig. 2.1(b), the SRR will act as a magnetic dipole with strong magnetic activity. The magnetic resonance resulting from internal capacitance and inductance of SRRs is based on Faraday's law of induction. A schematic diagram of one dimensional array of SRR units with lattice spacing a is shown in Fig. 2.2. Each unit cell acts as a LC oscillator in an external magnetic field causing sharp absorption of power corresponding to the resonant frequency. The charge distribution in an SRR and its equivalent circuit is given in Fig. 2.3 (a) and Fig. 2.3 (b) respectively. Since the

capacitance due to the splits in the rings is negligibly small in comparison with the gap capacitance between rings, it is not taken into account in certain situations.

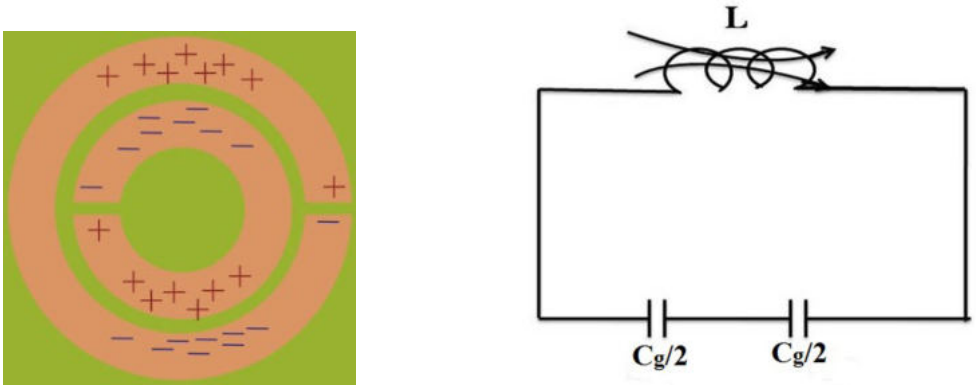

(a) (b)

Figure 2.3: SRR structure with (a) charge distribution and (b) its equivalent circuit.

The resonant frequency of this structure in terms of its intrinsic inductance L and capacitance C is given by

$$f = \frac{1}{2\pi\sqrt{LC}} \tag{2.6}$$

For a homogeneous medium of SRR having inner radius r, lattice constant a, gap between rings s and metal width w, the resonant frequency is given by [107]

$$\omega_{mo} = \sqrt{\frac{3sc^2}{\pi^2 r^3}} \tag{2.7}$$

where c is the velocity of light and the magnetic plasma frequency ω_{mp} is given by

$$\omega_{mp} = \sqrt{\frac{3sc^2}{\pi^2 r^3 (1 - \frac{\pi r^2}{a^2})}} \tag{2.8}$$

The SRR structure gives negative values for permeability in the frequency range of $\omega_{mo} < \omega < \omega_{mp}$ which is a narrow band.

Different research groups have thoroughly examined the magnetic resonance behaviour of SRR structure and they also proposed different equivalent circuits by considering their elemental behaviour. Marques et al. proposed an equivalent circuit model for SRR by examining the bianisotropic properties [108]. J. D. Baena et al. reported equivalent circuit models with split capacitance and dielectric losses [109, 110]. M. F. Wu et al. designed an equivalent circuit model for a rectangular SRR using modelling methods of spiral inductors for multiple frequency bands [111]. An improved equivalent circuit for three dimensional array of SRR is designed by Chen et al [112]. Later Shamonin et al. reported a modified circuit model for SRR [113]. Bilotti et al. investigated an equivalent circuit model by considering the conductor and dielectric losses for various types of resonators [114].

In 2009, Cui et al. suggested a symmetrical circuit model for all types of metamaterials [115]. Yasar Orten et al. developed an equivalent circuit model for SRR arrays in 2010 [116]. The transmission characteristics of single SRR is proposed and an expression for total capacitance which is the sum of gap capacitance and surface capacitance is derived by Sydoruk et al [117]. Another important conceptual development in the analysis of SRR is proposed by Sreedevi et al. where they have considered the effect of capacitive contribution from both sides of the split rings, a noticeable advancement from the previous reported works [99].

SRRs of different geometries are reported by various research groups. S. Maslovski et al. introduced metasolenoid, a new artificial magnetic material in microwave region and also verified by simulation [23]. Joseph Helszajn and David S. James theoretically and experimentally investigated planar triangular resonators in 1978 [118]. Ittipiboon et al. proposed aperture-fed rectangular and triangular shaped dielectric resonators [119]. Sabah et al. reported S and C band tunable metamaterials using triangular SRR and wire strips [120, 121]. Resonator structures with various shapes like Hexagonal

[122, 123], Rhombic [124] and Oval [125] were also reported by different authors. A schematic representation of commonly used ECSRR geometries are depicted in Fig. 2.4.

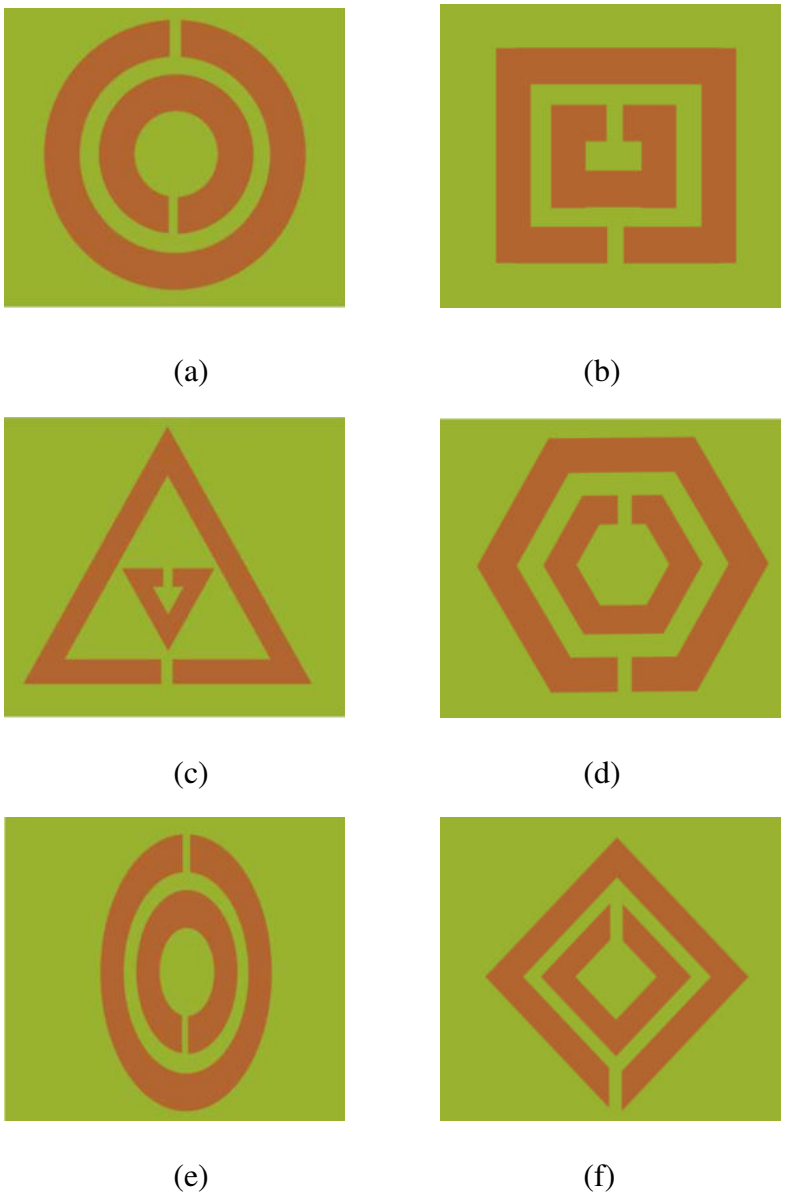

Figure 2.4: Schematic diagrams of ECSRRs showing different geometrical shapes (a) circular, (b) rectangular, (c) triangular, (d) hexagonal, (e) oval and (f) rhombic.

The SRR shows bianisotropic characteristics which arises from the magnetoelectric coupling or cross polarization effects. It is undesirable in some applications and hence to avoid the bianisotropic behavior of SRR, new forms of structures were investigated by researchers. A significant discussion on the role of bianisotropic nature of ECSRR is given by R. Marques et al [108]. In order to eliminate the bianisotropy, they have introduced a new structure called Broadside Coupled Split Ring Resonator (BCSRR). A discussion on BCSRR is followed in the next section.

2.2 Broadside Coupled Split Ring Resonator Structure

In order to overcome the limitations of ECSRR like bianisotropy, lower limit for resonant frequency etc., several other designs have been proposed and analysed. Broadside Coupled SRR (BCSRR) proposed in 2002 by R. Marques et al. [108] is one among the most explored structures. Conventional BCSRR units are fabricated on double sided PCBs by etching split rings on both sides of the substrate co-axially with the splits at diametrically opposite ends. The schematic representation of BCSRR with a transparent substrate is given in Fig. 2.5. Marques et al. performed a comparative analysis of the properties of conventional ECSRR and BCSRR [126]. The important parameters that influence the resonant frequency of BCSRR are the permittivity and the thickness of the substrate material. The resonant frequency varies inversely with square root of both substrate thickness and permittivity of substrate.

The effect of substrate parameters on the resonant frequency of BCSRR was theoretically investigated by Ekmecki et al. and Sheng et al [127, 128]. In 2009 Ekmecki et al. reported an equivalent circuit model for BCSRR and ECSRR and presented a comparison between them [129]. They also reported tunable THz metamaterial using BCSRR [130]. Different numerical and experimental studies related to the electrical

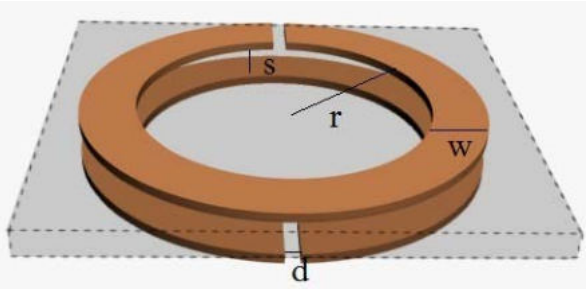

Figure 2.5: Schematic representation of BCSRR showing the structural parameters having circular geometry.

size and resonant frequency of BCSRR are also performed by them [131]. Tunable and modified BCSRR (MBCSRR) are proposed by J. Wang et al [132]. The experimental and theoretical study of mutual coupling of BCSRR are done by J. Machac et al [133]. A novel type of BCSRR loaded frequency tunable monopole patch antenna is presented by K. Joe et al [63].

2.3 Other Types of Magnetic Resonator Structures

Other types of resonator structures explored are Double sided SRR (DSRR), Complimentary SRR (CSRR), multi-ring SRR, spiral resonators, labyrinth-based metamaterial structures, S-shaped, V-shaped and Ω-shaped resonators are also attempted.

2.3.1 Double Sided SRR (DSRR)

Another structure called Double sided SRR (DSRR), analyzed by different researchers, is a mixture of both ECSRR and BCSRR, where two ECSRRs are placed on the two sides of a dielectric substrate. A schematic representation of DSRR with circular geometry on a transparent glass subsrate is shown in Fig. 2.6.

A comparative study using numerical simulation of ECSRR, DSRR and BCSRR

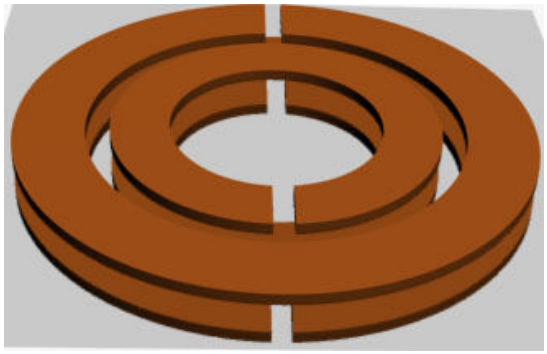

Figure 2.6: Schematic representation of a circular double sided SRR on a transparent substrate.

structures showed that DSRR can provide better miniaturization and can have wider half-power bandwidth when compared to other conventional structures [129]. Effects of substrate parameters on resonant frequency of DSRR structure under magnetic and electric excitations are also investigated [127].

2.3.2 Complimentary SRR

Complimentary SRR (CSRR) is proposed by F. Falcon in 2004 and is fabricated by removing the conducting parts of perfectly thin sheet in the shape of SRR. The Fig. 2.7 shows the schematic representation of CSRR. The designing of CSRR is based on the

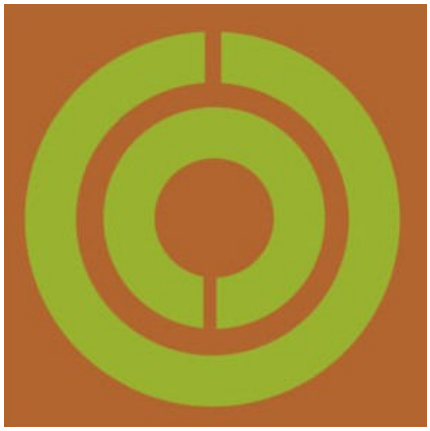

Figure 2.7: Schematic representation of CSRR.

Babinet's principle. A metamaterial antenna using CSRR with enhanced performance and reduced coupling effects is proposed by Bisht et al [134]. It is claimed to be suitable for different types of filters also. A compact antenna for improving isolation requirements of antenna array suitable for 5G communication elements is designed and proposed using CSRR by R. Selvaraju et al [135]. CSRR can also be used for various applications like satellite communication [136], material characterization [137], sensors [138] and wireless applications [139].

2.3.3 Multi-ring SRR

Figure 2.8: Schematic representation of multi-ring SRR.

A novel structure using multi-ring SRR is introduced by O. Turkmen et al. and variation of its resonant frequency with respect to the changes in structural parameters are investigated [140]. Fig. 2.8 shows the schematic representation of multi-ring SRR. F. Bilotti proposed an accurate method to realize this structure and also analyzed the quasi-static behaviour of multi-ring SRR [141]. A hexagonal shaped multi-ring SRR is designed by M. Jagadish et al. and studied the effect of variation of side length on its resonant frequency numerically [142]. A filter which can be used for wireless applications using multi-ring CSRR is presented by Imene Sassi et al [143].

2.3.4 Spiral resonators

Spiral resonators are the planar version of swiss roll and it is introduced by J. D. Baena et al [109]. Spiral Resonators are non-bianisotropic elements having small electrical size. A schematic representation of spiral resonator structure is given in Fig. 2.9. The major applications of spiral resonators are in low profile microwave antennas

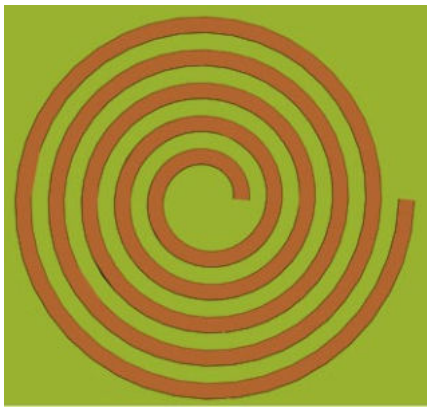

Figure 2.9: Schematic representation of spiral resonator structure.

[144], miniaturized band pass filters [145] and Radio Frequency Identification (RFID) tags [146]. Zunfu Jiang et al. computed the distributed capacitance and equivalent inductance of spiral structures [147]. Theoretical and experimental study of spiral resonators with elevated temperature, which can be used for applications in the field of superconducting metamaterial, are reported by Behnood G. et al [148]. A novel spiral resonator designed by modifying the spiral structure with embedded capacitors is proposed by Di Wu et al. which can be used for designing compact filters with good filter characteristics [149].

2.3.5 Labyrinth structures

The major problems that have been encountered with SRRs are bianisotropy and the coupling between electric and magnetic resonances. Irfan Bulu et al. proposed a labyrinth based material structure and experimentally confirmed its magnetic resonance property [150, 151]. A schematic representation of labyrinth resonator structure is given in Fig. 2.10. E. Ozbay et al. studied the transmission, refraction and focusing properties of labyrinth based structures [152, 153]. J. S. Dong et al. proposed symmetric square labyrinth ring structure and investigated its application in horn antennas [154]. Marques et al. analyzed different geometries of SRR like double slit SRR, non bianisotropic SRR and two turns spiral resonators with equivalent circuits [155].

Figure 2.10: Schematic representation of labyrinth resonator structure.

2.3.6 S-shaped structures

Instead of using a combination of negative permittivity wire structure and negative permeability structure to form a negative refractive media, S-shaped resonator structures are proposed which have both electric and magnetic resonances at a desired frequency. Hongsheng Chen et al. proposed this structure and confirmed the

left handed property of this material [156]. The experiments showed that the negative permittivity and negative permeability regions are overlapped in such structures. A schematic representation of S-shaped resonator structure is given in Fig. 2.11. They have also designed a combined double S-shaped structure that showed negative index property over a wide range of frequencies [157]. M. F. Khan and M. J. Mughal investigated the tuning properties of S-shaped materials [158, 159]. Hayet Benosman and Nouredine Boukli Hacene simulated a double S-shaped structure and investigated its effective parameters [160]. Some proposed applications of S-shaped resonators are differential filters, Ultra Wide Band (UWB) antennas etc [161, 162].

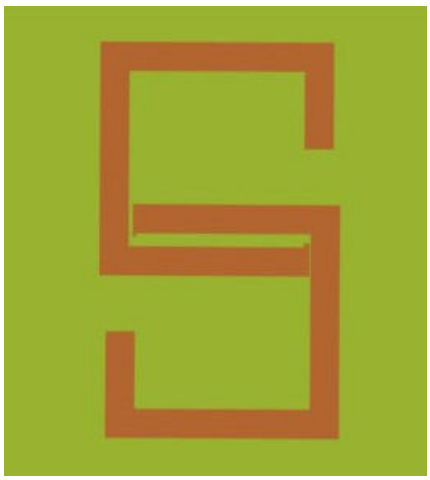

Figure 2.11: Schematic representation of S-shaped resonator structure.

2.3.7 V-shaped structures

Ekmekci et al. numerically investigated V-shaped resonator design for sensor applications [83]. A schematic representation of V-shaped resonator structure is given in Fig. 2.12. A bio-sensor is proposed by A. M. Soehartono et al. using V-shaped resonators made of gold [163]. A multi band metamaterial is designed by Sabah et al. using concentric type V-shaped resonators [164]. V-shaped resonators are also used for

applications in the field of antennas [165].

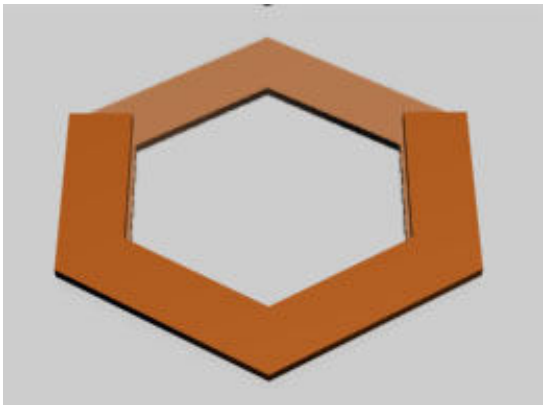

Figure 2.12: Schematic representation of V-shaped double resonator structure.

2.3.8 Ω-shaped structures

Another structure that shows negative permeability over a certain frequency regime is Ω-shaped structure. This bianisotropic pseudochiral medium was introduced by Mamdouh M. I. Saadoun and Nader Engheta [166]. A schematic representation of Ω-shaped resonator structure is given in Fig. 2.13.

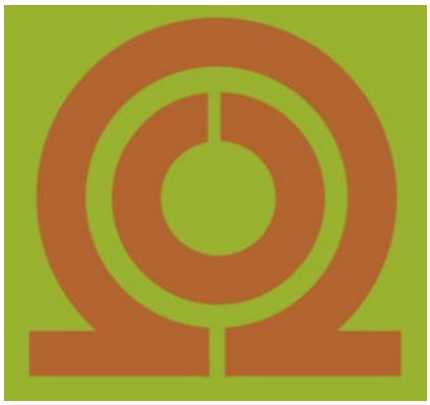

Figure 2.13: Schematic representation of Ω-shaped resonator structure.

An isotropic negative metamaterial fabricated by Ω-shaped elements is analyti-

cally analyzed by Simovski et al [167]. The negative index property of Ω-shaped structures are confirmed by Jiangtao Huang fu et al. [168]. V. V. Varadan and Sravanthi Penumarthy proposed a new design named Ω-image pairs and investigated its negative index and reciprocal behavior using resonance property [169]. They also reported the switching of electric and magnetic resonances of Ω-shaped elements by reflection [170]. Tretyakov et al. realized a backward wave medium using Ω-shaped composites [171]. Aydin et al. reported the transmission properties of various Ω-shaped materials [172, 173]. The major application areas of this type of structures include wireless communication [174], bowtie antennas [175], terahertz detection[176] and sensing [177].

2.4 Review of Properties and Applications of SRR

The metamaterial era begins from the invention of the first metamaterial by Smith et al. in the year 2000 [17]. After that a lot of research activities have been carried out in this specific area, particularly in the microwave frequency regime. SRR is the main constituent for providing negative permeability. Owing to the exotic properties of these meta molecules like near field sensing capability, they are used for various applications.

Some important research works using SRRs were reported by Koray Aydin et al. They demonstrated the magnetic resonance of SRR and studied its transmission characteristics [178, 179, 180]. The magnetoelectric coupling and bianisotropic characteristics of SRR are investigated by R. Marques [108]. Philippe Gay-Balmaz et al. reported a crossed SRR structure which acted as magnetic resonator and showed isotropic nature [181, 182]. Yi-Jang Hsu et al. investigated a deformed SRR which showed the resonance characteristics similar to conventional one with low power loss [183]. A novel method is proposed by Hee-Jo Lee et al. to detect biomolecular binding at microwave

frequencies using arrays of SRR [184].

A broadband metamaterial absorber is designed using multilayer SRR by Jingbo Sun et al [185]. Using circular cavity method, E. Li et al. proposed a system to measure dielectric properties of low loss microwave materials for broadband frequency ranges even at high temperatures [186]. To determine the surface strain of different materials R. Melik et al. proposed wireless sensor using SRR metamaterial structure [187]. The experimental measurement and numerical simulation of wide-angle metamaterial absorber by utilizing the coupling of SRR are also presented [188, 189]. A split ring resonator can be shifted in position to tune its nonlinear characteristics [190]. Using a couple of electric ring resonators and its complementary form, a compact metamaterial absorber is designed in L-band by Z. X. Cao et al [191]. For environmental applications, a wireless temperature sensor is designed by Hasanul Kairm using closed ring resonator [192].

A low cost passive sensor for dielectric characterization of solids and liquids is presented by Galindo Romera et al [193]. Chakyar et al. proposed a new resonant perturbation method using SRR to measure relative permittivity of different solid materials and the permittivity measurements of food samples like pulses and cereals for quality analysis [87]. They have also reported dielectric constant measurements of different wax samples with temperature variations [85, 86, 99]. A SRR sensor for the characterization of dielectric permittivity based on near field profile is also reported [194]. A stop band filter is designed using diamond SRR with good attenuation characteristics by Betsy George et al [195]. A method to determine the thickness of dielectric films/sheets using transmission line coupled SRR is presented by H. Thomas et al [92]. A novel method for liquid concentration measurement is proposed using BCSRR structure by Anju Sebastian et al. by considering its near field perturbation effects [90]. A sensitive tunable sensor using BCSRR for efficient detection of mechanical vibrations

is proposed by Sikha Simon et al [88].

Some specific applications of SRR demand tuning of its resonant frequency. A number of methods for tuning the resonant frequency are reported by various researchers. Tuning the permeability using varactor diode is demonstrated by some researchers [196, 197, 198, 199]. K. Aydin and E. Ozbay designed a tunable metamaterial using capacitor loaded SRRs [200]. Thomas H. Hand and Steven A. Cummer reported ferroelectric loaded SRR with frequency tunability [201]. Qian Zhao et al. proposed liquid crystal based negative permeability tuning using an array of SRRs [202]. Shumin Xiao et al. investigated thermally tunable negative permeability metamaterials using liquid crystals at optical frequencies [203]. Using an array of SRRs and ferrite rods, Lei Kang et al. demonstrated tunable negative permeability metamaterial composites experimentally [204, 205]. Jiaguang Han et al. numerically simulated a thermally and magnetostatically tunable metamaterials at THz frequencies [206]. Z. Sheng and V. V. Varadan studied the tuning properties by changing substrate thickness and dielectric permittivity [128]. Ekmecki et al. studied the resonant characteristics of SRR, BCSRR and DSRR by varying substrate parameters [129, 207].

2.5 Measurement Methods

In order to analyze the resonant characteristics of SRR, three different methods are commonly employed. They are waveguide method, free space method and transmission line method. Fig. 2.14 shows a schematic representation of these different measurement arrangements. Resonance measurement by free space method can be done in two ways. For measuring the resonant frequency of a single SRR molecule, a setup as shown in Fig. 2.14 (a) is used. In this case the SRR is placed in between two monopole antennas, one acts as a transmitting probe and the other acts as a receiving probe, which are

connected to a Vector Network Analyzer (VNA).

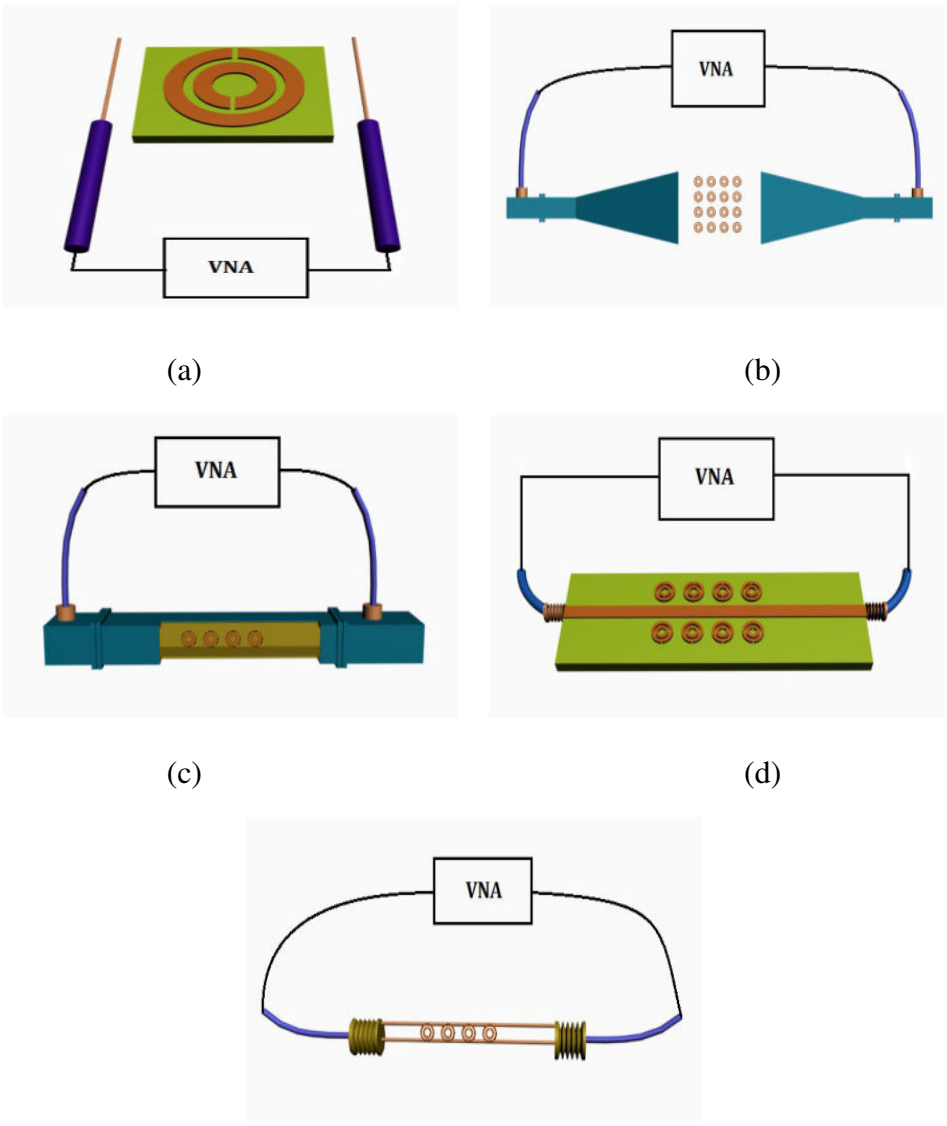

(a) (b)

(c) (d)

(e)

Figure 2.14: Schematic representation of different measurement methods used to study SRR magnetic resonance: (a) & (b) Free space measurements using probes and horn antennas respectively, (c) Waveguide method, (d) & (e) Transmission line methods.

The SRR should be arranged in the reactive rear field region between the probes in such a way that the plane of the resonator rings is perpendicular to the direction of the magnetic field component of the incident electromagnetic field [178].

In the case of a bulk medium, a measurement setup as depicted in Fig. 2.14(b) is employed [178]. The SRR bulk sample is placed between two wide band horn antennas connected to the transmitting and receiving ports of the VNA. In this case also, the orientation of the plane of SRRs should be perpendicular to the magnetic field direction. In waveguide method, the second measurement method, SRRs are arranged inside the waveguide at the middle region along the wave propagation direction with the plane of the rings perpendicular to the magnetic field direction as depicted in Fig. 2.14(c) [109]. This method is found to be effective for small SRRs.

Third method is the transmission line method. Conventional transmission lines are metallic structures used to guide electromagnetic energy. A micro-strip transmission line of specific length fabricated on certain dielectric substrates as depicted in Fig. 2.14(d) is usually used for the resonance study. When the SRR structure is placed near the microsrtip line, resonant absorption of power takes place corresponding to the magnetic plasma frequency of the structure. Since the transmission line is fabricated on the substrate, a good part of power is confined within the material. So the resonance absorption dip is found to be less in this case [208]. For the purpose of avoiding the dielectric related absorption losses, a new transmission line structure for finding the resonant frequency of SRR is also proposed. This structure is fabricated using thin wires. Fig. 2.14(e) shows the schematic representation of transmission line set up. The SRR under study is arranged between two lines of the structure as shown. The absorption dip corresponding to the resonant frequency obtained in this case is higher compared to the conventional transmission line method.

2.6 Experimental Setup Used for the Study

Resonance properties of various structures introduced in this thesis are analyzed using the free space methods. Resonance behaviour of single flexible SRR, single flexible wire-SRR, single flexible BCSRR and single flexible wire-BCSRR are carried out by free space method using the transmitter-receiver probe set up depicted in Fig. 2.14 (a). In order to analyze the wide band absorption properties of bulk samples, the free space method with wide band horn antennas is used (Fig. 2.14(b)). The measurements are done using a Keysight vector network analyzer set up for the frequency band of 2 GHz to 9 GHz.

2.7 Conclusion

The theory behind the widely used negative permeability SRR structure is discussed. Another important type of SRR structure known as BCSRR structure in which bianisotropic behaviour eliminated is also presented. Various types of other resonating structures and their applications are also detailed. A detailed review of different types of SRRs is also presented. The various measurement methods and their experimental setups to study the resonant characteristics of proposed structures are also presented.

CHAPTER 3

Flexible Split Ring Resonator Metamaterial Structure

In this chapter a novel flexible SRR metamaterial structure is introduced and its design, fabrication and resonance behaviour are discussed in detail. The effect of structural and dielectric parameter variations of the proposed structure on its resonant frequency along with its transmission properties are presented. The experimental results obtained for the proposed structure are analyzed in terms of possibility of tuning the resonant frequency to any desired values by introducing changes in its structural parameters or in the substrate material used or in the thickness of the substrate. The results obtained by simulation method are also presented for comparison purpose.

3.1 Introduction

The widely used negative permeability metamaterial molecule is split ring resonator (SRR). Apart from using it along with wire medium to form a composite negative refractive index medium, it is used for a variety of applications both in bulk form and as individual structure. In bulk form, the most cited applications of SRR are in the fields of frequency selective surfaces (FSS) and absorbers, whereas the major use of individual SRR is in the field of various sensor applications. Almost all applications of SRRs are confined around its magnetic resonance property and it is totally related to its intrinsic capacitance and inductance. For a particular SRR geometry the resonance tunable properties are mostly depend on the capacitive part rather than inductive part. The near field perturbations of the SRR in view of some sort of changes happening to the dielectric environment of the rings drastically affect its resonance. Keeping all these features into account, a new form of SRR fabricated with the advantage of flexibility is presented in the following sections.

SRR also known as Edge Coupled SRR (ECSRR), consists of two circular or square metallic rings with small splits situated diametrically at opposite ends. These concentric flat rings have negligible thickness and are usually fabricated on planar dielectric substrates. The resonance characteristics of these structures mainly depend upon their structural dimensions and dielectric substrate parameters. Different researchers have tried to investigate on these issues.

Aydin et al. investigated the resonant properties and the transmission characteristics of SRR structures both numerically and experimentally [180]. They have also reported the transmission characteristics and left handed behavior of a composite medium which consists of SRR and thin wires [209, 210, 211]. The effect of alignment disorder and periodicity are also studied [212]. In all such studies, the SRR is fabricated

on the solid substrate of printed circuit board (PCB). Along with the rigid nature of this structure, the non-vanishing loss factor of the substrate material forces the SRR to behave as a LCR resonator instead of a LC resonator, causing reduction in Q-factor. For particular applications of metamaterial like FSSs and cloaking, the flexibility in structure is a necessity. A flexible metamaterial structure at THz frequencies is reported by R. Miyamuru et al. in 2009 [213]. The development of a flexible structure at microwave frequencies is one of the objectives of this thesis. This work is the first of this kind which introduces a flexible SRR structure fabricated on a negligibly thin inert dielectric film substrate for applications at microwave frequencies [214].

3.2 Fabrication of the Flexible Split Ring Resonator Structure

Since the size of SRR molecules is very small with structural dimensions ranging from few millimeters at certain regions to much less than a millimeter at certain other regions, etching technique using PCBs is usually adopted for the manufacture of conventional SRRs. Chemical etching based on photolithographic method or computer aided milling method is used for this purpose. For the present flexible SRR case, since there is no rigid substrate present, the chance of milling method is out of question. Here SRR unit cell is fabricated on a thin polypropylene film of thickness 18 μm using a copper foil of 20 μm thickness. Two different methods are used for the purpose. One method is the conventional photolithographic etching method while the second one is a novel but simple method which uses direct printing of the SRR pattern on the copper film followed by chemical etching. For the purpose of comparison, conventional SRR on PCB is also fabricated for the present study. Both photochemical etching method and milling method are used for it. Various steps followed for the photolithographic etching method and direct printing method are detailed below.

3.2.1 Photolithographic method

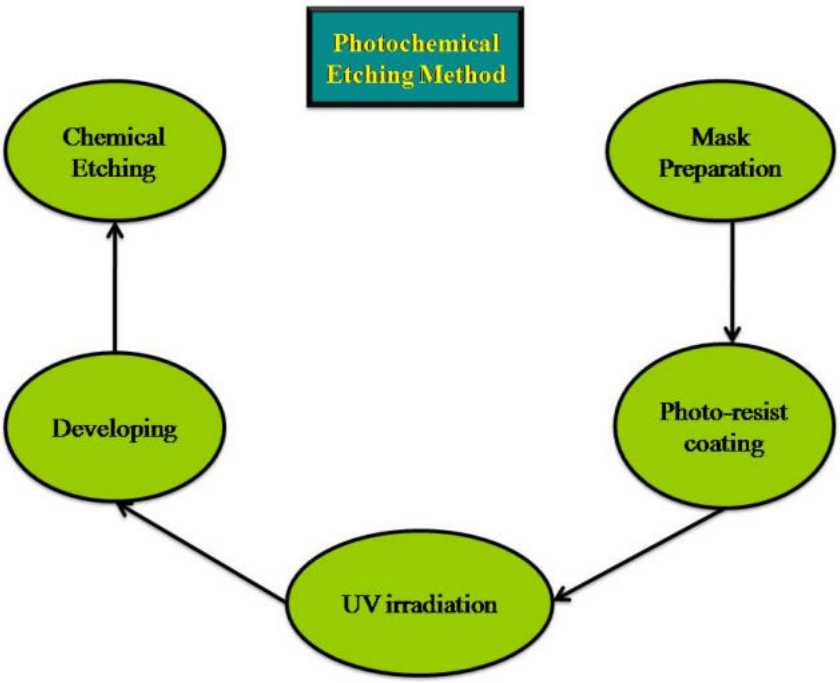

Figure 3.1: The flowchart showing the photolithographic chemical etching method used for the fabrication of flexible SRR.

In this method, the copper sheet after cleaning is fixed on a thin polymer film. It is then dipped in a photo-resist solution and is exposed to ultraviolet rays with suitable mask after drying. The copper sheet is then treated with ferric chloride solution for chemically etching the unwanted portion. This method is little complex, tedious and time consuming. Fig. 3.1 shows a flowchart of the photolithographic etching method. A schematic representation of the entire process is also given in Fig. 3.2.

3.2.2 Direct printing method

Another novel technique introduced in this thesis for the fabrication of SRR pattern on the flexible film substrate is a modification of the photochemical method. In

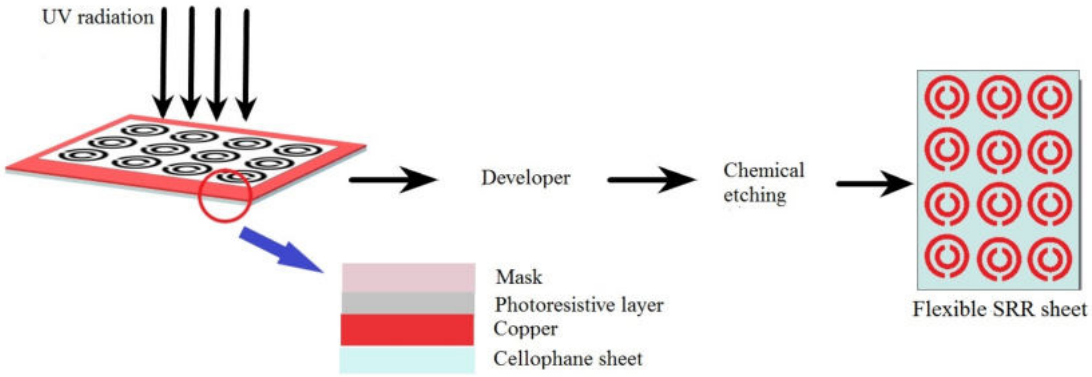

Figure 3.2: Schematic diagram showing the different steps of photolithographic chemical etching method for the fabrication of flexible SRR.

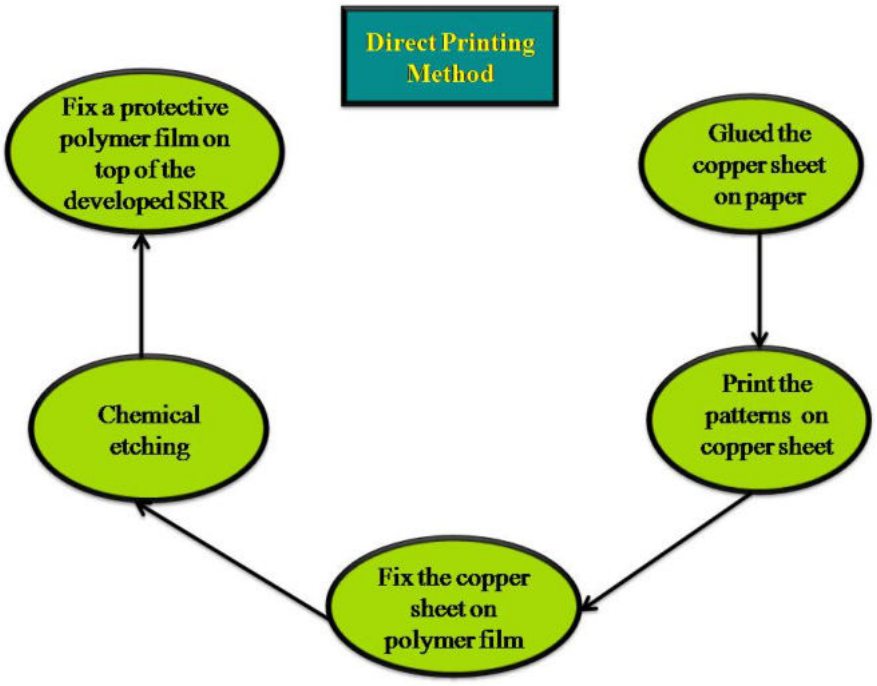

Figure 3.3: The chart showing direct printing method used for the fabrication of flexible SRR.

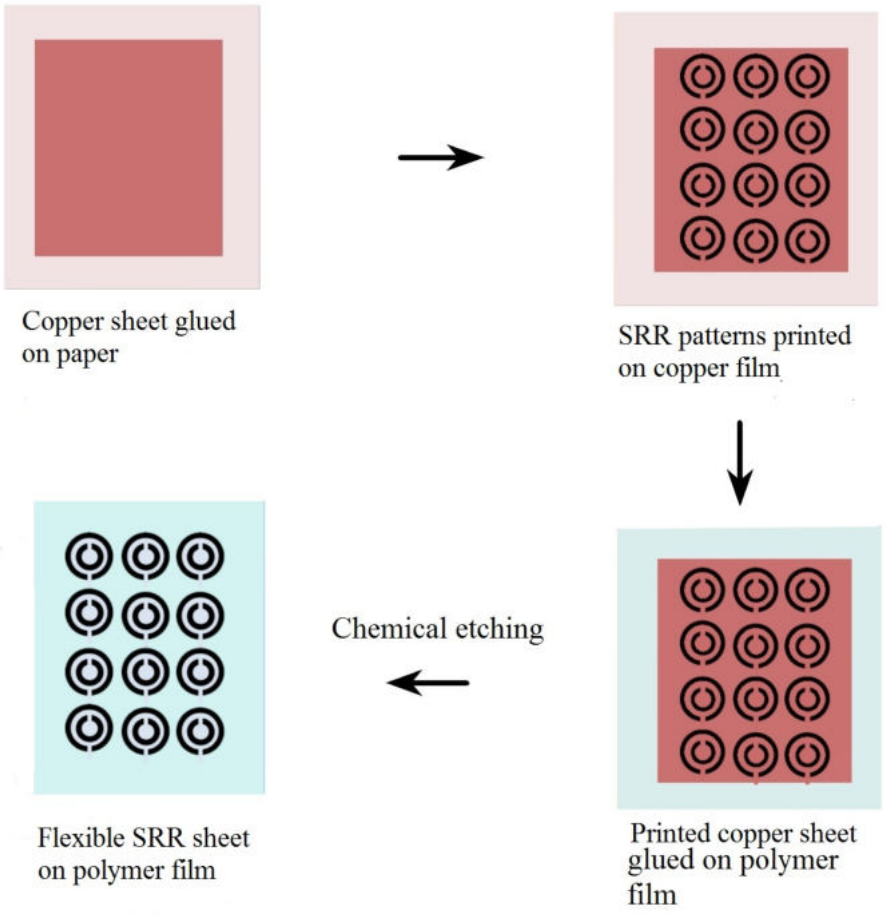

Figure 3.4: Schematic diagram showing different steps of the direct printing method.

this method no photomasking or UV irradiation is required. The desired patterns are printed on the copper film directly using a printer and is then subjected to chemical etching. This method seems to be easier and also simpler than the conventional photochemial method. The flowchart and schematic diagram of the direct printing method is shown in Fig. 3.3 and Fig. 3.4.

3.3 SRRs, Substrates and Methods used

Various types of structures used for the study are detailed in this section. Different substrates used for analyzing the resonance effect on permittivity of the near field environment of the SRR is also presented. The simulation technique used for the study is also mentioned.

3.3.1 Experimental studies

The resonance characteristics of the flexible SRR is analyzed with respect to the structural and dielectric parameters. Flexible SRRs of different structural parameters (inner radius, split width, gap distance and metallic width) are fabricated for this purpose. For comparison purposes SRRs are also fabricated on flame retardant PCB laminates. A photograph of certain SRR structures used for the study is given in Fig. 3.5.

For measuring the magnetic resonance of SRR experimentally the free space method explained in chapter 2 section 2.5 is used. For single SRR, the measurement method using transmitting and receiving probes is employed. In the case of bulk samples, free space method using wide band antennas is used. In order to study the effect of dielectric constant on the resonant frequency in the near field environment of the SRR, substrates of thin polymethylmethacrylate (PMMA) and wax sheets are used.

PMMA is a vinyl polymer made by free radical polymerization from the monomer methyl methacrylate (MMA). It is a substituent of glass with a hard and silky finish. This transparent thermoplastic has good weather resistance, less cost and easiness to handle and process. The fabrication of PMMA films from MMA is simple. MMA solution is mixed with benzoylperoxide and is stirred for atleast one hour. It is then

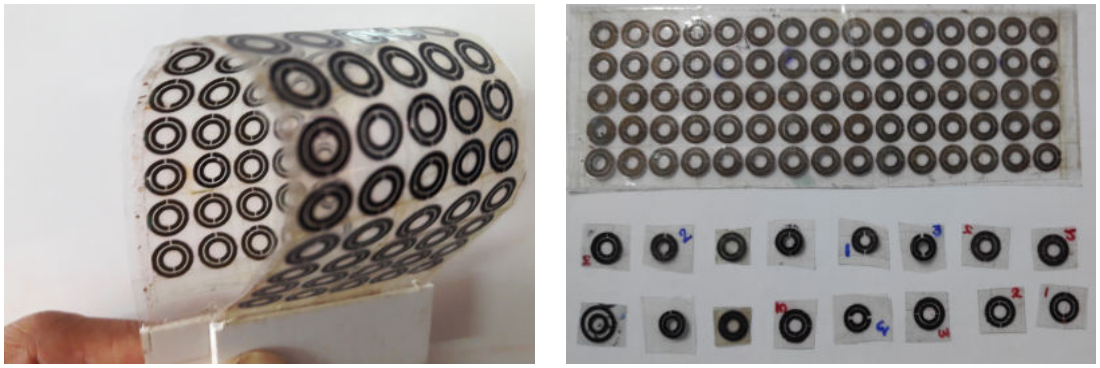

(a) (b)

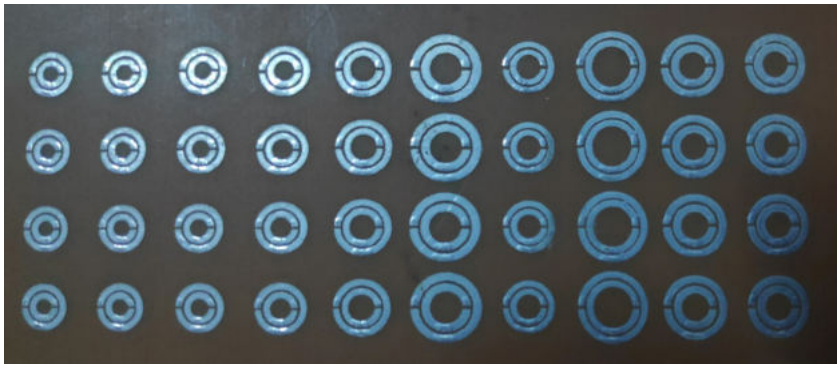

(c)

Figure 3.5: Photograph of different SRR structures used for the study (a) flexible SRR on a polymer film, (b) flexible SRR with different dimensions, (c) SRR with different dimensions fabricated on PCB.

kept in molds of different thicknesses and set for 30 minutes for drying. The molded PMMA films of different thicknesses are then cut into square shapes using a crystal cutter and the film is polished. Screw gauge is used to measure the thickness of the film. Wax is a soft colorless saturated hydrocarbon derived from petroleum or coal. Molten wax is kept in the mold, of required thickness and is allowed to solidify. It is then cut into square shape and polished.

3.3.2 Simulation studies

High Frequency Structure Simulator (HFSS) is one of the commonly used three dimensional electromagnetic simulator from Ansys. It uses the finite element method as a computational technique for designing various types of structures, electronic circuit elements, antennas etc. In this simulator the simulation domain with the structure is divided into small meshes in the form of tetrahedral shape and then Maxwell equations are evaluated inside it. In the present study, the simulation studies of the proposed structures are also carried out and the results are compared with the experimental values.

3.4 Resonant Characteristics Study of Flexible SRR

The resonant characteristics of a single SRR is studied using free space measurement method. The unit cell is placed between two monopole antennas which is connected to VNA. A photograph of the experimental setup showing a schematic of the probe-SRR arrangement is given in Fig. 3.6. The resonance graph obtained for a typical flexible SRR unit and its phase plot is shown in Fig. 3.7 and Fig. 3.8. The structural dimension of the SRR used for investigating the resonant characteristics are inner radius $r = 1.6$ mm, gap distance between rings $s = 0.2$ mm, metal width $w = 0.9$ mm and slit width $d = 0.2$ mm. The resonance frequency obtained is around 4.8 GHz.

The resonant properties of SRR fabricated on PCB ($\epsilon_r = 4.4$) having the same dimensions, is also measured for comparison study. The absorption graph and phase plot obtained is given in Fig. 3.9. In this case the resonant frequency observed is around 4.4 GHz. The decrease in resonant frequency is due to the presence of the dielectric substrate material. When the dielectric constant of the substrate increases, resonant

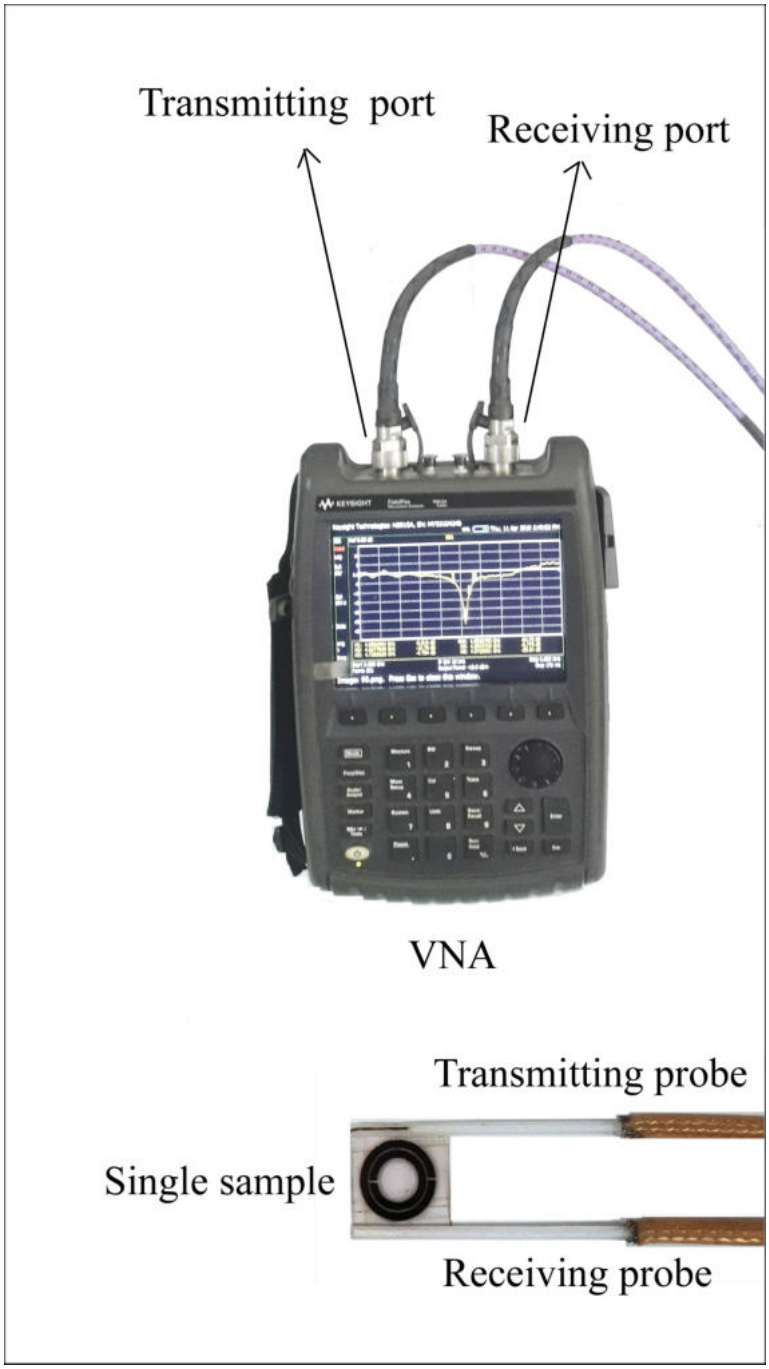

Figure 3.6: Schematic representation of probe-SRR experimental setup.

frequency decreases due to the increase in capacitive contribution of the resonance.

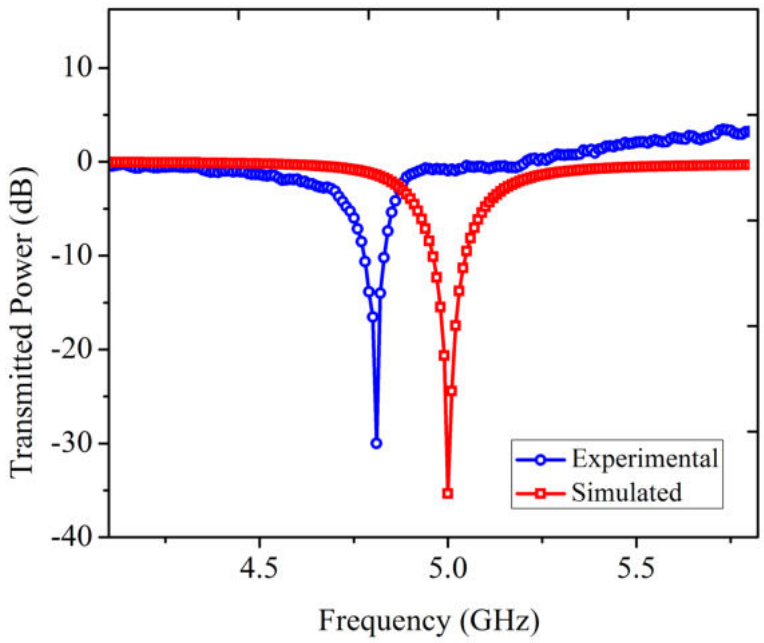

Figure 3.7: Magnetic resonance curves obtained for flexible SRR units with structural dimensions inner radius r = 1.6 mm, gap distance s = 0.2 mm, metal width w = 0.9 mm and slit width d = 0.2 mm.

Another important point worth mentioning is regarding the resonance dip. The flexible SRR fabricated on the thin inert substrate shows high absorption of microwave power around -35 dB as is evident from Fig. 3.7. It is about 10 to 15 dB higher than that corresponding to the SRR fabricated on the PCB (Fig. 3.9) . The decrease in power for the case with PCB substrate is due to the finite (non-zero) conductivity of the material and also may be due to some scattering effects.

In order to analyze the resonance behaviour of bulk sample, sheets of 2-dimensional SRR arrays fabricated with lattice spacing 10 mm is arranged as shown in Fig. 3.10 (a). The SRR sheets are fixed on rectangular foamex ($\epsilon_r = 1.6$) frame as depicted. The spacing between sheets is 10 mm. SRR arrays fabricated on FR4 PCB laminates with the same spacing are also arranged in bulk form to compare the resonance character-

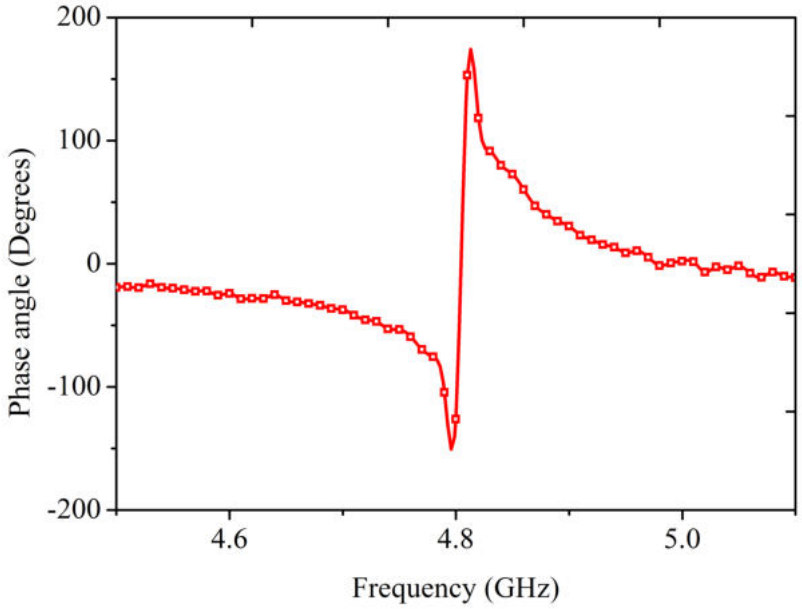

Figure 3.8: The phase plot of flexible SRR units with structural dimensions inner radius r = 1.6 mm, gap distance s = 0.2 mm, metal width w = 0.9 mm and slit width d = 0.2 mm.

istics (Fig. 3.10 (b)). The schematic representation of the SRR array within the bulk form showing different layers is given in the inset of Fig. 3.10. The magnetic resonance graphs obtained for both bulk samples are given in Fig. 3.11 (a) and (b) respectively. In this case also the high Q-value of the flexible sample is quite evident.

3.5 Effect of Substrate Permittivity on the Resonant Frequency of Flexible SRR Structure

The two important near field permittivity related parameters of the SRR that affect its resonant frequency are the dielectric constant and thickness of the substrate. When these two factors change, the capacitance also changes and the corresponding resonant frequency varies. In this study the effect of thickness and permittivity of the substrate on the resonant frequency of the SRR are analyzed experimentally with the

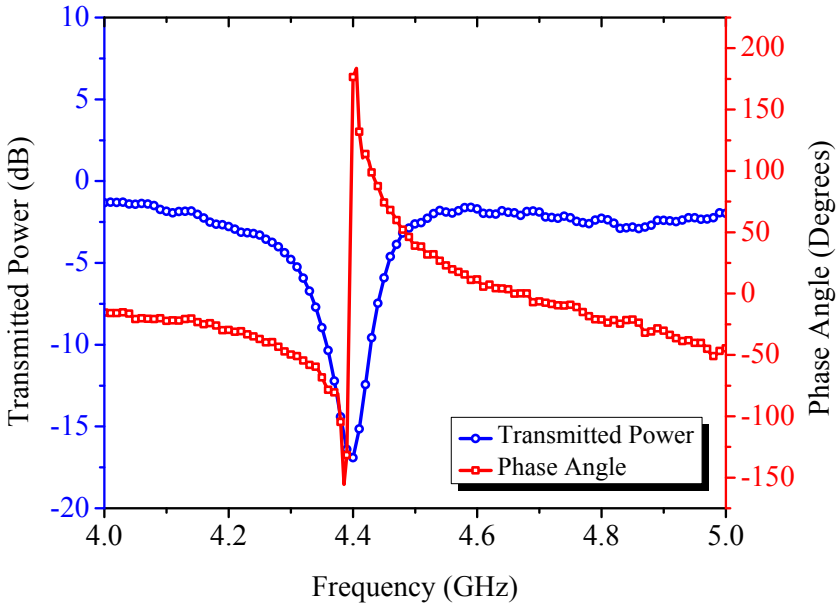

Figure 3.9: Resonance absorption and phase plots of SRR fabricated on PCB of thickness 1.8 mm (ϵ_r = 4.4) with structural dimensions inner radius r = 1.6 mm, gap distance s = 0.2 mm, metal width w = 0.9 mm and slit width d = 0.2 mm.

help of the new SRR structure fabricated.

Some researchers numerically addressed this problem and analyzed the effect of substrate permittivity on resonance frequency. A numerical study of the effect of substrate on the resonant frequency of particular SRR with two different thicknesses is performed by Zhongyan et al. [128]. E. Ekmeckci et al. investigated the absorption characteristics of double sided SRR, BCSRR and conventional SRR for different substrate parameters [129, 127, 215]. Since the resonant frequency of the SRR, given by equation

$$f = \frac{1}{2\pi\sqrt{LC}} \tag{3.1}$$

is inversely related to the square root of its capacitance C, any increase in capacitance produces a corresponding decrease in resonance frequency. If the entire near field region of the SRR is filled with any dielectric, the increase in capacitance will be of ϵ_r times.

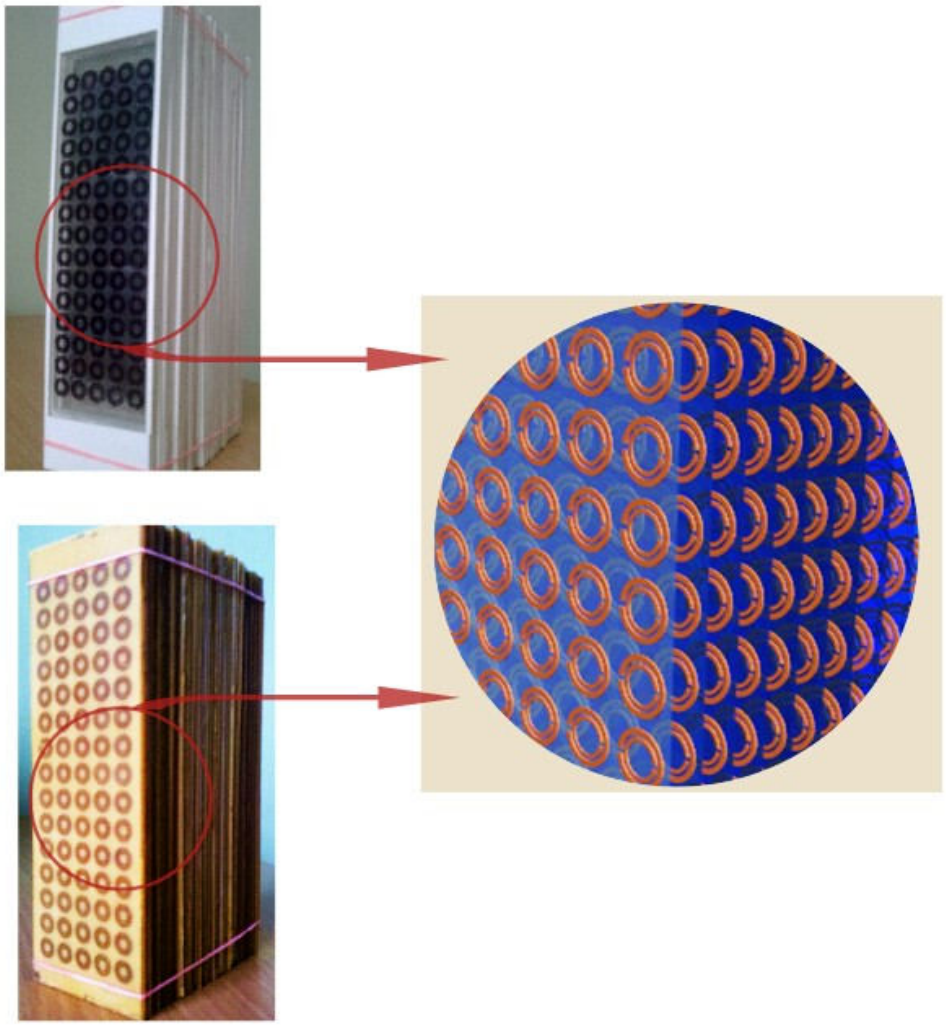

Figure 3.10: Photograph of the bulk samples of (a) flexible SRR and (b) SRR on PCB. Inset : SRR arrays within the bulk sample.

For thin substrate, the capacitance change is partial since in such cases the equivalent circuit behaves as a partially filled capacitor. For a particular substrate as its thickness

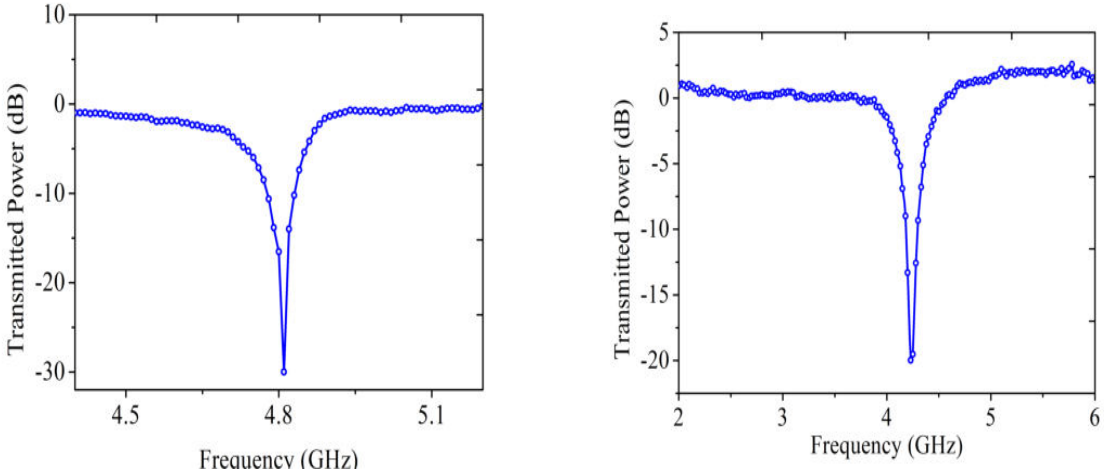

Figure 3.11: Experimental absorption plots of bulk sample of (a) flexible SRR and (b) SRR fabricated on PCB.

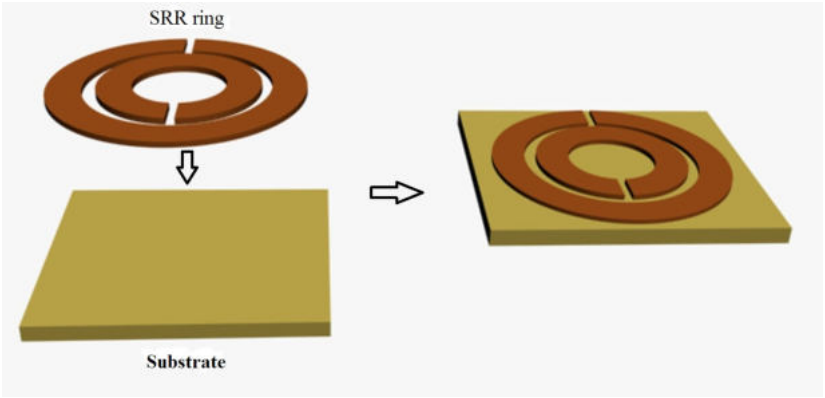

Figure 3.12: Construction of SRR test probe for studying the effect of substrate dielectric constant on resonant frequency.

increases, the filling space also increases resulting in maximum capacitive contribution leading to the lowering of resonance frequency to minimum values. To perform this experiment, two dielectrics, wax and PMMA are selected as substrates and flexible SRR units of geometrical parameters having inner radius $r = 3$ mm, metal width $w = 1.25$ mm, gap between rings $s = 0.5$ mm and slit width $d = 0.3$ mm are fixed on them

as depicted in Fig. 3.12 and resonance frequencies are taken. A photograph of PMMA and wax sample used for the study is given in Fig. 3.13.

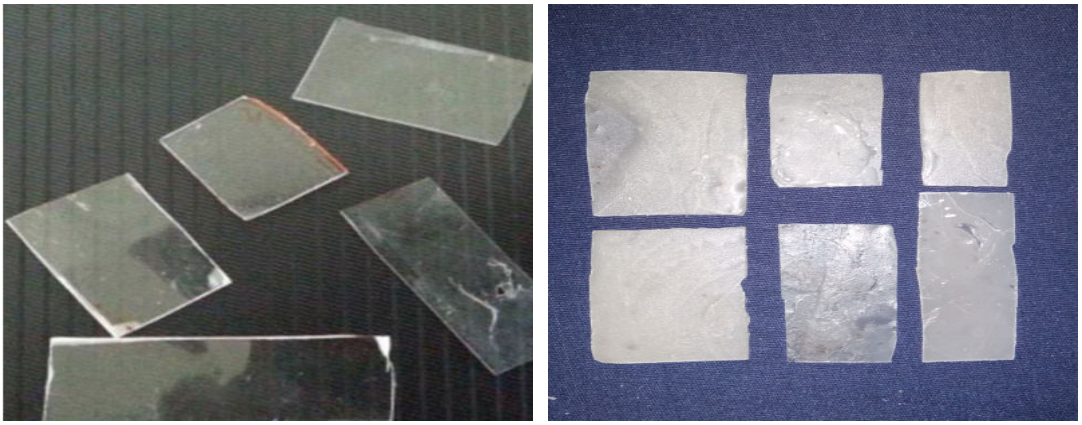

(a) (b)

Figure 3.13: Photograph of (a) PMMA and (b) Wax samples used for study.

3.5.1 PMMA and wax substrates

Three PMMA samples of thickness t equal to 0.15 mm, 0.24 mm and 0.29 mm are used for the study. Using the PMMA substrate of 0.15 mm thickness, the resonant frequency observed is 6.37 GHz . By increasing the thickness to 0.24 mm and 0.29 mm, the resonant frequency shifts to lower regions to 6.32 GHz and 6.23 GHz respectively. The resonance graphs obtained are plotted as Fig. 3.14. In the case of wax samples, the three different thicknesses 0.68 mm, 0.91 mm and 1.07 mm are used. The observed resonant frequencies are 6.41 GHz, 6.39 GHz and 6.35 GHz as shown in Fig. 3.15. The investigation shows that the increase in dielectric constant or thickness of substrate will reduce the resonant frequency to lower value. It shows that the tuning of resonant frequency of SRR to any desired value is possible by means of substrates of different permittivity or thicknesses. Thus the new SRR structure because of its special design allows frequency tunability also.

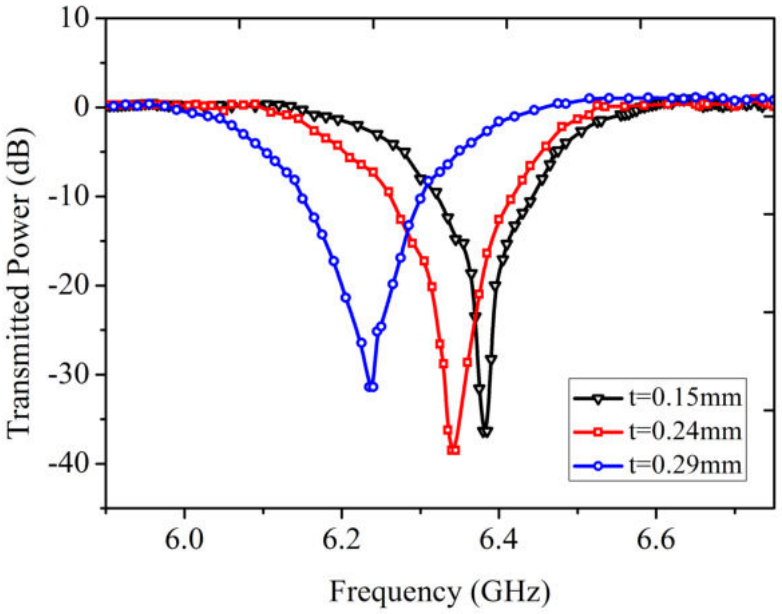

Figure 3.14: Resonant frequency variation of SRR with PMMA substrates of different thicknesses.

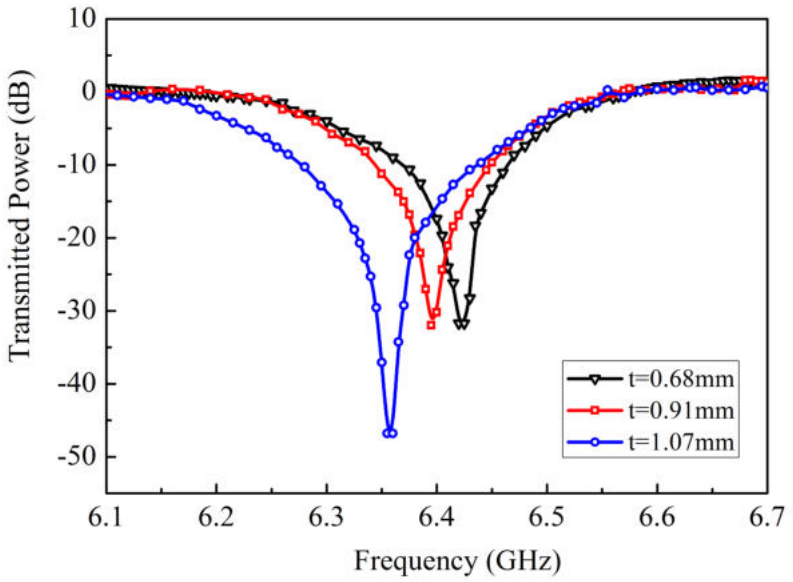

Figure 3.15: Resonant Frequency variation of SRR with wax substrates of different thicknesses, t.

3.6 Effect of Structural Parameters on the Resonant Frequency of Flexible SRR Structures

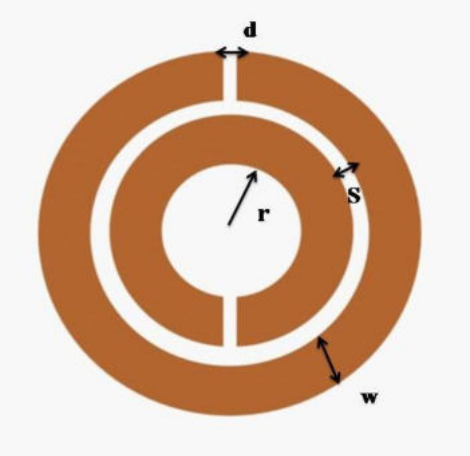

Figure 3.16: Schematic diagram of SRR with structural parameters.

The effect of structural parameter variation on the magnetic resonance frequency of the flexible SRR meta molecule is carried out in this section. The four structural parameters of interest are inner radius r, width of metalisation w, gap distance between the rings s and split width d. SRRs are fabricated using copper sheet of thickness 20 μm and are fixed on flexible polymer film of thickness 18 μm. A schematic diagram of the SRR showing the structural parameters is shown in Fig. 3.16. The experimental setup in which the SRR arranged between transmitting and receiving probe antennas is used for taking the transmission spectra. In order to compare the geometry related resonance effects of the flexible SRR with that fabricated on rigid substrate ($\epsilon_r = 4.4$), SRRs of the same dimensions are fabricated on PCB also.

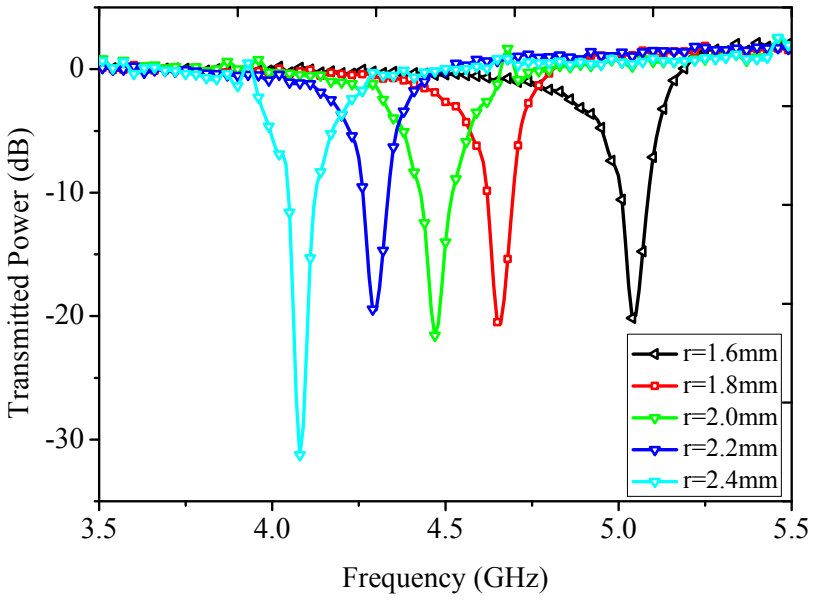

Figure 3.17: Experimental transmission curves of the flexible SRR for different inner radius r.

3.6.1 Effect of variation of inner radius on resonant frequency

To study the effect of variation of inner radius r on resonant frequency, five SRR unit cells of varying inner radius from 1.6 mm to 2.4 mm for a 0.2 mm separation are fabricated keeping all other parameters constant and their resonance curves are plotted. The result shows that for an increase of inner radius, the resonant frequency of SRR decreases. It is due to the following reason. As the inner radius increases keeping metal width, spacing between rings and split width constant, the size of ring and hence area of the rings increases. This causes the total effective capacitance of the structure to increase, which produces a corresponding reduction in resonant frequency. The resonance curves obtained for different inner radii are plotted in Fig. 3.17.

The results obtained by experiment are also verified by simulation . The resonance graphs obtained by simulation are given in Fig. 3.18. A graph is plotted between inner

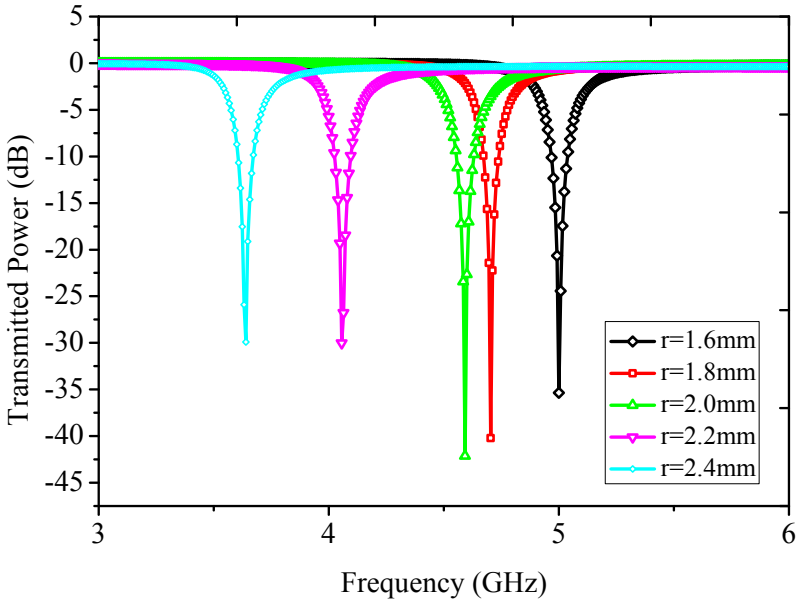

Figure 3.18: Simulated transmission curves of flexible SRR for different values of inner radius r.

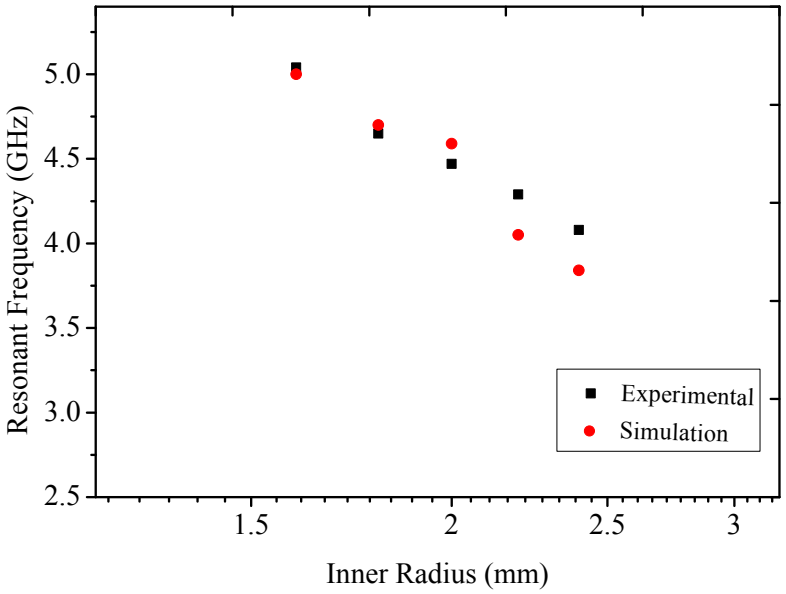

Figure 3.19: Experimental and simulated values of resonance frequency for the flexible SRR for different values of inner radius r.

radius and resonant frequency by taking values from experiment and simulation and is shown in Fig. 3.19. Experimental resonance graphs and simulation graphs are studied for SRRs fabricated on PCB also. The results are tabulated in Table 3.1. The resonant frequency decrease obtained for flexible SRR will increase with inner radius and is found to be similar to that of the conventional SRR fabricated on PCB ($\epsilon_r = 4.4$). But the result shows large variation in resonant frequency with the conventional one. Here it varies from 4.2 GHz to 3.1 GHz. The resonant frequencies are shifted to lower regions more than that for flexible SRR and which is due to the effect of dielectric substrate.

Table 3.1: Resonance frequency variation with inner radius for SRR with PCB substrate.

Structural Parameters (mm)			Resonance frequency (GHz)	
r	*w*	*s*	Experimental	Simulation
1.6	0.9	0.2	4.2	4.08
1.8	0.9	0.2	4.0	3.0
2.0	0.9	0.2	3.9	2.28
2.2	0.9	0.2	3.2	2.26
2.4	0.9	0.2	3.1	2.19

3.6.2 Effect of variation of metal width on resonant frequency

For investigating the effect of metal width w on resonant frequency of flexible SRR, five samples with different metal widths ranging from 0.9 mm to 1.7 mm are fabricated. Increasing the metal width of the rings by 0.2 mm by keeping the inner radius, gap distance and split width constant, the resonant frequency is found to shifted to lower frequency end as that of the previous case. Increase in metal width directly enhances the area of the SRR capacitor, which in turn increases the effective capacitance and hence a decrease in resonant frequency.

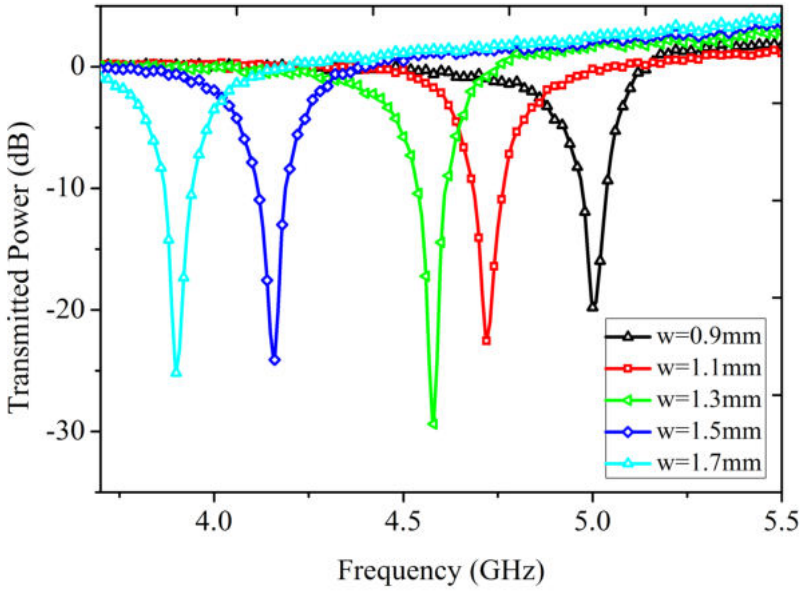

Figure 3.20: Experimental transmission curves of the flexible SRR for different values of metal width w.

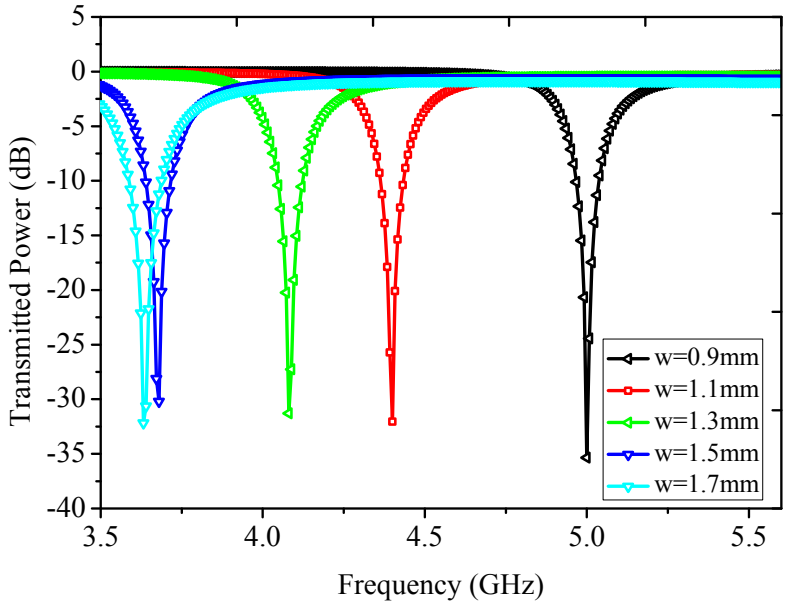

Figure 3.21: Simulated transmission curves of flexible SRR for different values of metal width w.

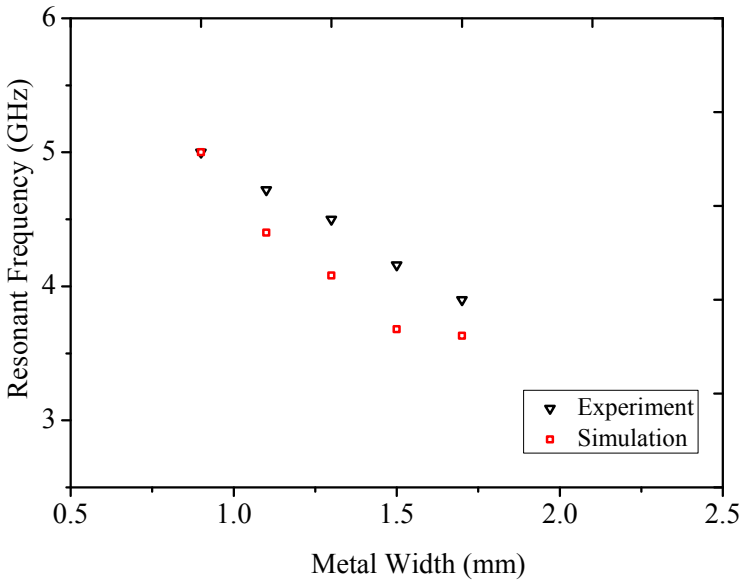

Figure 3.22: Experimental and simulated values of resonance frequency for the flexible SRR for different values of metal width w.

Table 3.2: Resonant frequency variation with metal width w for SRR with PCB substrate.

Structural Parameters (mm)			Resonance frequency (GHz)	
r	*w*	*s*	Experimental	Simulation
1.6	0.9	0.2	4.2	4.08
1.6	1.1	0.2	3.8	3.65
1.6	1.3	0.2	3.55	3.01
1.6	1.5	0.2	3.34	2.85
1.6	1.7	0.2	3.24	2.77

Fig. 3.20 depicts the variations of resonant frequency with metal width. The shift obtained is from 5 GHz to 3.7 GHz. The simulated results are also taken and is shown in Fig. 3.21. A graph showing the resonant frequency shift with metal width obtained for both experiment and simulation is given in Fig. 3.22. The metal width variation of SRR with PCB substrate is also measured and the corresponding resonant frequency is shown in Table 3.2, which shows the same behaviour as that for the flexible case.

3.6.3 Effect of variation of gap distance on resonant frequency

For studying the effect of gap distance on resonant frequency, five different structures with gap distance from 0.2 mm to 1 mm are fabricated. The transmission spectra obtained for gap variations is shown in Fig. 3.23. In this case also, a decrease in gap distance between the rings of the SRR causes the capacitance to increase. It is equivalent to a reduction in spacing between the plates of the SRR capacitor.

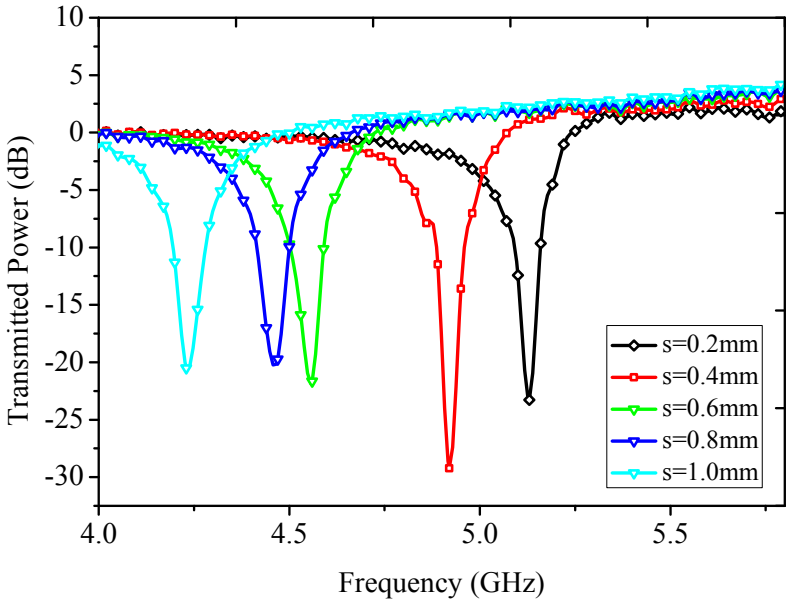

Figure 3.23: Experimental transmission curves of the flexible SRR for different values of distance between rings s.

The resonance variation of SRR fabricated on PCB for different gap distances is shown in Table 3.3. The result shows same nature as that for flexible SRR fabricated without substrate, but with lower value.

Table 3.3: Resonant frequency variation with gap distance s for SRR with PCB substrate.

Structural Parameters (mm)			Resonance frequency (GHz)	
r	w	s	Experimental	Simulation
1.6	0.9	0.2	4.2	4.08
1.6	0.9	0.4	3.85	4.07
1.6	0.9	0.6	3.78	4.04
1.6	0.9	0.8	3.6	3.93
1.6	0.9	1.0	3.57	3.86

3.6.4 Effect of variation of split width of SRR on resonant frequency

Different structures with varying split width d from 0.2 mm to 1 mm are fabricated for this study. The split width in the SRR acts like parallel plate capacitor and in-

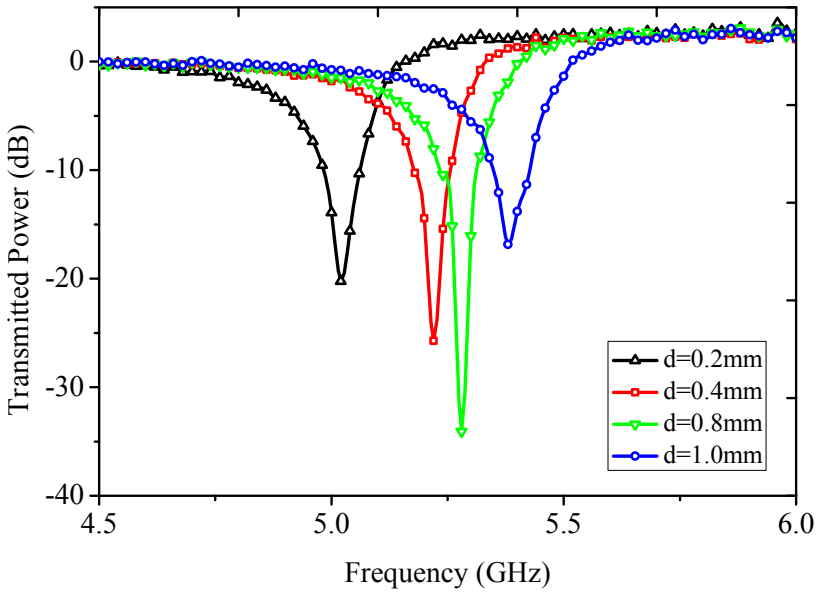

Figure 3.24: Experimental transmission curves of the flexible SRR for different values of slit width d.

creasing the split width decreases the capacitance, and correspondingly the resonance frequency increases. Since the capacitive contribution to the total capacitance of the SRR by split capacitance is small compared to that of the gap capacitance, the variation in resonance frequency is not much appreciable here. The graph given in Fig. 3.24 shows the variation of resonant frequency with slit width. The slit width variation of SRR with substrate is also measured and is tabulated in Table 3.4. It also shows the same result with values lower than that of flexible SRR.

Table 3.4: Resonant frequency variation with slit width d for SRR with PCB substrate.

Structural Parameters (mm)			Resonance frequency (GHz)
r	w	d	Experimental
1.6	0.9	0.2	4.01
1.6	0.9	0.4	4.44
1.6	0.9	0.6	4.51
1.6	0.9	0.8	4.58
1.6	0.9	1.0	4.6

3.7 Conclusion

From the resonance property study of flexible SRR the following conclusions may be derived. Conventional SRRs are made on rigid circuit board laminates and hence along with the limitations of rigid nature, possibilitiy of the presence of loss factors causing low Q-resonance cannot be ruled out. Since this proposed novel SRR is fabricated on a negligibly thin loss less polymer film substrate, very good absorption of microwave power corresponding to the resonance frequency is expected and also the dielectric induced losses may be avoided.

Another important highlight of this metamaterial resonator is regrading its flexibility. This is the first work of this kind reported. Since metamaterials have lot of

potential applications in fields like cloaking and frequency selective surfaces, flexibility is a much important factor. Any object can be effectively covered by the novel flexible metamaterial structure for cloaking or frequency selective applications.

Being void of any rigid substrate, the structure here got wide possibility of tunability in respect of geometrical parameters or dielectric parameters. So by the proper choice of structural parameters and substrate permittivity the resonance can be tuned to a large extend. So this low loss structure having possibilities for flexibility and tunability may find good number of applications in the field of negative index metamaterials and the advantages may be extended for the realization of negative index medium having added properties.

CHAPTER 4

Flexible Broadside Coupled Split Ring Resonator Metamaterial Structure

A modified version of flexible SRR called flexible broadside coupled SRR (BCSRR) structure is introduced in this chapter. Fabrication method and resonance tuning properties of the proposed structure are presented. Three methods for tuning the resonant frequency are described. The two methods adopted for tuning the resonant frequency of the flexible SRR structure, by changing its geometrical parameters and the dielectric substrates are possible in the present flexible BCSRR structure also. Moreover a third method, by changing the spacing between the rings of the BCSRR, is introduced for resonant frequency tuning. An important application of this proposed BCSRR structure as a wide band absorber is also presented.

4.1 Introduction

Out of the varieties of split ring resonators, BCSRR possesses some specific properties. Researchers are focusing on BCSRR because of its isotropic nature and small electrical size. Apart from having a 2-D planar structure possessed by most members of the SRR family, BCSRR takes a 3-D solid like structure. As discussed in Chapter 2-Section 2.2, it is usually fabricated using double sided PCB-like laminates. The flexible BCSRR proposed in this thesis is prepared in a slightly different way so as to have a possibility to change the substrate material and also its thickness. This introduces attractive features to the structure in relation to its resonance frequency tuning methods. In view of the wide band tunability achieved by virtue of its special fabrication technique, the possibility of the design of a wide band frequency selective surface is also presented.

4.2 Fabrication of Flexible BCSRR Metamaterial Structure

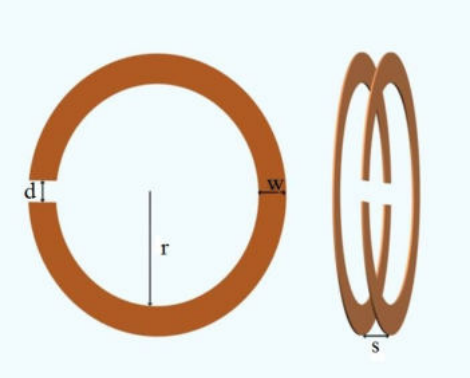

Figure 4.1: Schematic diagram of the BCSRR with structural parameters.

As discussed earlier, conventional BCSRRs are fabricated using laminates like double sided printed circuit boards. Usually photolithographic etching method or computer aided milling method is used for its fabrication. Along with the ring radius and ring

width, the thickness and permittivity of the substrate strongly affect its resonance behaviour. The parallel plate approximation for evaluating intrinsic capacitance of the BCSRR resonator is quite valid for this structure. So the effect of thickness and permittivity on the resonant frequency will be much higher for this structure in comparison to other commonly used SRR structures. The new design of the flexible SRR proposed in chapter 3 of this thesis provides novel methods for achieving wide band frequency tunability by enabling the BCSRR to change the spacing and the dielectric between the rings of the structure.

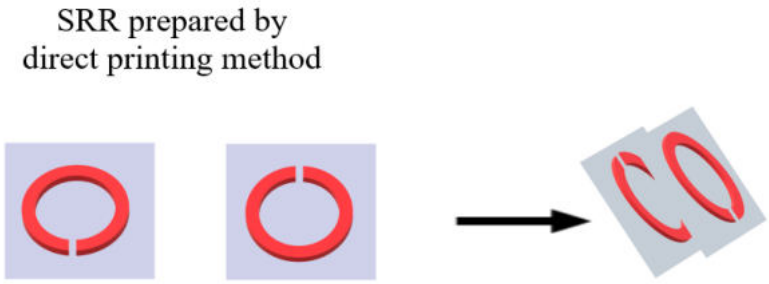

Figure 4.2: Schematic representation of making of the BCSRR on transparent film.

For the fabrication of the new flexible BCSRR, photolithographic or direct printing method introduced for flexible SRR is used. The two rings of the BCSRR are separately etched on two thin polymer flexible sheets of micrometer thickness using copper foil of thickness 20 μm. The rings are then arranged co-axially with the splits of the rings in opposite ends as shown in Fig. 4.1 to form the BCSRR. The structural parameters are also shown in figure. Flexible or rigid substrates may be used to keep the spacing between the rings as required. For flexibility related applications, the space between the rings may be filled with cotton, sponge, tissue paper or even air filled polymer bags. The second way to keep the spacing fixed is by using some rigid substrates like glass, perspex, mica and wood of required thickness and permittivity. A schematic diagram

of the process of making flexible BCSRR is given in Fig. 4.2. A photograph showing BCSRR structures with flexible polymer and paper substrates are given in Fig. 4.3.

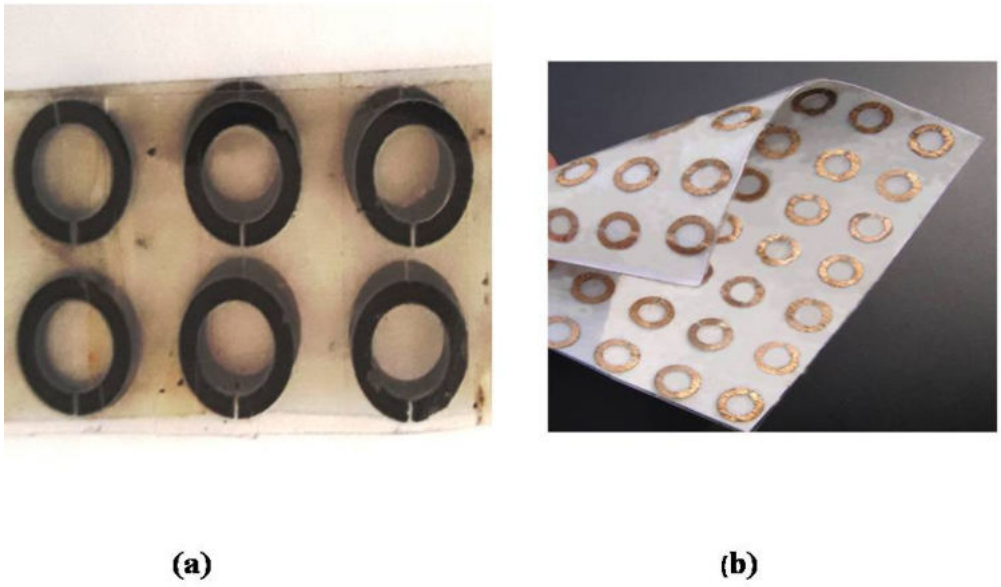

Figure 4.3: Photographs of flexible BCSRR structures fabricated with (a) polymer substrate and (b) paper substrate.

4.3 Resonance Characteristics Study of the Flexible BCSRR

In order to study the transmission spectra (S_{21}) of the BCSRR structure, free space method discussed in chapter 2 section 2.5 is used. For single BCSRR, the method consisting of transmitting and receiving probes connected to the VNA is used. A schematic design of the BCSRR-probe setup is given in Fig. 4.4. The structural parameters that mainly affect the resonance frequency of the BCSRR are spacing between rings s, inner radius r, width of metallization w and permittivity of the dielectric substrate ϵ_r. Since the capacitive contribution between the ring is very high compared to that of split

capacitance for the BCSRR design, the effect of split width d on resonance frequency is very small. In the following section the effect of resonance frequency on the above mentioned four parameters are presented.

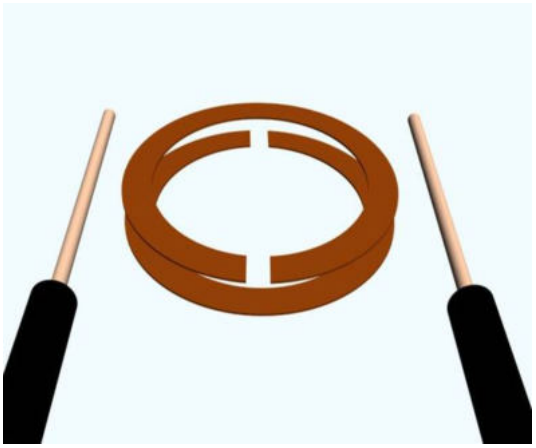

Figure 4.4: Schematic diagram showing the BCSRR unit cell between transmitting and receiving probes.

4.3.1 Effect of variation of substrate dielectric constant on the resonant frequency of flexible BCSRR

The dielectric constant and thickness of the substrate are two important factors that affect the resonant frequency of the BCSRR. As for the case of flexible SRR, the same substrate materials PMMA (perspex) and wax are used for this purpose. BCSRR with inner radius $r = 2$ mm and metal width $w = 0.4$ mm is used for the study. PMMA samples of thickness 0.1 mm, 0.15 mm, 0.24 mm and 0.29 mm are used as substrates. The rings fabricated on copper film are fixed on either sides of the substrate coaxially with the splits positioned diametrically at opposite ends to form a BCSRR unit and their resonance graphs are plotted. Fig. 4.5 represents the resonance graphs obtained for the PMMA samples. For the substrates with 0.1 mm thickness, the resonant frequency obtained is 3.97 GHz. When it is increased to 0.24 mm, the

resonant frequency also increases to 4.87 GHz, i.e. a change of 0.9 GHz is observed for a thickness change of 0.19 mm. A plot between the resonant frequency and thickness of the PMMA substrates of the BCSRR is depicted in Fig. 4.6.

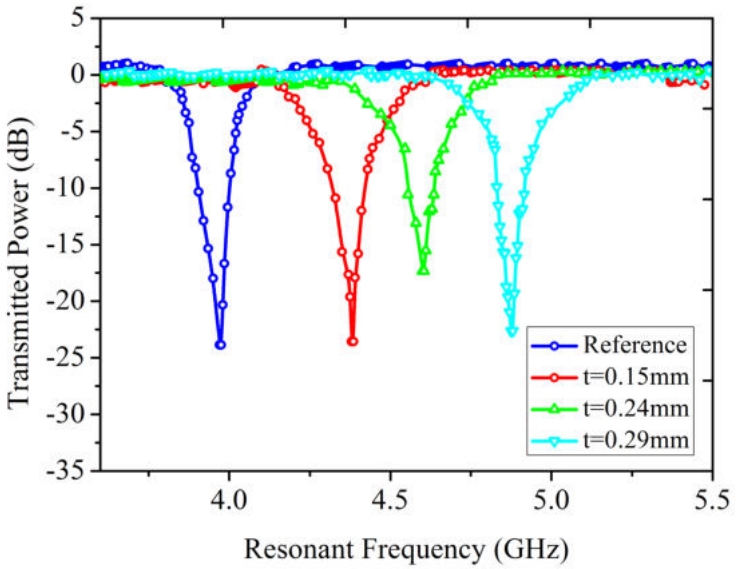

Figure 4.5: Experimental resonance curves obtained for the BCSRR with PMMA substrate of different thicknesses.

Wax samples used for the study are of thicknesses 0.68 mm, 0.91 mm and 1.07 mm. In this case also, results similar to that of PMMA are obtained. Since the dielectric constant of wax ($\epsilon_r = 2.2$) is less than that of the PMMA ($\epsilon_r = 2.5$), the resonance shift obtained for wax will be greater than that of PMMA. Experimental transmission curves obtained for the wax substrates of different thicknesses are given in Fig. 4.7. The resonant frequency versus thickness graph is given in Fig. 4.8.

4.3.2 Effect of changing the spacing between the rings

The two rings of BCSRR are fabricated separately and the spacing between them is varied for studying its effect on resonant frequency. Strips of tissue paper is used for

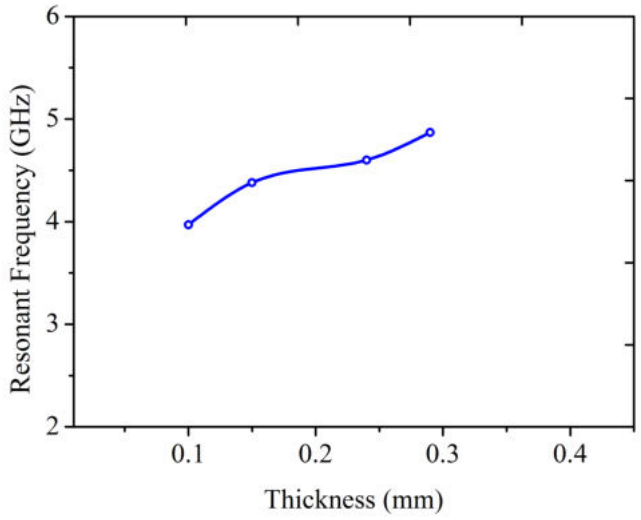

Figure 4.6: Variation of resonant frequency of the BCSRR with thickness of PMMA substrates.

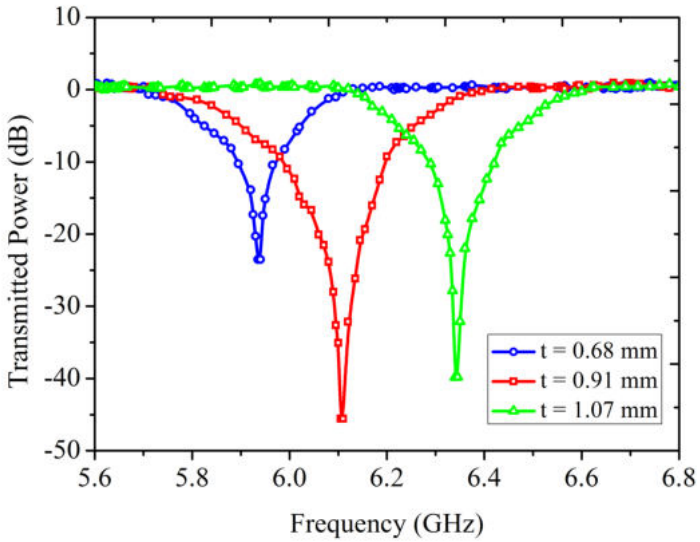

Figure 4.7: Experimental resonance curves obtained for the BCSRR with wax substrate of different thicknesses.

changing the spacing. The small dielectric constants of the tissue paper ($\epsilon_r = 1.35$) is neglected for the present study. The transmission spectra given in Fig. 4.9 shows the

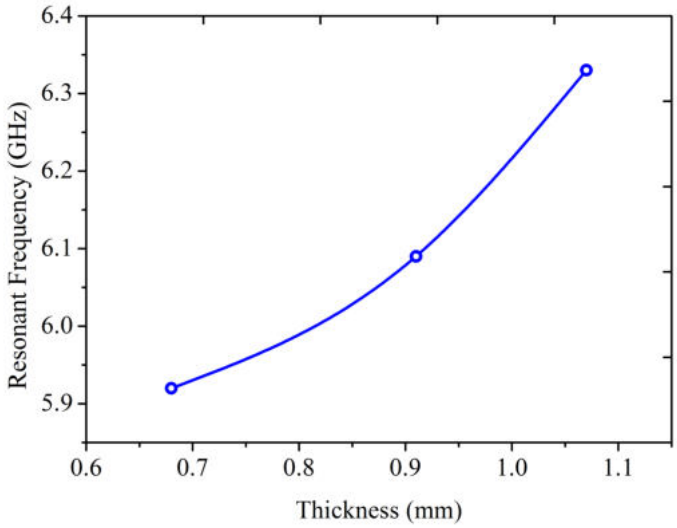

Figure 4.8: Variation of resonant frequency of the BCSRR with thickness of wax substrates.

variation of resonant frequency with respect to the spacing between rings. For a small change in spacing, a remarkable shift in the resonant frequency is obtained. The plane of the rings is arranged perpendicular to the excited magnetic field.

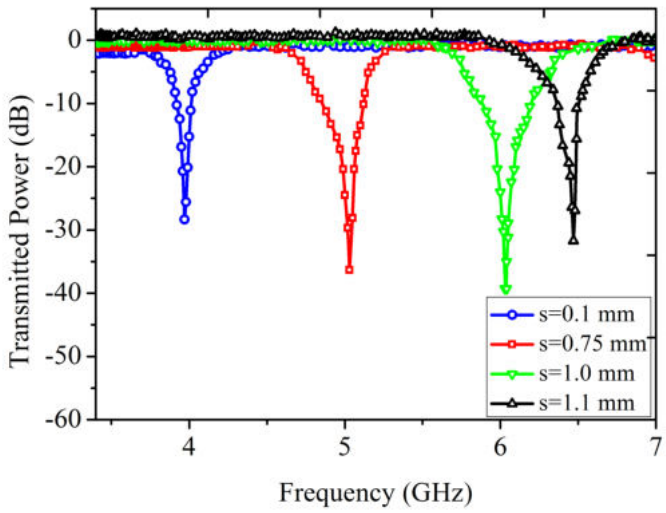

Figure 4.9: Experimental resonance curves obtained for different spacing of the BC-SRR.

When the spacing between rings is increased from 0.1 mm to 0.9 mm, the resonant frequency is observed to shift from 3.97 GHz to 5.03 GHz. For spacings of 1.0 mm and 1.1 mm, the resonant frequency obtained are 6.03 GHz and 6.47 GHz respectively. With increase in spacing between the rings, the effective capacitance between the rings of the BCSRR decreases and hence the resonant frequency increases.

The resonance graph shows that a frequency shift of 2.5 GHz is obtained for a spacing variation of 1 mm. A graph between the resonant frequency and spacing is given in Fig. 4.10. This remarkable shift observed predicts that the resonant frequency can be tuned to any desired wide frequency range by properly adjusting the spacing between the rings. It may find applications in wide bandwidth cloaking applications and frequency selective surfaces.

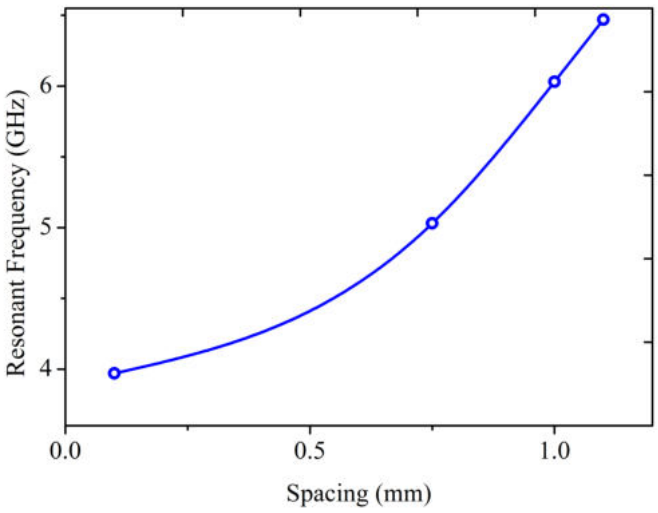

Figure 4.10: Variation of spacing between rings on resonant frequency of BCSRR.

4.3.3 Effect of variation of inner radius on resonant frequency

Similar to the case of flexible SRR detailed in Chapter 3, there is significant effect on the resonant frequency for the inner radius. In this case, the increase in radius causes

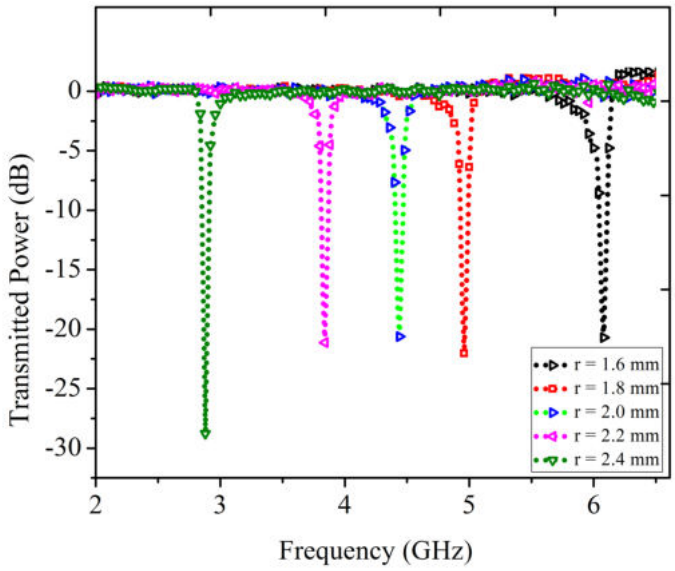

Figure 4.11: Experimental resonance curves obtained for the flexible BCSRR for different inner radius r.

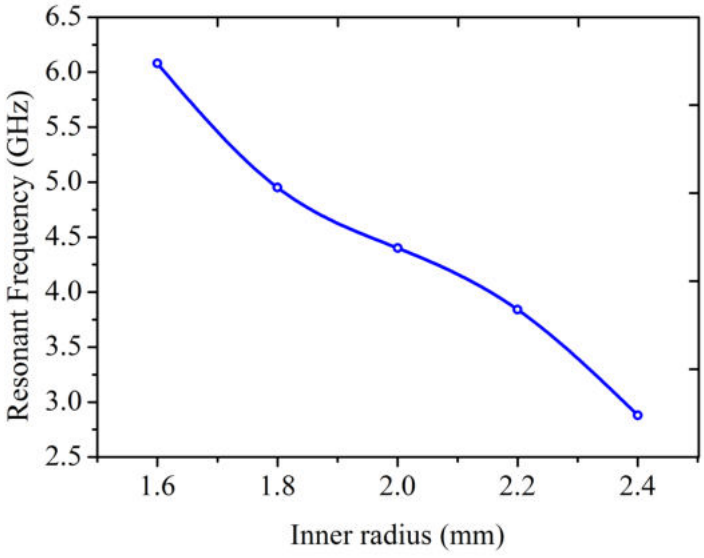

Figure 4.12: Variation of resonant frequency of the BCSRR with inner radius.

the area of the rings to increase which in turn increases the capacitance, and therefore it reduces the resonant frequency. For the purpose of analyzing this properties, BCSRR

with inner radius 1.6 mm, 1.8 mm, 2 mm, 2.2 mm and 2.4 mm are fabricated and studied. Fig. 4.11 gives the experimental resonance curves obtained for different inner radii of the BCSRR. The graph between resonance frequency and inner radius is given in Fig. 4.12.

4.3.4 Effect of variation in metal width on resonant frequency of flexible BCSRR

The other parameter that may have some effect on the resonant frequency of the BCSRR is metallic width w of the ring. As verified for the case of flexible SRR, in this case also, an increase of metal width directly increases the capacitance contribution of the BCSRR structure. So an increase in metal width reduces the resonant frequency as expected. The frequency tuning obtained in relation to this parameter is depicted in Fig: 4.13. Fig. 4.14 gives the graph between resonant frequency and metal width.

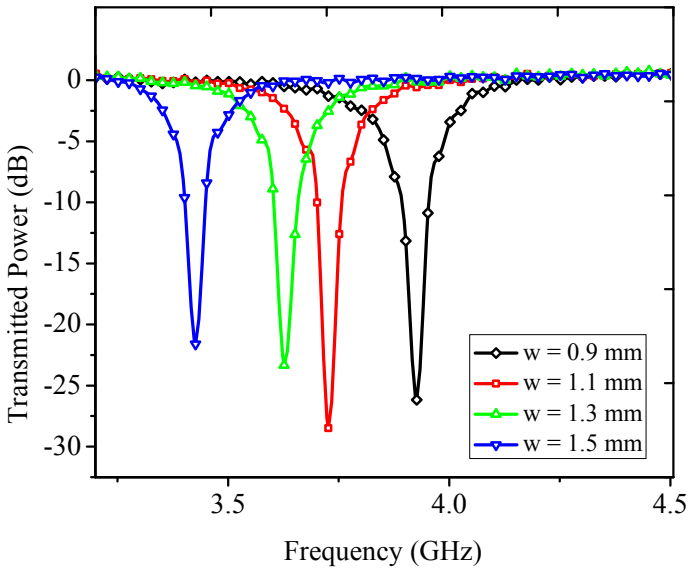

Figure 4.13: S_{21} characteristics vs frequency for BCSRR having different metal widths.

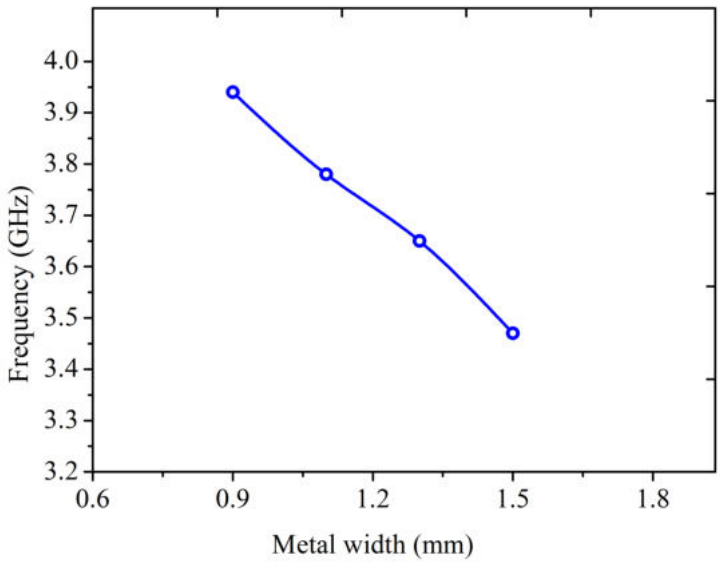

Figure 4.14: Variation of resonant frequency of BCSRR with metal width.

4.4 Application of the Flexible BCSRR as a Wide Band Microwave Absorber

One noteworthy result observed during the study of the resonant frequency dependence of the BCSRR on its structural parameters is regarding the wide frequency tunability obtained for the variation of spacing between the rings. By varying the spacing to few fractions of a millimeter using some lossless and flexible sheets like paper and cotton fabric, resonant frequency shifts upto 2 GHz or even a higher value can be achieved. It is observed that a shift of 3 GHz can be achieved by a spacing variation of 1 mm in certain cases. By making use of this principle a wide band frequency selective surface which may have potential applications in the field of metamaterial microwave absorber is materialized in this study.

In order to realize a wide band frequency selective microwave metamaterial absorber, flexible BCSRRs with three structural dimensions are fabricated. Each struc-

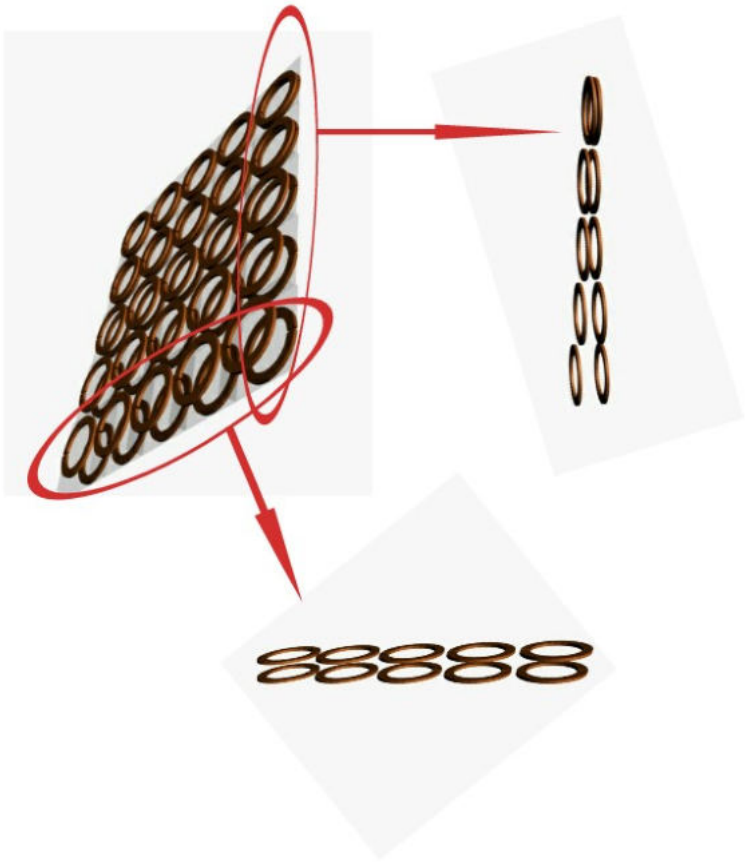

Figure 4.15: Schematic arrangement showing one layer of the wide band BCSRR within the bulk sample.

ture is arranged in a bulk form with $5 \times 5 \times 8$ units to have a specific but different wide band frequency tunability. In order to achieve this, the BCSRRs of each group are arranged with different spacings between the rings. Since the geometrical parameters are different for the three sets of selected BCSRRs, the resonance absorption bands also will be different. If three frequency bands adjacent to each other combine together to form a bulk medium, it will result in a wide band absorption with bandwidth equal to the sum of the three bandwidths.

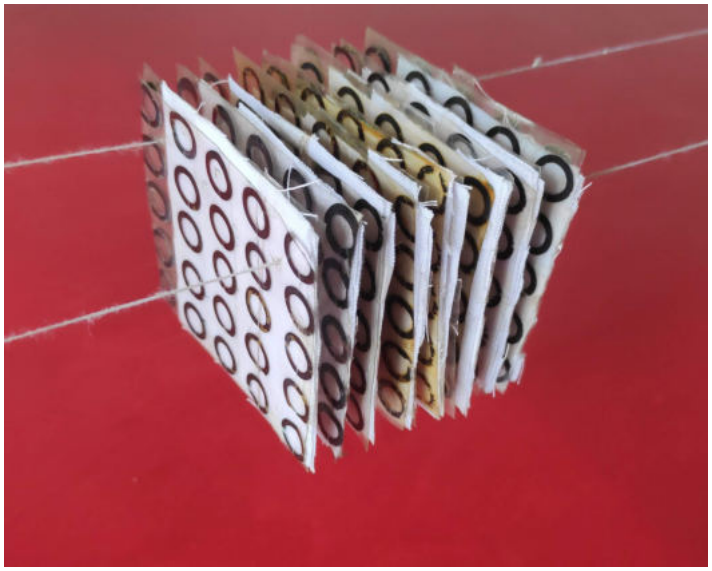

Figure 4.16: Photograph of a typical bulk sample of BCSRR medium used to study the wide band frequency selective property.

In this study BCSRR units with three different dimensions are fabricated and are arranged in planar form with lattice spacing 12 mm. It consists of five columns each having 5 BCSRR units with progressively increasing spacing from 0.1 mm to 0.5 mm using layers of cotton fabric as depicted in the schematic diagram Fig. 4.15 (cotton fabric pieces between the layers are avoided in the drawing for getting clarity). The three different sample sets are formed with 8 layers each. Fig. 4.16 is a photograph of one typical bulk sample of the BCSRR wideband medium. Resonance graphs obtained for BCSRRs of different spacing corresponding to one set is given in Fig. 4.17. Table 4.1 gives all the values obtained for the resonance frequency of the three sets together. The spacing variation of three different samples with their corresponding resonant frequency is plotted in Fig. 4.18.

The dimensions used for fabricating three different set samples are as follows. The inner radius $r = 5.4$ mm and metal width $w = 2.7$ mm for set 1; $r = 4.7$ mm and $w = 1.8$ mm for set 2; $r = 3.0$ mm and $w = 2.0$ mm for set 3. The results show that the

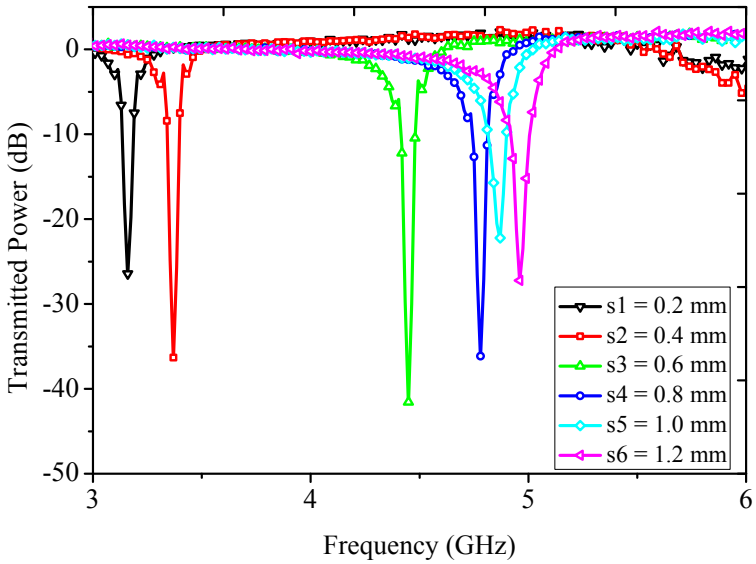

Figure 4.17: Resonance graphs of BCSRR samples having different spacing s with inner radius r = 5.4 mm and metal width w = 2.7 mm.

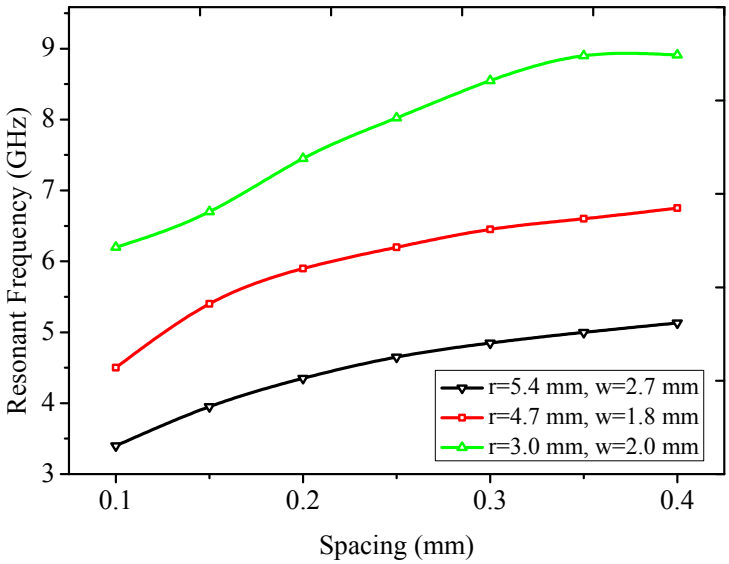

Figure 4.18: The resonant frequency variation with spacing for the individual BCSRR units of the three bulk samples.

resonant frequency is varied from 3.5 GHz to 5.3 GHz (bandwidth : 1.8 GHz) for the first set of samples. The second and third set of samples show a bandwidth of 2.4 GHz

Table 4.1: Resonant frequency variation for the 3 sets of sample of BCSRR with spacing.

Spacing(mm)	Resonant frequency (GHz)		
	Set 1	Set 2	Set 3
0.1	3.4	4.5	6.2
0.15	3.95	5.4	6.7
2.0	4.35	5.9	7.45
2.5	4.65	6.2	8.02
3.0	4.85	6.45	8.55
3.5	5.0	6.6	8.9
4	5.13	6.75	8.91

for a frequency variation from 4.5 GHz to 6.9 GHz and another bandwidth of 2.8 GHz from 6.2 GHz to 9 GHz respectively. Fig. 4.19 gives a photograph of the experiment setup used to study the bulk resonance.

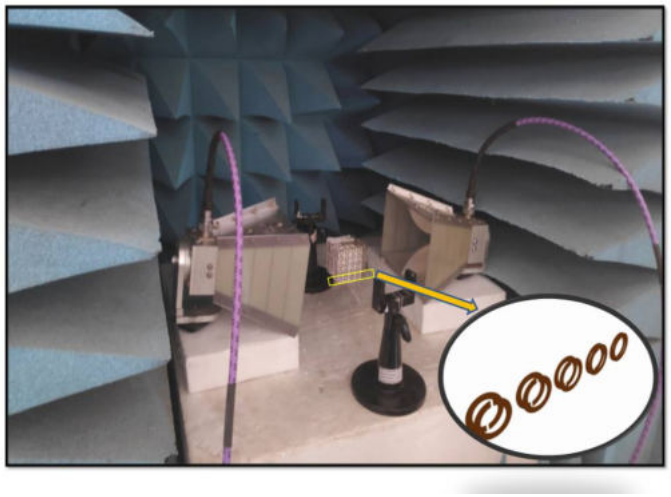

Figure 4.19: Photograph showing the experiment set up to study the resonance characteristics of the bulk BCSRR sample placed between horn antennas inside an anechoic test box.

Even using a single set of samples with proper spacing variation, the resonant

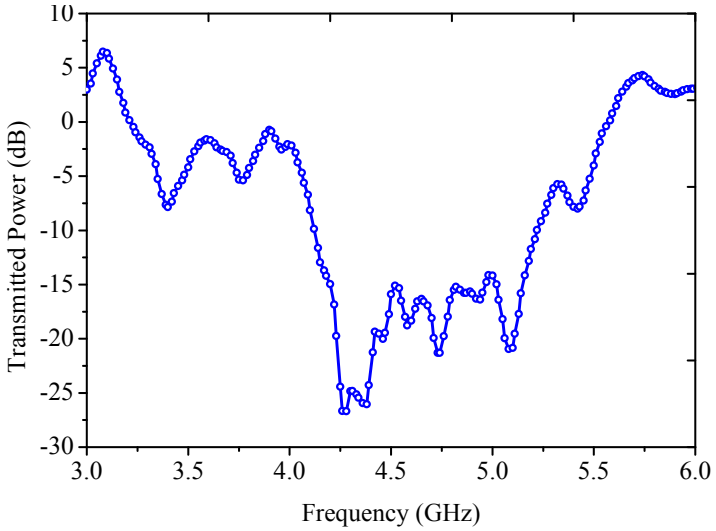

Figure 4.20: The wide band absorption curve obtained for BCSRR bulk sample set 1 with r = 5.4 mm and w = 2.7 mm.

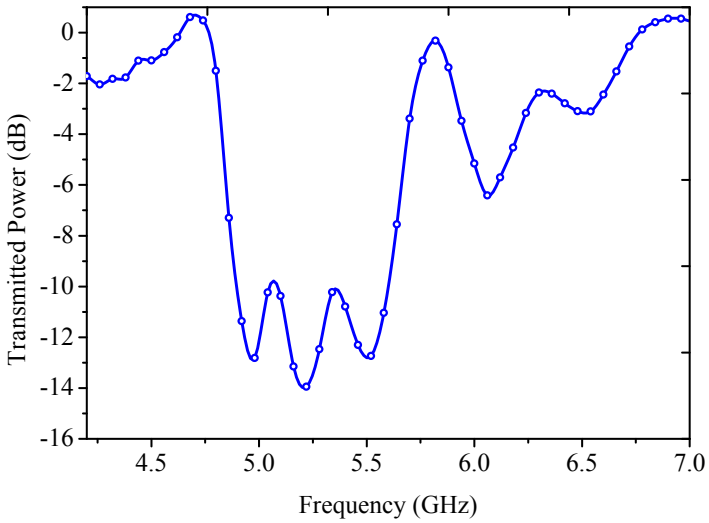

Figure 4.21: The wide band absorption curve obtained for BCSRR bulk sample set 2 with r = 4.7 mm and w = 1.8 mm.

frequency can be tuned in a wide range. The wideband absorption graph obtained for the set with inner radius $r = 5.4$ mm and $w = 2.7$ mm as shown in Fig. 4.20. Fig. 4.21 and Fig. 4.22 give the absorption graphs obtained for set 2 and set 3 with dimensions

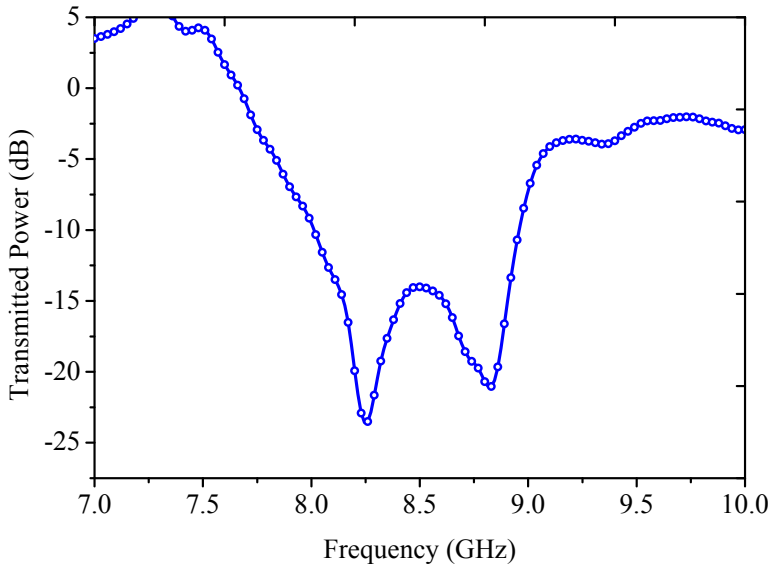

Figure 4.22: The wide band absorption curve obtained for BCSRR bulk sample set 3 with r = 3.0 mm and w = 2.0 mm.

r = 4.7 mm, w = 1.8 mm and r = 3.0 mm, w = 2.0 mm respectively. A wide band absorption ranging from 3 GHz to 9 GHz results when these three sets of bulk forms combined together.

4.5 Conclusion

Fabrication methods and tunable properties of a flexible BCSRR metamaterial structure at microwave frequencies have been presented. Along with the property of flexibility, the structure provides added advantage of wide band frequency tuning possibility. The resonant frequency tuning of BCSRR can be done effectively by this proposed method. The result shows that, by changing the dielectric constant of the substrate, spacing between the rings and the structural geometrical parameters, the resonant frequency of the proposed BCSRR structure can be tuned to any desired value. By changing the spacing between the rings of the BCSRR unit, extensive shifts

in resonance frequency is achieved. The structure may find applications in the design of frequency selective surfaces and cloaking media of wide bandwidths. The method of fabrication can be easily extended to flexible and tunable negative index metamaterials.

CHAPTER 5

Flexible Wire-Split Ring Resonator and Wire-Broadside Coupled Split Ring Resonator

This chapter introduces a novel negative permeability metamaterial structure called as Wire-Split Ring Resonator (W-SRR) constructed using copper wires. Different units of this new resonator are fixed on a thin flexible polymer film and the tuning characteristics of this proposed structure at microwave frequencies are investigated for both single and bulk form. This chapter also discusses the effect of structural parameter variation on the resonant frequency of the W-SRR along with a comparative study with conventional SRR. The theoretical and numerical verification of the result are also included in this chapter. The resonant characteristics of Wire-BCSRR (W-BCSRR) is also studied and its structural parameter variation effects are investigated.

5.1 Introduction

Different types of negative permeability metamaterial SRRs are detailed in chapter 2. Out of these different structures discussed, ECSRR and BCSRR are the most explored ones. Novel variants of these structures called Flexible ECSRR and Flexible BCSRR introduced in this thesis are presented in chapter 3 and chapter 4 respectively. Yet another addition to these groups of metastructures named as Wire-Edge Coupled Split Ring Resonator (W-ECSRR or simply W-SRR) and Wire-Broadside Coupled Split Ring Resonator(W-BCSRR) both made on flexible substrates are introduced in this chapter. These newly introduced structures differ specifically in many aspects compared to their conventional counterparts.

The newly proposed W-SRR and W-BCSRR are fabricated using thin conducting wires of circular cross section in circular geometry like the conventional circular SRR and BCSRR. The area of cross section of metalization of these new wire SRRs are higher in comparison to conventional SRRs that use thin flat rings. For achieving flexibility for the structure, wire SRRs are fixed on flexible polymer film substrate as in the case of flexible structures discussed in chapter 3 and 4. It also helps to avoid the substrate related loss factors. The fabrication, resonance characteristics, structural specialties and some theoretical aspects of this newly proposed structures are presented in the coming sections.

5.2 Fabrication and Measurements

The fabrication of W-SRR is simple compared to other SRR structures. The circular conducting rings of W-SRR are formed by bending copper wires into the form of circular split rings. Complex procedures like photolithographic etching process are

not involved in this fabrication process. The rings are made using a cylindrical cavity shaped mold and are glued on a thin flexible adhesive polypropylene film of 18 μm thickness. The small possible asymmetries in the fabrication of these rings may be reduced by using any standard engineering procedures. The same method is extended for the fabrication of wire-BCSRR also. The two rings of the W-BCSRR are made separately on two polymer films and joined co-axially providing required spacing using low loss dielectric materials to form the W-BCSRR. W-SRRs and W-BCSRRs with different dimensions are fabricated using copper wires of different diameters for studying the effect of structural parameters on their resonant frequencies. Fig. 5.1 gives the schematic diagram of W-SRR and W-BCSRR designs with their structural parameters. Fig. 5.2 show photographs of W-SRR and W-BCSRR along with a flexible sheet of W-SRR.

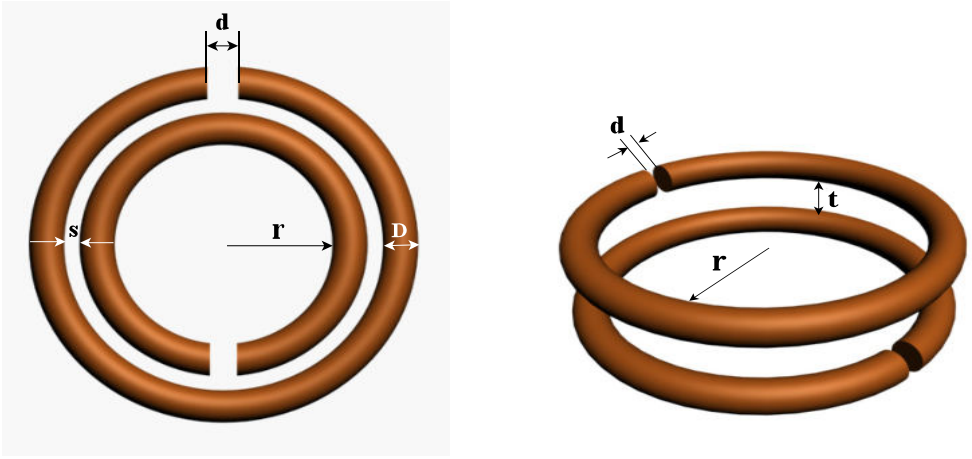

Figure 5.1: Schematic diagram of (a) W-SRR and (b) W-BCSRR units with structural parameters.

The transmission properties of individual W-SRR are studied by placing it between two monopole antennas connected to VNA. For analyzing the effect of structural parameters on the resonant frequency, W-SRR unit cells of different inner radius r and

(a)

(b)

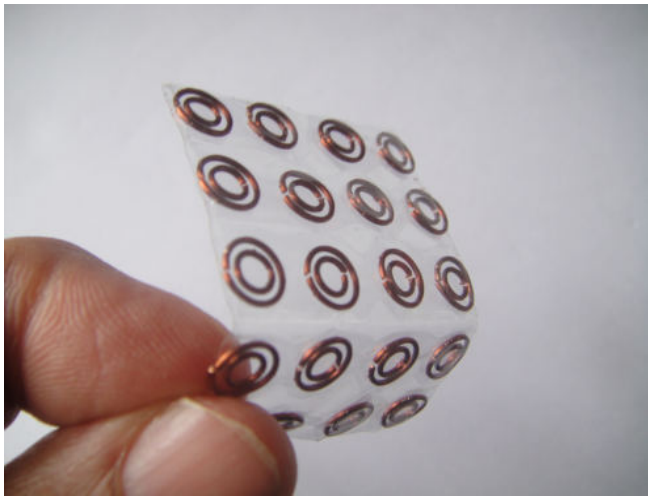

(c)

Figure 5.2: Photographs of (a) W-SRR , (b) W-BCSRR and (c) a flexible W-SRR sheet.

gap between inner and outer rings s are fabricated. Copper wires with different diameters ranging from 0.4 mm to 0.8 mm are used for this purpose. For comparative study, flat ring flexible SRR structures are also fabricated with the same geometrical dimensions as that of WSRRs used. These flexible SRR units are fabricated using the

(a)

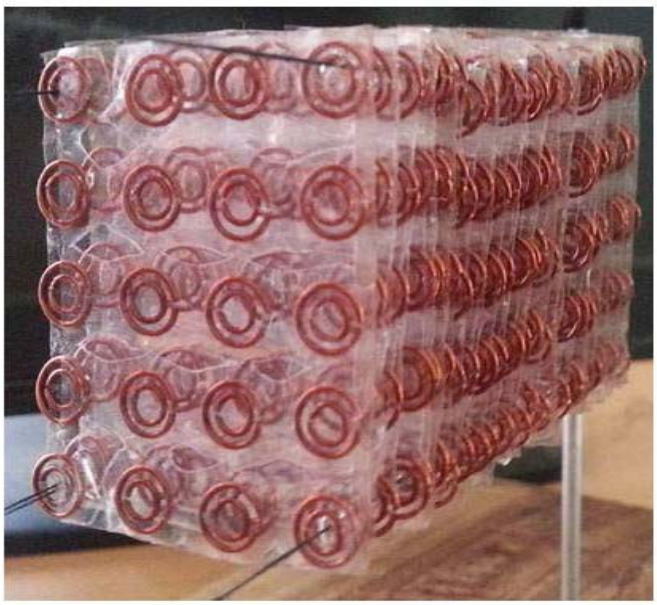

(b)

Figure 5.3: The photographs of (a) W-SRR sheets used for making the bulk form and (b) bulk W-SRR medium having $4 \times 5 \times 12$ elements.

photolithographic etching method on the same type of thin polymer film substrate, which is used in the fabrication of W-SRR. For the study of absorption properties of bulk W-SRR medium, unit cells are arranged periodically in the form of sheets of $4 \times$

5 elements with periodicity 10 mm and 12 such sheets are set parallel to each other with spacing 10 mm. The photograph of the W-SRR structures arranged in sheet and bulk forms are shown in Fig. 5.3. To plot the transmission spectra of the bulk medium , free space method with the sample arranged between the transmitting and receiving wide band antennas is used.

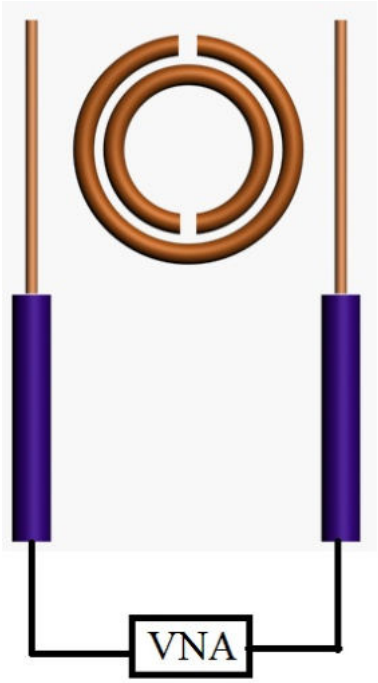

Figure 5.4: Schematic diagram of W-SRR unit placed between probe antennas to study the transmission properties.

5.3 Study of Resonant Characteristics of W-SRR

The transmission curves of individual W-SRR are measured by placing it between two monopole antennas connected to a VNA as depicted in Fig. 5.4. The magnetic resonance curve and phase plot curve obtained for a typical W-SRR with geometrical parameters (inner radius r = 2.45 mm, gap distance between the rings s = 0.8 mm,

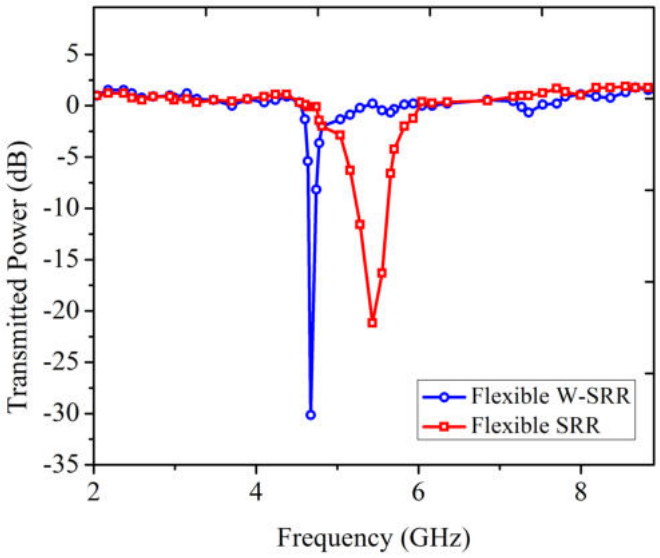

Figure 5.5: Experimental tranmission spectra of WSRR and flat flexible SRR. The parameters are inner radius r = 2.45 mm, gap distance between the rings s = 0.8 mm, and slit width d = 0.5 mm, diameter of the wire D = 0.7 mm. (The wire diameter of W-SRR $D = w$ for flexible SRR)

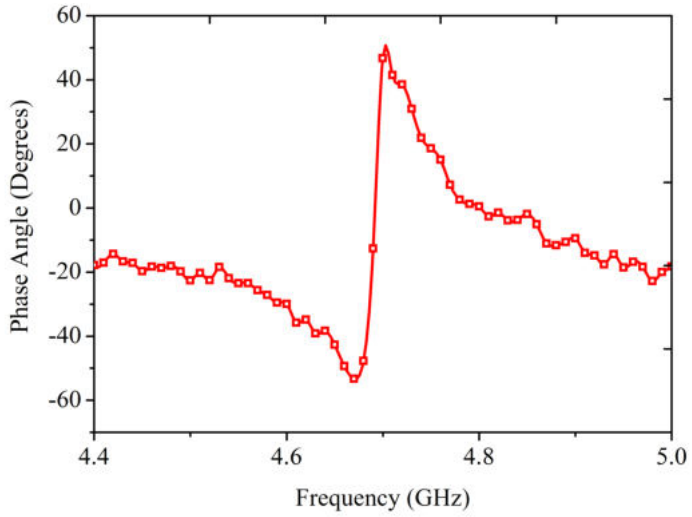

Figure 5.6: The phase plot obtained for W-SRR with parameters inner radius r = 2.45 mm, gap distance between the rings s = 0.8 mm, and slit width d = 0.5 mm, diameter of the wire D = 0.7 mm.

and slit width $d = 0.5$ mm, diameter of the wire $D = 0.7$ mm) are shown in Fig. 5.5 and Fig. 5.6. The structure gives very sharp absorption of power with high Q value,

which is evident from the narrow bandwidth and high absorption level of the resonance curve. Transmission spectra of a flat ring flexible SRR with width of metalization w equal to the diameter of wire D used for W-SRR is also plotted and given in Fig. 5.5. The result clearly shows that equivalent flexible flat SRR have higher bandwidth than W-SRR. Since the bandwidth is inversely proportional to the Q factor, it is evident that the proposed W-SRR have high Q - factor than the flat SRR structure. The results are also verified by simulation and the graphs obtained are given in Fig. 5.7 and observed to be in good agreement with the experimental values.

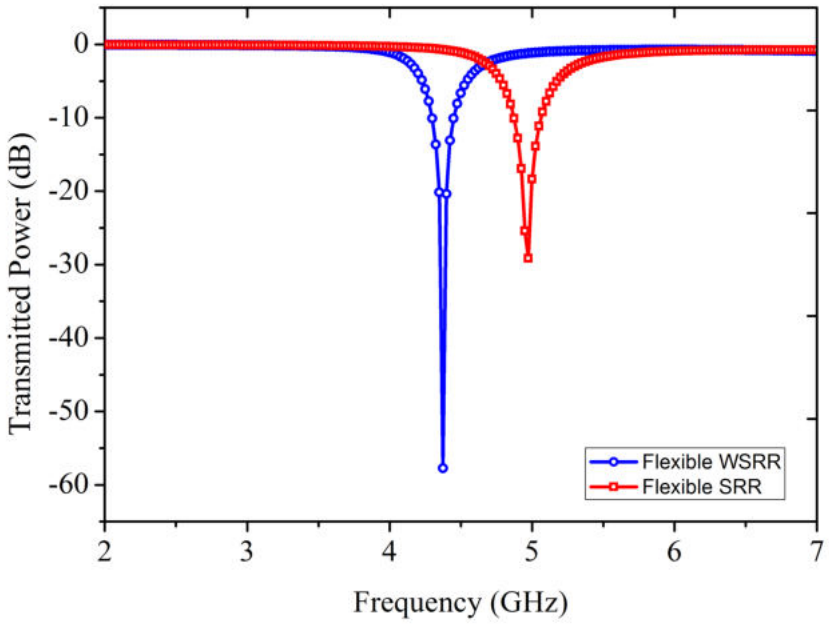

Figure 5.7: Simulated transmission spectra of W-SRR and flat flexible SRR. The parameters are inner radius r = 2.45 mm, gap distance between the rings s= 0.8 mm, and slit width d = 0.5 mm, diameter of the wire D = 0.7 mm.

The absorption curve for the bulk W-SRR medium is plotted using the free space method by employing transmitting and receiving horn antennas as depicted in Fig. 5.8. The absorption graph obtained for the bulk sample shown in Fig. 5.3 is plotted in Fig. 5.9. The resonance is observed around 5.4 GHz. The geometrical parameters

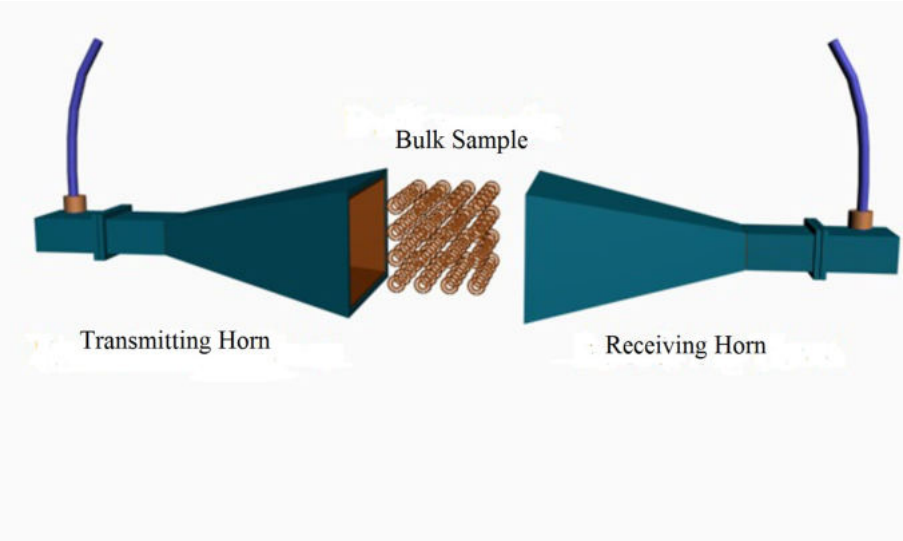

Figure 5.8: Schematic diagram of measurement setup used to study the resonance curve of bulk W-SRR sample.

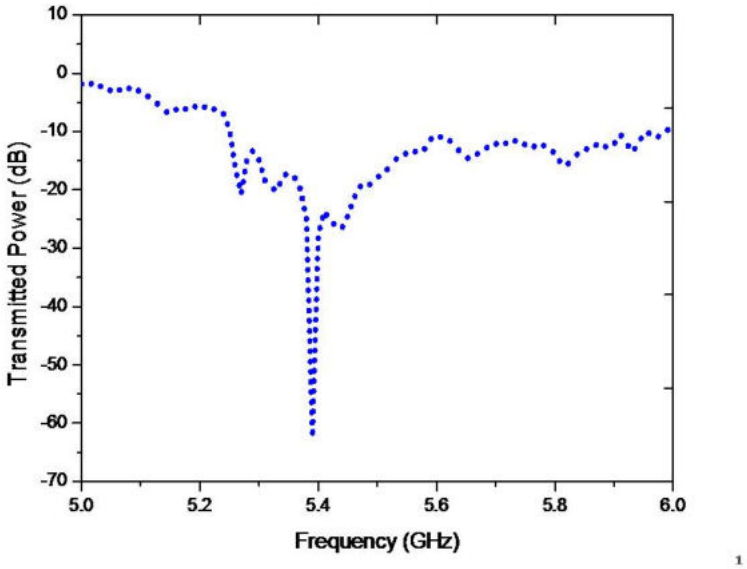

Figure 5.9: Experimental transmission characteristics curve of W-SRR bulk medium.

for the individual W-SRRs used for making the bulk sample for this study are r = 1.68 mm, D = 0.4 mm, s = 0.5 mm and d = 0.5 mm with lattice spacing $10mm \times 10mm \times 10mm$. The broadening of the bandwidth observed is due to slight deviation of the structural parameters of individual W-SRRs from the stipulated values occured during fabrication.

5.4 Theoretical Analysis of Resonant Frequency of W-SRR

The expression for the resonant frequency of the W-SRR in terms of its capacitance and inductance is,

$$f = \frac{1}{2\pi\sqrt{LC}} \tag{5.1}$$

The gap capacitance between two rings of W-SRR as parallel plate capacitor is given by

$$C = \frac{\epsilon_o A}{d} \tag{5.2}$$

where A is the area and d is the distance between plates. In order to consider it as a parallel plate capacitor the following expressions are made. The two wires used for the fabrication of W-SRR is approximated as straight wires of equal length with spacing s as pictured in Fig. 5.10 (a) and (b). Since the field distribution is between the curved portions, direct application of the parallel plate approximation is not possible here. The spacing between the plates of the capacitor d is taken as s which is a variable quantity here. It is reasonable to assume that the capacitive effect is only due to semicircular structure regions of the rings. For a small region defined in terms of r' dθ, the capacitive contribution dC is given by

$$dC = \frac{\epsilon_o 2\pi r_o r' d\theta}{s} \tag{5.3}$$

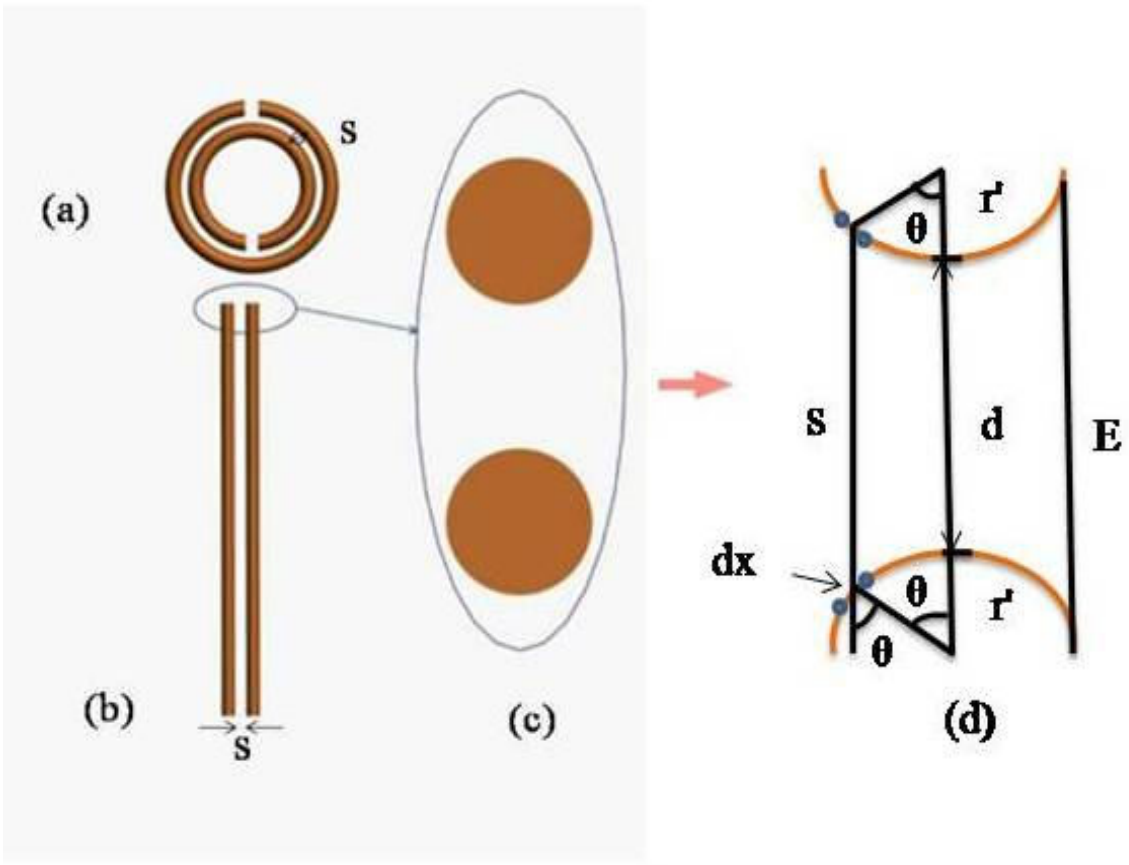

Figure 5.10: Schematic diagram for evaluating the effective capacitance of W-SRR.

$$= \frac{\epsilon_o 2\pi r_o r' d\theta}{E - 2r' cos\theta} \tag{5.4}$$

$$= \frac{\epsilon_o 2\pi r_o r' d\theta}{E(1 - \frac{2r'}{E} cos\theta)} \tag{5.5}$$

where r_o is the average ring radius, r' is the wire radius, E is the maximum value of the distance and d is the minimum distance between rings. Fig. 5.10 (c) shows the cross section of the W-SRR. This equation is for a small element dx or r'dθ. To find the total capacitance integrate the equation from 0 to $\pi/2$ as

$$C = \int_0^{\pi/2} 2(\frac{\epsilon_0 2\pi r_0}{E} \frac{r' d\theta}{1 - \frac{2r'}{E} cos\theta}) \tag{5.6}$$

After integration, along with a small correction applied to account for the fringing field (deduction of 25%) at the end region, the equation for capacitance becomes,

$$C = 1.5(\frac{\epsilon_0 2\pi r_0 r'}{\sqrt{E^2 + 4r'^2}} cos^{-1}(\frac{-2r'}{E})) \tag{5.7}$$

The self inductances of the rings are given by

$$L_1 = \mu_o \pi r_1^2 \tag{5.8}$$

and

$$L_2 = \mu_o \pi r_2^2 \tag{5.9}$$

The mutual inductance M is given by [216]

$$M = \frac{\mu_o \pi r_1^2}{2r_2} \tag{5.10}$$

where D is the wire diameter, r_1 is the average radius of the inner ring and r_2 is the average radius of the outer ring. r_1 and r_2 are given by

$$r_1 = (r + \frac{D}{2}) \tag{5.11}$$

$$r_2 = (r + D + d + \frac{D}{2}) \tag{5.12}$$

where r is the inner radius of the ring. Then the resonant frequency f is given by

$$f = \frac{1}{2\pi\sqrt{(L_1 + L_2 + M)C}} \tag{5.13}$$

The resonance frequencies calculated using this numerical relation are compared with the experimental values. The correction applied for the capacitance is for getting a reasonable agreement with the experimental results.

5.5 Effect of Structural Parameter on the Resonant Frequency of Flexible W-SRR

To study the structural parameter variation with resonant frequency, different samples with varying inner radius r, wire diameter D and gap between the rings s are fabricated and their resonant frequencies are analyzed. Wire diameter, inner radius and gap distance between rings are the parameters selected for investigation. In all cases the results obtained are verified by simulation. The results are also verified by numerical equation (eqn 5.13) derived for the resonant frequency.

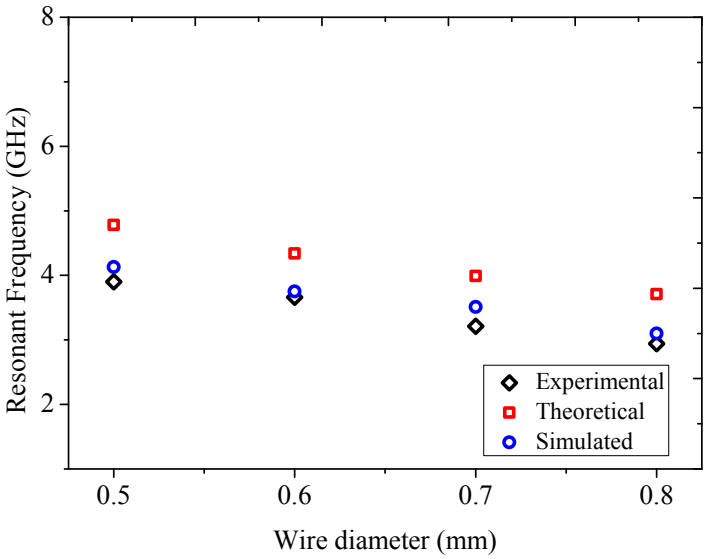

Figure 5.11: Variation of resonant frequency with wire diameter for a typical gap distance of 0.5 mm.

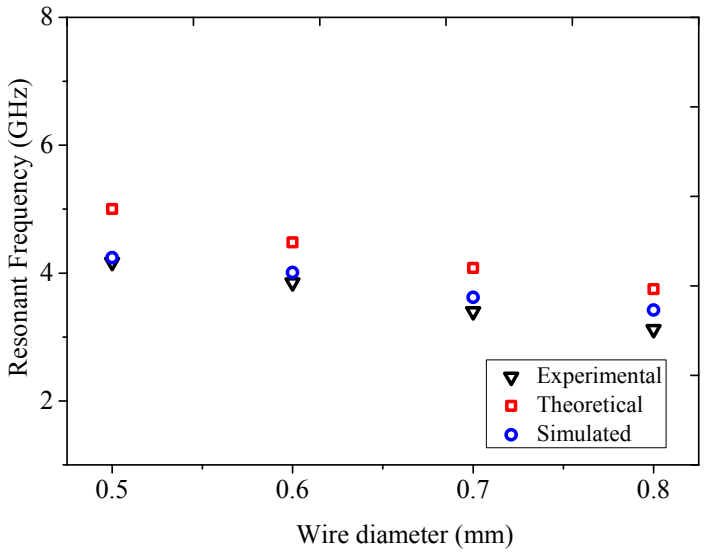

Figure 5.12: Variation of resonant frequency with wire diameter for a typical gap distance of 1.4 mm.

5.5.1 Effect of variation of wire diameter on resonant frequency

The effect of variation of wire diameter on the resonant frequency keeping inner radius r and gap distance s fixed is studied for wire diameter 0.5 mm, 0.6 mm, 0.7

mm and 0.8 mm. Graphs are plotted for wire diameter variation for two different gap distances 0.5 mm and 1.4 mm. Results are also evaluated by theoretical and simulation methods. Figs. 5.11 and 5.12 show the wire diameter variation of the W-SRR with resonant frequency for gap distances of $s = 0.5$ mm and $s = 1.4$ mm respectively. As the wire diameter increases, the resonant frequency decreases as shown by the figure which is a result opposite to that of the conventional type SRR with metal width in place of wire diameter. This may be due to the difference in capacitance which arised from the structural difference of SRR and W-SRR.

5.5.2 Effect of variation of inner radius on resonant frequency

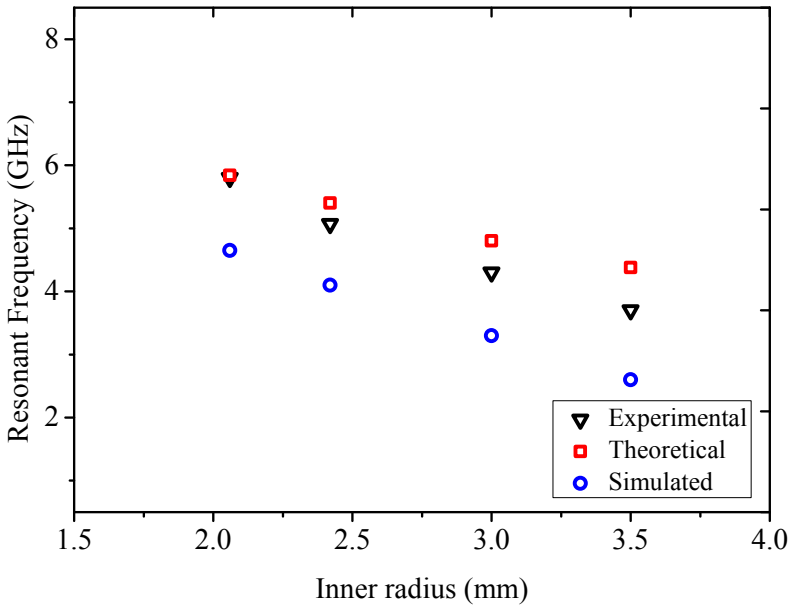

Figure 5.13: Variation of resonant frequency with inner radius of W-SRR for a typical wire diameter 0.4 mm.

For studying the effect of inner radius r on resonant frequency, the gap distance between the rings is kept constant. Two sets of readings with different wire diameter 0.4 mm and 0.7 mm are taken. Fig. 5.13 and Fig. 5.14 show the variation of resonant

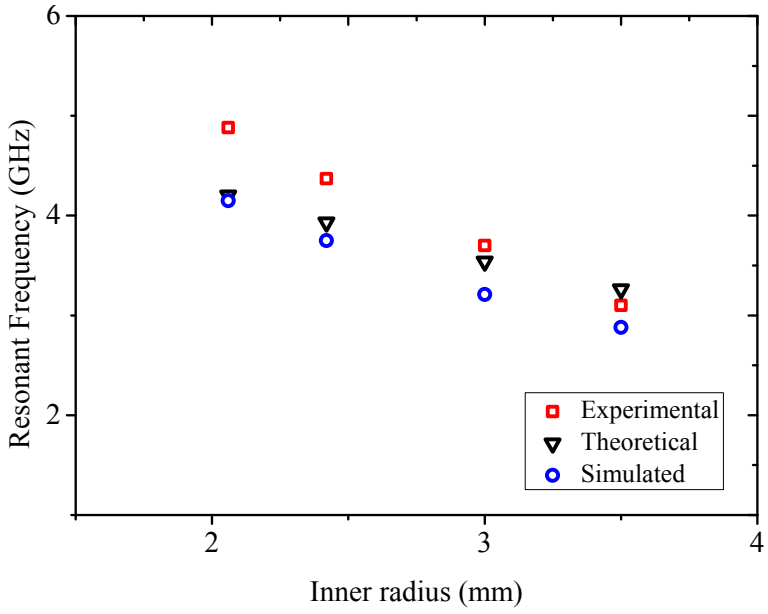

Figure 5.14: Variation of resonant frequency with inner radius of W-SRR for a typical wire diameter 0.7 mm.

frequency with respect to the inner radius for these set of data. The simulated and theoretical results are also plotted for comparison. As the inner radius increases, the capacitance between the rings increases and correspondingly the resonant frequency decreases. This result is similar to that of conventional SRR but the variation is higher for the case of W-SRR.

5.5.3 Effect of gap distance between rings on resonant frequency

The effect of gap distance between rings on resonant frequency is studied by keeping wire diameter constant. By increasing the gap distance, the capacitance between rings decreases and hence the resonant frequency increases. Figs. 5.15 and 5.16 show the variation of resonant frequency with spacing for two W-SRRs with inner radius r = 2.42 mm and r = 2.47 mm respectively. This result also show similarity with that of the conventional SRR structure.

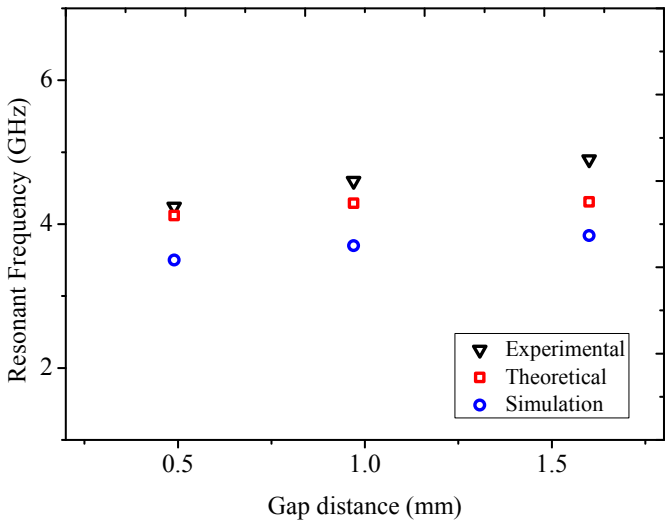

Figure 5.15: Variation of resonant frequency of W-BCSRR with gap distance for a typical inner radius 2.42 mm.

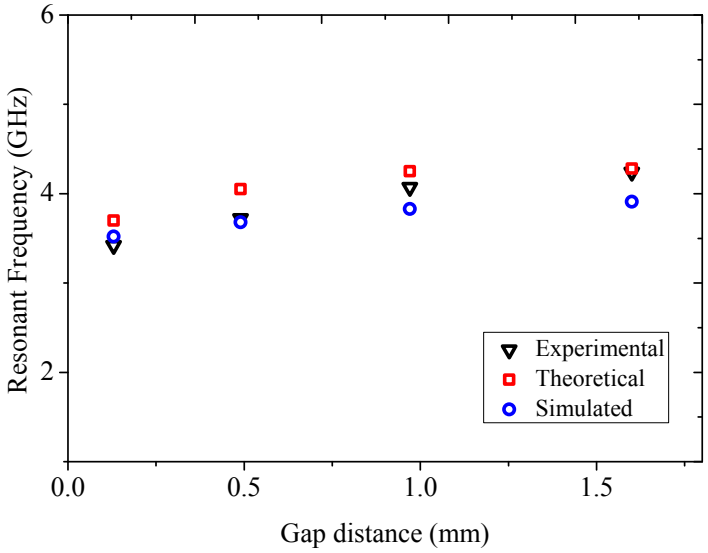

Figure 5.16: Variation of resonant frequency of W-BCSRR with gap distance for a typical inner radius 2.47 mm.

5.6 Resonance Characteristics of W-BCSRR

Magnetic resonance studies of W-BCSRR structures fabricated as mentioned in section 5.2 are carried out using the transmitting-receiving probe setup. A typical

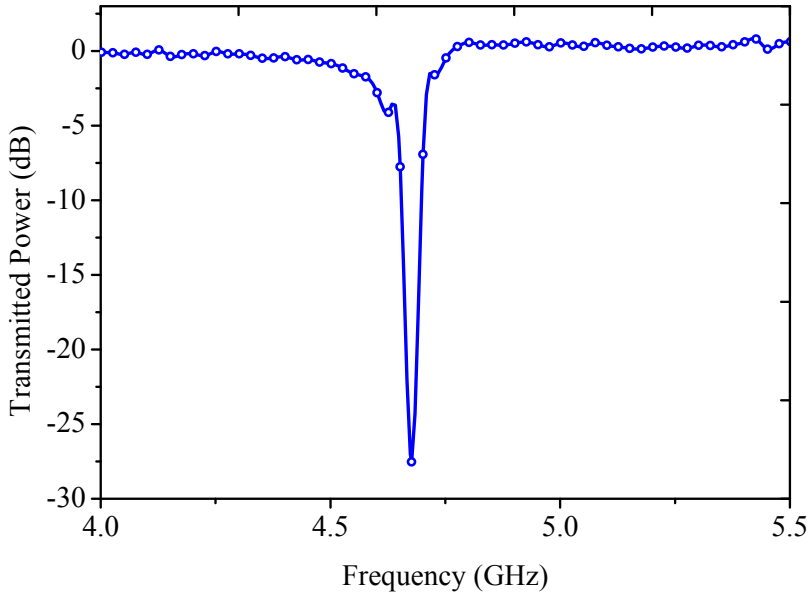

Figure 5.17: Experimental resonance curve of W-BCSRR with parameters inner radius r = 2.06 mm, wire diameter D = 0.4 mm, split width d = 0.2 mm and spacing s = 0.2 mm.

resonance curve for W-BCSRR having ring inner radius $r = 2.06$ mm, wire diameter $D = 0.4$ mm, split width $d = 0.2$ mm and spacing $s = 0.2$ mm is given in Fig. 5.17. As per the case of W-SRR, W-BCSRR also gives magnetic resonant absorption with high Q-value.

5.7 Structural Parameter Variation Study of Flexible W-BCSRR

In order to investigate the effect of structural parameter variations on the resonant frequency of W-BCSRR, different units of W-BCSRR with varying r, D and s are constructed. The experimental results obtained for these three parameters are presented in the following sections.

5.7.1 Effect of variation of wire diameter on resonant frequency

For the purpose of investigating the effect of wire diameter on the resonant frequency, W-BCSRR structures are constructed using wires of diameter 0.5 mm, 0.6 mm and 0.7 mm. The inner radius and spacing are kept constant as 3.0 mm and 0.2 mm. The resonance graph obtained are plotted in Fig. 5.18.

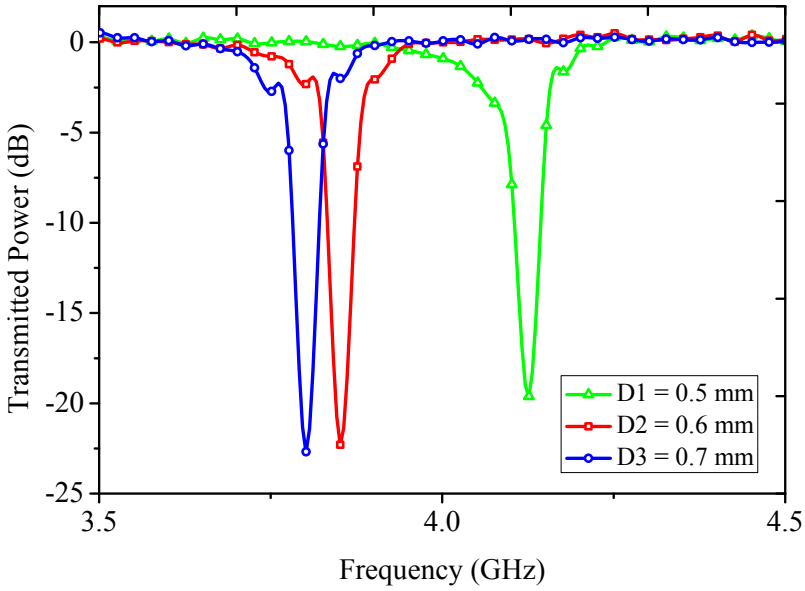

Figure 5.18: Transmission spectra showing the variation of resonant frequency with respect to wire diameter of W-BCSRR.

5.7.2 Effect of variation of inner radius on resonant frequency

In the case of W-BCSRR, as the inner radius increases, the capacitance increases owing to the corresponding increase in surface area of wires which may result in a reduced resonant frequency. The resonance graph obtained for different experimental W-BCSRRs and given in Fig. 5.19. Fig. 5.20 depicts the resonant frequency variation of W-BCSRR with inner radius. The wire diameter D and spacing of the rings s are

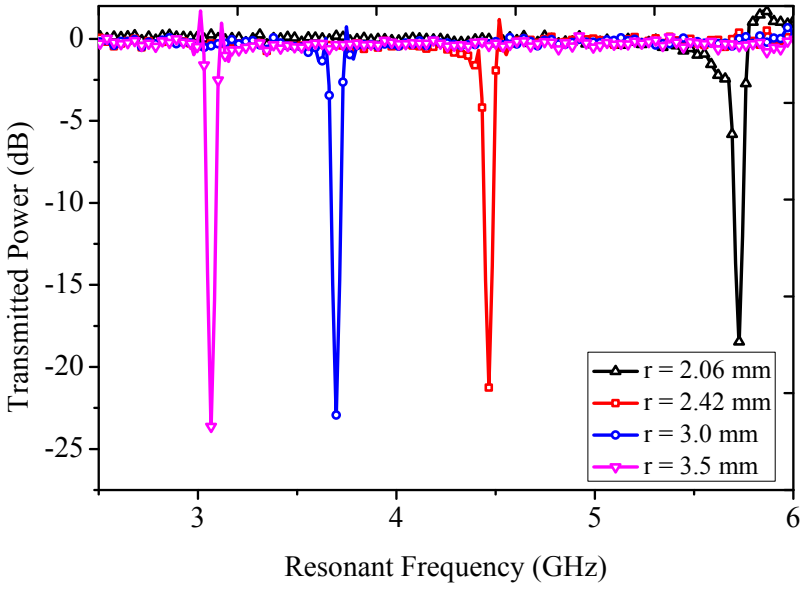

Figure 5.19: S_{21} characteristics versus frequency with respect to different inner radii of W-BCSRR.

kept constant.

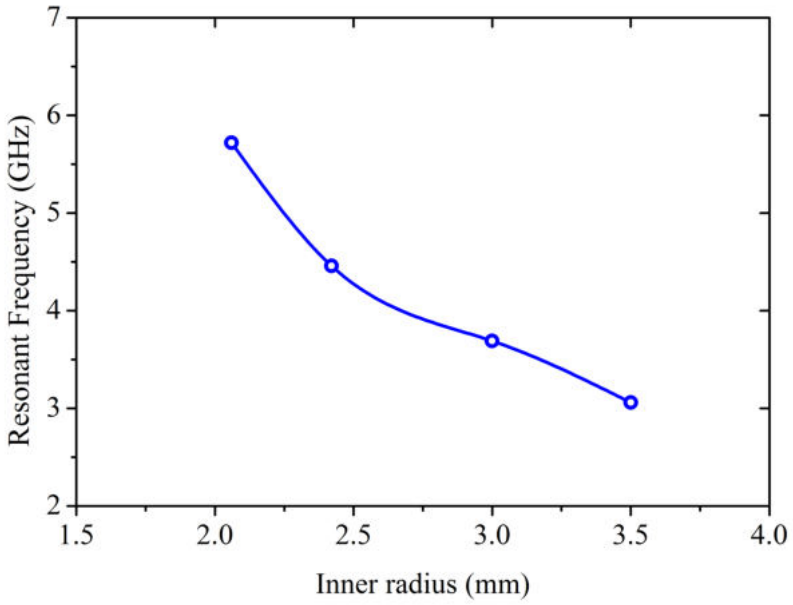

Figure 5.20: Variation of resonant frequency with respect to inner radii of the rings of W-BCSRR.

5.8 Advantages and Applications of Flexible W-SRR

One of the main advantages of the proposed W-SRRs over the conventional SRR with same structural dimensions is the high Q resonance performance. The metal width of the SRR is considered as wire diameter in W-SRR. The induced current flowing through the rings of W-SRR is increased due to the large amount of metallization. In conventional SRR, the rings are fabricated with flat metallization and are in tight contact with the substrate. In such cases major portions of evanescent field passes through this supporting dielectric. So the dielectric loss is high in conventional SRR.

But in the case of W-SRR, the metallization is in semi spherical form and there is no question of a rigid substrate tightly attached to the rings. So the dielectric losses will be low in W-SRR which may lead to high Q-value. The ohmic losses also reduced in W-SRR due to the greater area of cross section than flat SRR. Another advantage of WSRR over conventional SRR is the higher structural tunability. The flexibility is another advantage of W-SRR. The novel structure may find applications in the field of high sensitive sensors, frequency selective surfaces and material characterization studies.

5.9 Conclusion

The design, fabrication and resonant characteristics of this novel flexible W-SRR made of metallic wires are presented. The resonance characteristics of both W-SRR and W-BCSRR are taken and the results are compared with that of conventional SRRs. The results are also verified using simulation.The study of structural parameter variations on the resonant frequency is also performed and it is observed that W-SRR shows higher structural tunability than ordinary SRR. The proposed structures are

fabricated without a solid substrate and they showed high quality factor. These thin low loss flexible structures with high Q-value can be used for applications in various fields like frequency selective surfaces and sensors.

CHAPTER 6

Summary and Scope of Future Work

Structures with negative permeability nature is not common in nature. Some ferro and ferri magnetic materials show negative permeability at particular frequency regions which are rare and of narrow bandwidth. So different negative permeability structures for specific applications in microwave frequency ranges have to be artificially fabricated. Split ring resonators are the commonly used microwave structures showing the negative permeability. But all studies in the literature show that the samples are fabricated on solid substrate.

Structures having flexibility and tunability for particular applications like frequency selective surfaces and cloaking are of much importance. In this thesis different types of flexible structures are introduced and the resonant and dielectric characteris-

tics study of these novel structures are presented. The effect of structural parameters on the resonant frequency of these different structures are also investigated. The different types of structures presented include flexible split ring resonator (SRR), broad side coupled split ring resonator (BCSRR), wire-SRR (W-SRR) and wire-BCSRR (W-BCSRR).

The first section presented the novel flexible SRR metamaterial structure fabricated on a thin inert substrate of polypropylene film with negligible thickness. A new method is introduced to fabricate the flexible structure other than photolithographic method called direct printing method which prints the desired pattern on the thin film using printer. This method of fabrication is easier than conventional complex method. The structure shows sharp resonance absorption at microwave frequencies. The dielectric constant and thickness of substrate are the two main factors which depend on the resonant frequency of the SRR structure. By increasing the permittivity and thickness of substrate, the resonant frequency shifts to a lower frequency range, due to increase in capacitance.

For the experimental study, the substrates of PMMA and wax are used. A comparative study is performed to investigate the effects of structural parameters on the resonant frequency of flexible SRR fabricated on thin film with the conventional one which is fabricated on PCB. The parameters considered are the inner radius, gap distance between rings and metal width. Varying these parameters, the resonant frequency decreases, a similar result which is obtained for conventional SRR. By varying the permittivity, thickness and structural parameters of this flexible SRR, the resonant frequency can be tuned to any desired range. The proposed thin flexible structure having low loss makes it suitable for variety of metamaterial applications like frequency selective surfaces and cloaking.

A modified version of flexible SRR called flexible BCSRR is introduced in the next section. The design, fabrication and resonance characteristics of flexible BCSRR are also included. The fabrication of flexible BCSRR is quite different from conventional one. The two rings are fabricated separately on two thin films rather than fabricated on the two sides of the same substrate in conventional SRR. This makes it suitable for tuning the resonant frequency of BCSRR by varying the spacing between rings.

The effect of dielectric constant of the substrate on the resonance frequency is investigated by using substrates of PMMA and wax. By using different dielectric materials, the resonant frequency shift obtained is remarkable. The effect of the structural parameter variations of BCSRR with resonant frequency is studied and the results show that by varying these parameters, the resonant frequency tuning is possible to great extends. By varying the spacing between the rings of BCSRR using cotton fabric with increasing thickness, a wide band microwave absorber is designed. For that study, three sets of samples with different dimensions are fabricated. The spectra shows a wide band absorption curve and by combining the three set of samples to make it a bulk form, a wide band ranging from 3 GHz to 9 GHz is observed. By varying the permittivity, thickness and spacing of the BCSRR units, the resonant frequency can be tuned to any desired value. This structure can be used in potential applications of metamaterials like absorbers, frequency selective surfaces and sensors.

Another novel structure introduced in this thesis is W-SRR. It is fabricated using simple engineering technique. Photo masking and etching techniques are not used in the fabrication process. The structure is fabricated using metallic wires bend into the form of split rings and glued on a thin polymer film. The W-SRR shows sharp absorption characteristics than conventional SRR. A comparative study of W-SRR and flexible SRR is performed by using a SRR with the same geometrical configuration as W-SRR. The experimental and simulated results are in good agreement. WSRR

shows sharp absorption compared to SRR and has narrow bandwidth thereby shows high-Q performance. The absorption characteristics of bulk sample of WSRR are also investigated.

A novel wire BCSRR structure is proposed and the resonance and structural characteristics are analyzed. The effect of variations in structural parameters on the resonant frequency is also studied. The study reveals that the structural dependence of W-SRR is higher than SRR and shows similar result as conventional SRR except wire diameter variation in which it behaves oppositely. Since the structure is fabricated using thin substrate, the scattering and absorption losses due to the solid substrate are reduced. The sensitivity of the structure is also high. The theoretical and simulated results are in quite agreement with experimental values. The structure may find applications in the field of senors, frequency selective surfaces and material characterization studies.

The fabrication can be extended to design a flexible negative index material in the microwave frequencies. Tuning the resonant frequency of the proposed structures is easier by varying any of the following parameters - substrate permittivity, substrate thickness, spacing or structural parameters. So a wideband tunable negative index medium can be designed using these tuning techniques. These thin low loss flexible structures can be used in a variety of applications in the field of microwave engineering.

Bibliography

[1] Winston E Kock. Metallic delay lenses. Bell System Technical Journal, 27(1):58–82, 1948.

[2] Viktor G Veselago. The electrodynamics of substances with simultaneously negative values of and μ. Soviet physics uspekhi, 10(4):509, 1968.

[3] John B Pendry, Anthony J Holden, David J Robbins, and WJ Stewart. Magnetism from conductors and enhanced nonlinear phenomena. IEEE transactions on microwave theory and techniques, 47(11):2075–2084, 1999.

[4] John B Pendry, AJ Holden, WJ Stewart, and I Youngs. Extremely low frequency plasmons in metallic mesostructures. Physical review letters, 76(25):4773, 1996.

[5] David R Smith, Willie J Padilla, DC Vier, Syrus C Nemat-Nasser, and Seldon Schultz. Composite medium with simultaneously negative permeability and permittivity. Physical review letters, 84(18):4184, 2000.

[6] David R Smith and Norman Kroll. Negative refractive index in left-handed materials. Physical Review Letters, 85(14):2933, 2000.

[7] Lord Rayleigh. Lvi. on the influence of obstacles arranged in rectangular order upon the properties of a medium. The London, Edinburgh, and Dublin Philosophical Magazine and Journal of Science, 34(211):481–502, 1892.

[8] Filippo Capolino. Theory and phenomena of metamaterials. CRC press, 2017.

[9] Robert E Collin. Field theory of guided waves. 1960.

[10] Jagadis Chunder Bose. On the rotation of plane of polarisation of electric wave by a twisted structure. Proceedings of the Royal Society of London, 63(389-400):146–152, 1898.

[11] Ismo V Lindell, Ari H Sihvola, and Juhani Kurkijarvi. Karl f. lindman: The last hertzian, and a harbinger of electromagnetic chirality. IEEE Antennas and Propagation Magazine, 34(3):24–30, 1992.

[12] Sergei Alexander Schelkunoff and Harald T Friis. Antennas: theory and practice, volume 639. Wiley New York, 1952.

[13] AN Lagarkov, VN Semenenko, VA Chistyaev, DE Ryabov, SA Tretyakov, and CR Simovski. Resonance properties of bi-helix media at microwaves. Electromagnetics, 17(3):213–237, 1997.

[14] MCK Wiltshire, JB Pendry, IR Young, DJ Larkman, DJ Gilderdale, and JV Hajnal. Microstructured magnetic materials for radio frequency operation in magnetic resonance imaging (mri). MRI Paper Final, 10, 2001.

[15] Rodger M Walser. Electromagnetic metamaterials. In Complex Mediums II: Beyond Linear Isotropic Dielectrics, volume 4467, pages 1–16. International Society for Optics and Photonics, 2001.

[16] S Anantha Ramakrishna. Physics of negative refractive index materials. Reports on progress in physics, 68(2):449, 2005.

[17] David R Smith, Willie J Padilla, DC Vier, Syrus C Nemat-Nasser, and Seldon Schultz. Composite medium with simultaneously negative permeability and permittivity. Physical review letters, 84(18):4184, 2000.

[18] Walter Rotman. Plasma simulation by artificial dielectrics and parallel-plate media. IRE Transactions on Antennas and Propagation, 10(1):82–95, 1962.

[19] John B Pendry, AJ Holden, DJ Robbins, and WJ Stewart. Low frequency plasmons in thin-wire structures. Journal of Physics: Condensed Matter, 10(22):4785, 1998.

[20] D Schurig, JJ Mock, and DR Smith. Electric-field-coupled resonators for negative permittivity metamaterials. Applied physics letters, 88(4):041109, 2006.

[21] DF Sievenpiper, ME Sickmiller, and E Yablonovitch. 3d wire mesh photonic crystals.

Physical Review Letters, 76(14):2480, 1996.

[22] SI Maslovski, SA Tretyakov, and PA Belov. Wire media with negative effective permittivity: A quasi-static model. Microwave and Optical Technology Letters, 35(1):47–51, 2002.

[23] Stanislav I Maslovski, Pekka MT Ikonen, Igor Kolmakov, Sergei A Tretyakov, and Mikko Kaunisto. Artificial magnetic materials based on the new magnetic particle: Metasolenoid. Progress In Electromagnetics Research, 54:61–81, 2005.

[24] Martin Hudlicka, Jan Machac, and Igor S Nefedov. A triple wire medium as an isotropic negative permittivity metamaterial. Progress In Electromagnetics Research, 65:233–246, 2006.

[25] Murtala Aminu-Baba, Mohammad Kamal A Rahim, Farid Zubir, Mohd Fairus Mohd Yusoff, and Abdulkadir Bello Shallah. Microstrip antenna with csrr ground structure. In 2017 International Symposium on Antennas and Propagation (ISAP), pages 1–2. IEEE, 2017.

[26] Taha A Elwi, Z Abbas, Mohammed Noori, Yahiea Al-Naiemy, Ethar Y Salih, and Marwa M Hamed. Conformal antenna array for mimo applications. Journal of Electromagnetic Analysis and Applications, 6(04):43, 2014.

[27] Qiwei Ye, Ying Liu, Hai Lin, Minhua Li, and Helin Yang. Multi-band metamaterial absorber made of multi-gap srrs structure. Applied Physics A, 107(1):155–160, 2012.

[28] Chinmoy Saha and Jawad Y Siddiqui. A comparative analyis for split ring resonators of different geometrical shapes. In 2011 IEEE Applied Electromagnetics Conference (AEMC), pages 1–4. IEEE, 2011.

[29] Richard A Shelby, David R Smith, and Seldon Schultz. Experimental verification of a negative index of refraction. science, 292(5514):77–79, 2001.

[30] RA Shelby, DR Smith, SC Nemat-Nasser, and Sheldon Schultz. Microwave transmission through a two-dimensional, isotropic, left-handed metamaterial. Applied Physics Letters, 78(4):489–491, 2001.

[31] T Weiland, R Schuhmann, RB Greegor, CG Parazzoli, AM Vetter, DR Smith, DC Vier, and S Schultz. Ab initio numerical simulation of left-handed metamaterials: Comparison of calculations and experiments. Journal of Applied Physics, 90(10):5419–5424, 2001.

[32] Anthony Grbic and George V Eleftheriades. Experimental verification of backward-wave radiation from a negative refractive index metamaterial. Journal of applied physics, 92(10):5930–5935, 2002.

[33] Vladimir M Shalaev, Wenshan Cai, Uday K Chettiar, Hsiao-Kuan Yuan, Andrey K Sarychev, Vladimir P Drachev, and Alexander V Kildishev. Negative index of refraction in optical metamaterials. Optics letters, 30(24):3356–3358, 2005.

[34] Jiangfeng Zhou, Thomas Koschny, Lei Zhang, Gary Tuttle, and Costas M Soukoulis. Experimental demonstration of negative index of refraction. Applied Physics Letters, 88(22):221103, 2006.

[35] Ekmel Ozbay, Kaan Guven, and Koray Aydin. Metamaterials with negative permeability and negative refractive index: experiments and simulations. Journal of Optics A: Pure and Applied Optics, 9(9):S301, 2007.

[36] John Brian Pendry. Negative refraction makes a perfect lens. Physical review letters, 85(18):3966, 2000.

[37] David Schurig, JJ Mock, BJ Justice, Steven A Cummer, John B Pendry, AF Starr, and DR Smith. Metamaterial electromagnetic cloak at microwave frequencies. Science, 314(5801):977–980, 2006.

[38] Ulf Leonhardt. Optical conformal mapping. Science, 312(5781):1777–1780, 2006.

[39] Wenshan Cai, Uday K Chettiar, Alexander V Kildishev, and Vladimir M Shalaev. Optical cloaking with metamaterials. Nature photonics, 1(4):224, 2007.

[40] Wenshan Cai, Uday K Chettiar, Alexander V Kildishev, Vladimir M Shalaev, and Graeme W Milton. Nonmagnetic cloak with minimized scattering. Applied Physics Letters, 91(11):111105, 2007.

[41] Wenshan Cai and Vladimir M Shalaev. Designs of optical cloak with nonlinear transformations. In Lasers and Electro-Optics, 2008 and 2008 Conference on Quantum Electronics and Laser Science. CLEO/QELS 2008. Conference on, pages 1–2. IEEE, 2008.

[42] Su Xu, Yong Wang, BaiLe Zhang, and HongSheng Chen. Invisibility cloaks from forward design to inverse design. Science China Information Sciences, 56(12):1–11, 2013.

[43] Marco A Ribeiro and Carlos R Paiva. Invisibility cloaks and the equivalence principle

for electromagnetics. In 2008 IEEE Antennas and Propagation Society International Symposium, pages 1–4. IEEE, 2008.

[44] author=Gabor, D, journal=Pat. UK, volume=541, pages=753, year=1940.

[45] David R Smith, David Schurig, Marshall Rosenbluth, Sheldon Schultz, S Anantha Ramakrishna, and John B Pendry. Limitations on subdiffraction imaging with a negative refractive index slab. Applied Physics Letters, 82(10):1506–1508, 2003.

[46] MCK Wiltshire, JV Hajnal, JB Pendry, DJ Edwards, and CJ Stevens. Metamaterial endoscope for magnetic field transfer: near field imaging with magnetic wires. Optics Express, 11(7):709–715, 2003.

[47] Zhaowei Liu, Nicholas Fang, Ta-Jen Yen, and Xiang Zhang. Rapid growth of evanescent wave by a silver superlens. Applied Physics Letters, 83(25):5184–5186, 2003.

[48] Anthony Grbic and George V Eleftheriades. Overcoming the diffraction limit with a planar left-handed transmission-line lens. Physical Review Letters, 92(11):117403, 2004.

[49] Ashwin K Iyer and George V Eleftheriades. Free-space imaging beyond the diffraction limit using a veselago-pendry transmission-line metamaterial superlens. IEEE transactions on antennas and propagation, 57(6):1720–1727, 2009.

[50] Alessandro Salandrino and Nader Engheta. Far-field subdiffraction optical microscopy using metamaterial crystals: Theory and simulations. Physical Review B, 74(7):075103, 2006.

[51] Nader Engheta, Alessandro Salandrino, and Brian Edwards. Far-field sub-diffraction optical lenses (fasdol), February 14 2012. US Patent 8,116,009.

[52] Zubin Jacob, Leonid V Alekseyev, and Evgenii Narimanov. Optical hyperlens: far-field imaging beyond the diffraction limit. Optics express, 14(18):8247–8256, 2006.

[53] Igor I Smolyaninov, Yu-Ju Hung, and Christopher C Davis. Magnifying superlens in the visible frequency range. science, 315(5819):1699–1701, 2007.

[54] Wyatt Adams, Mehdi Sadatgol, Xu Zhang, and Durdu Ö Güney. Bringing the 'perfect lens' into focus by near-perfect compensation of losses without gain media. New Journal of Physics, 18(12):125004, 2016.

[55] Xu Zhang, Wyatt Adams, Mehdi Sadatgol, and Durdu Ö Güney. Enhancing the resolution of hyperlens by the compensation of losses without gain media. arXiv preprint

arXiv:1607.07466, 2016.

[56] WS Hart, AO Bak, and CC Phillips. Ultra low-loss super-resolution with extremely anisotropic semiconductor metamaterials. AIP Advances, 8(2):025203, 2018.

[57] Irfan Bulu, Humeyra Caglayan, Koray Aydin, and Ekmel Ozbay. Compact size highly directive antennas based on the srr metamaterial medium. New Journal of Physics, 7(1):223, 2005.

[58] Richard W Ziolkowski and Aycan Erentok. Metamaterial-based efficient electrically small antennas. IEEE Transactions on antennas and propagation, 54(7):2113–2130, 2006.

[59] Chunchen Lin, Iftekhar O Mirza, Shouyuan Shi, and Dennis W Prather. Tuneable meta-material split-ring resonators for impedance matching antennas for broadband applications. Technical report, DELAWARE UNIV NEWARK DEPT OF ELECTRICAL AND COMPUTER ENGINEERING, 2008.

[60] Prathaban Mookiah and Kapil R Dandekar. Metamaterial-substrate antenna array for mimo communication system. IEEE Transactions on Antennas and Propagation, 57(10):3283–3292, 2009.

[61] Adnan Sondaş, Mustafa Hikmet Bilgehan Ucar, and Yunus Emre Erdemli. Tunable srr-based substrate for a microstrip patch antenna. Turkish Journal of Electrical Engineering & Computer Sciences, 20(1):159–168, 2012.

[62] Joe Kizhakooden, Jovia Jose, Nees Paul, Sikha K Simon, Sreedevi P Chakyar, Jolly Andrews, and VP Joseph. Metamaterial inspired featherlight artificial plasma horn antenna for astronomical and communication applications. Microwave and Optical Technology Letters, 61(3):777–780, 2019.

[63] Joe Kizhakooden, Jovia Jose, Nees Paul, Sreedevi P Chakyar, Anju Sebastian, Sikha K Simon, KS Umadevi, C Bindu, Jolly Andrews, and VP Joseph. Broadside coupled split ring resonator based multiband monopole patch antenna for wireless communication applications. In AIP Conference Proceedings, volume 2162, page 020068. AIP Publishing, 2019.

[64] Winfield W Salisbury. Absorbent body for electromagnetic waves, June 10 1952. US Patent 2,599,944.

[65] Filiberto Bilotti, Luca Nucci, and Lucio Vegni. An srr based microwave absorber. Microwave and Optical Technology Letters, 48(11):2171–2175, 2006.

[66] N I? Landy, S Sajuyigbe, Jack J Mock, David R Smith, and Willie J Padilla. Perfect metamaterial absorber. Physical review letters, 100(20):207402, 2008.

[67] Jiafu Wang, Shaobo Qu, Zhentang Fu, Hua Ma, Yiming Yang, Xiang Wu, Zhuo Xu, and Meijuan Hao. Three-dimensional metamaterial microwave absorbers composed of coplanar magnetic and electric resonators. Progress In Electromagnetics Research, 7:15–24, 2009.

[68] Li Huang, Dibakar Roy Chowdhury, Suchitra Ramani, Matthew T Reiten, Sheng-Nian Luo, Antoinette J Taylor, and Hou-Tong Chen. Experimental demonstration of terahertz metamaterial absorbers with a broad and flat high absorption band. Optics letters, 37(2):154–156, 2012.

[69] LiangKui Sun, HaiFeng Cheng, YongJiang Zhou, and Jun Wang. Broadband metamaterial absorber based on coupling resistive frequency selective surface. Optics express, 20(4):4675–4680, 2012.

[70] YJ Yoo, HY Zheng, YJ Kim, JY Rhee, J-H Kang, KW Kim, H Cheong, YH Kim, and YP Lee. Flexible and elastic metamaterial absorber for low frequency, based on small-size unit cell. Applied physics letters, 105(4):041902, 2014.

[71] Jinfeng Zhu, Delong Li, Shuang Yan, Yijun Cai, Qing Huo Liu, and Timothy Lin. Tunable microwave metamaterial absorbers using varactor-loaded split loops. EPL (Europhysics Letters), 112(5):54002, 2015.

[72] Saptarshi Ghosh, Somak Bhattacharyya, Devkinandan Chaurasiya, and Kumar Vaibhav Srivastava. An ultrawideband ultrathin metamaterial absorber based on circular split rings. IEEE antennas and wireless propagation letters, 14:1172–1175, 2015.

[73] Hao Meng, Jihong Wen, Honggang Zhao, and Xisen Wen. Optimization of locally resonant acoustic metamaterials on underwater sound absorption characteristics. Journal of Sound and Vibration, 331(20):4406–4416, 2012.

[74] Changlin Ding, Huaijun Chen, Shilong Zhai, and Xiaopeng Zhao. Acoustic metamaterial based on multi-split hollow spheres. Applied Physics A, 112(3):533–541, 2013.

[75] Yu I Bobrovnitskii and TM Tomilina. Sound absorption and metamaterials: A review. Acoustical Physics, 64(5):519–526, 2018.

[76] Robert W Boyd and John E Heebner. Sensitive disk resonator photonic biosensor. Applied optics, 40(31):5742–5747, 2001.

[77] Akira Ishimaru, Sermak Jaruwatanadilok, and Yasuo Kuga. Generalized surface plasmon resonance sensors using metamaterials and negative index materials. Progress In Electromagnetics Research, 51:139–152, 2005.

[78] John F O'Hara, Ranjan Singh, Igal Brener, Evgenya Smirnova, Jiaguang Han, Antoinette J Taylor, and Weili Zhang. Thin-film sensing with planar terahertz metamaterials: sensitivity and limitations. Optics Express, 16(3):1786–1795, 2008.

[79] Rohat Melik, Emre Unal, Nihan Kosku Perkgoz, Christian Puttlitz, and Hilmi Volkan Demir. Metamaterial-based wireless strain sensors. Applied Physics Letters, 95(1):011106, 2009.

[80] Kenta Hattori, Keiichiro Shiraga, Yuichi Ogawa, and Naoshi Kondo. Sensing living cells using a terahertz split-ring resonator with reflection spectroscopy. In 2014 XXXIth URSI General Assembly and Scientific Symposium (URSI GASS), pages 1–4. IEEE, 2014.

[81] Jordi Naqui, Miguel Durán-Sindreu, and Ferran Martín. Novel sensors based on the symmetry properties of split ring resonators (srrs). Sensors, 11(8):7545–7553, 2011.

[82] Jordi Naqui, Miguel Durán-Sindreu, and Ferran Martín. Alignment and position sensors based on split ring resonators. Sensors, 12(9):11790–11797, 2012.

[83] Evren Ekmekci and Gonul Turhan-Sayan. Metamaterial sensor applications based on broadside-coupled srr and v-shaped resonator structures. In Antennas and Propagation (APSURSI), 2011 IEEE International Symposium on, pages 1170–1172. IEEE, 2011.

[84] Muhammed S Boybay and Omar M Ramahi. Metamaterial particles for near-field sensing applications, April 12 2012. US Patent App. 12/902,584.

[85] Sreedevi P Chakyar, Jolly Andrews, and VP Joseph. Temperature dependence of relative permittivity: A measurement technique using split ring resonators. International Journal of Mechanical and Mechatronics Engineering, 10(6):1134–1137, 2016.

[86] Sreedevi P Chakyar, TA Shanto, Aathira Murali, Nees Paul, Jolly Andrews, VP Joseph, et al. Measurement of dielectric constant of waxes at different temperatures using split ring resonator structure. In 2016 IEEE MTT-S International Microwave and RF Conference (IMaRC), pages 1–4. IEEE, 2016.

[87] Sreedevi P Chakyar, Aathira Murali, and Jolly Andrews. Determination of permittivity of pulses and cereals using metamaterial split ring resonator. In AIP Conference Proceedings, volume 1849, page 020024. AIP Publishing, 2017.

[88] Sikha K Simon, Sreedevi P Chakyar, Anju Sebastian, Jovia Jose, Jolly Andrews, and VP Joseph. Broadside coupled split ring resonator as a sensitive tunable sensor for efficient detection of mechanical vibrations. Sensing and Imaging, 20(1):17, 2019.

[89] Sikha K Simon, Sreedevi P Chakyar, Anju Sebastian, Jolly Andrews, and VP Joseph. Direct amplitude modulation technique using metamaterial broadside coupled split ring resonator (bcsrr) structure. In 2019 Thirteenth International Congress on Artificial Materials for Novel Wave Phenomena (Metamaterials), pages X–390. IEEE, 2019.

[90] Anju Sebastian, Sikha K Simon, Sreedevi P Chakyar, Jovia Jose, VP Joseph, and Jolly Andrews. Broadside coupled split ring resonator metamaterial structure for sensitive measurement of liquid concentrations. In AIP Conference Proceedings, volume 2082, page 070002. AIP Publishing, 2019.

[91] Anju Sebastian, Sreedevi P Chakyar, C Bindu, VP Joseph, and Jolly Andrews. Rotation sensor based on near field perturbations of metamaterial split ring resonator. In 2019 Thirteenth International Congress on Artificial Materials for Novel Wave Phenomena (Metamaterials), pages X–378. IEEE, 2019.

[92] Hazel Thomas, Sreedevi P Chakyar, and Jolly Andrews. Transmission line coupled split ring resonator as dielectric thickness sensor. In AIP Conference Proceedings, volume 1849, page 020003. AIP Publishing, 2017.

[93] Christian Debus and Peter Haring Bolivar. Frequency selective surfaces for high sensitivity terahertz sensing. Applied Physics Letters, 91(18):184102, 2007.

[94] Farhad Bayatpur and Kamal Sarabandi. Single-layer high-order miniaturized-element frequency-selective surfaces. IEEE Transactions on Microwave Theory and Techniques, 56(4):774–781, 2008.

[95] Farhad Bayatpur and Kamal Sarabandi. Tuning performance of metamaterial-based frequency selective surfaces. IEEE Transactions on Antennas and Propagation, 57(2):590–592, 2009.

[96] Farhad Bayatpur and Kamal Sarabandi. A tunable metamaterial frequency-selective surface with variable modes of operation. IEEE Transactions on Microwave Theory and Techniques, 57(6):1433–1438, 2009.

[97] Homayoon Oraizi and Majid Afsahi. Design of metamaterial multilayer structures as frequency selective surfaces. Progress In Electromagnetics Research, 6:115–126, 2009.

[98] Safiullah Khan and Thomas F Eibert. A multifunctional metamaterial-based dual-band

isotropic frequency-selective surface. IEEE Transactions on Antennas and Propagation, 66(8):4042–4051, 2018.

[99] Sreedevi P Chakyar, Sikha K. Simon, C Bindu, Jolly Andrews, and VP Joseph. Complex permittivity measurement using metamaterial split ring resonators. Journal of Applied Physics, 121(5):054101, 2017.

[100] Erick Reyes-Vera, G Acevedo-Osorio, Mauricio Arias-Correa, and David E Senior. A submersible printed sensor based on a monopole-coupled split ring resonator for permittivity characterization. Sensors, 19(8):1936, 2019.

[101] Kuiwen Xu, Yang Liu, Shichang Chen, Peng Zhao, Liang Peng, Linxi Dong, and Gaofeng Wang. Novel microwave sensors based on split ring resonators for measuring permittivity. IEEE Access, 6:26111–26120, 2018.

[102] Rammah Ali Alahnomi, Zahriladha Zakaria, Eliyana Ruslan, Siti Rosmaniza Ab Rashid, and Amyrul Azuan Mohd Bahar. High-q sensor based on symmetrical split ring resonator with spurlines for solids material detection. IEEE Sensors Journal, 17(9):2766–2775, 2017.

[103] Muhammed Said Boybay and Omar M Ramahi. Material characterization using complementary split-ring resonators. IEEE Transactions on Instrumentation and Measurement, 61(11):3039–3046, 2012.

[104] Chieh-Sen Lee and Chin-Lung Yang. Complementary split-ring resonators for measuring dielectric constants and loss tangents. IEEE Microwave and Wireless Components Letters, 24(8):563–565, 2014.

[105] Chieh-Sen Lee and Chin-Lung Yang. Single compound complementary split-ring resonator for simultaneously measuring permittivity and thickness. In 2014 IEEE MTT-S International Microwave Symposium (IMS2014), pages 1–3. IEEE, 2014.

[106] Chieh-Sen Lee and Chin-Lung Yang. Thickness and permittivity measurement in multilayered dielectric structures using complementary split-ring resonators. IEEE Sensors Journal, 14(3):695–700, 2013.

[107] Peter W Milonni. Fast light, slow light and left-handed light. CRC Press, 2004.

[108] Ricardo Marqués, Francisco Medina, and Rachid Rafii-El-Idrissi. Role of bianisotropy in negative permeability and left-handed metamaterials. Physical Review B, 65(14):144440, 2002.

[109] Juan D Baena, Ricardo Marqués, Francisco Medina, and Jesús Martel. Artificial magnetic metamaterial design by using spiral resonators. Physical review B, 69(1):014402, 2004.

[110] Juan Domingo Baena, Jordi Bonache, Ferran Martin, R Marqués Sillero, Francisco Falcone, Txema Lopetegi, Miguel AG Laso, Joan Garcia-Garcia, Ignacio Gil, M Flores Portillo, et al. Equivalent-circuit models for split-ring resonators and complementary split-ring resonators coupled to planar transmission lines. IEEE transactions on microwave theory and techniques, 53(4):1451–1461, 2005.

[111] MF Wu, FY Meng, Q Wu, J Wu, and LW Li. A compact equivalent circuit model for the srr structure in metamaterials. In 2005 Asia-Pacific Microwave Conference Proceedings, volume 1, pages 4–pp. IEEE, 2005.

[112] Hongsheng Chen, Lixin Ran, Jiangtao Huangfu, Tomasz M Grzegorczyk, and Jin Au Kong. Equivalent circuit model for left-handed metamaterials. Journal of applied physics, 100(2):024915, 2006.

[113] M Shamonin, E Shamonina, V Kalinin, and L Solymar. Resonant frequencies of a split-ring resonator: Analytical solutions and numerical simulations. Microwave and optical technology letters, 44(2):133–136, 2005.

[114] Filiberto Bilotti, Alessandro Toscano, Lucio Vegni, Koray Aydin, K. B. Alici, and E. Ozbay. Equivalent-circuit models for the design of metamaterials based on artificial magnetic inclusions. IEEE Transactions on Microwave Theory and Techniques, 55:2865–2873, 2007.

[115] Tie-Jun Cui, Hui-Feng Ma, Ruo Peng Liu, Bo Zhao, Qiang Cheng, and Jessie Yao Chin. A symmetrical circuit model describing all kinds of circuit metamaterials. Progress In Electromagnetics Research, 5:63–76, 2008.

[116] P Yasar-Orten, E Ekmekci, and G Turhan-Sayan. Equivalent circuit models for split-ring resonator arrays. In PIERS Proceedings, pages 534–537, 2010.

[117] O Sydoruk, E Tatartschuk, E Shamonina, and L Solymar. Analytical formulation for the resonant frequency of split rings. Journal of applied physics, 105(1):014903, 2009.

[118] Joseph Helszajn and David S James. Planar triangular resonators with magnetic walls. IEEE Transactions on Microwave Theory and Techniques, 26(2):95–100, 1978.

[119] A Ittipiboon, R Kumar Mongia, YMM Antar, P Bhartia, and M Cuhaci. Aperture fed rectangular and triangular dielectric resonators for use as magnetic dipole antennas.

Electronics Letters, 29(23):2001–2002, 1993.

[120] Cumali Sabah. Tunable metamaterial design composed of triangular split ring resonator and wire strip for s-and c-microwave bands. Progress In Electromagnetics Research, 22:341–357, 2010.

[121] SS Chaudhury, C Saha, and JY Siddiqui. Triangular split ring resonator backed coplanar wave guide for stop band applications. In The 8th Annual International Conference ATMS, 2015.

[122] Zhang Fu-Li, Zhao Qian, Liu Ya-Hong, Luo Chun-Rong, and Zhao Xiao-Peng. Behaviour of hexagon split ring resonators and left-handed metamaterials. Chinese Physics Letters, 21(7):1330, 2004.

[123] Neema C Babu and Sreedevi K Menon. Analysis of hexagonal split ring resonator. In Progress in Electromagnetic Research Symposium (PIERS), pages 3478–3481. IEEE, 2016.

[124] Nornikman Hassan, Badrul Hisham Ahmad, Mohamad Zoinol, and Zahriladha Zakaria. Microstrip patch antenna with a complementary unit of rhombic split ring resonator (r-srr) structure. World Applied Sciences Journal, 21:85–90, 2013.

[125] Carolin Reimann, Margarita Puentes, Matthias Maasch, Frank Hübner, Babak Bazrafshan, Thomas Vogl, Christian Damm, and Rolf Jakoby. Planar microwave sensor for theranostic therapy of organic tissue based on oval split ring resonators. Sensors, 16(9):1450, 2016.

[126] Ricardo Marqués, Francisco Mesa, Jesus Martel, and Francisco Medina. Comparative analysis of edge-and broadside-coupled split ring resonators for metamaterial design-theory and experiments. IEEE Transactions on Antennas and Propagation, 51(10):2572–2581, 2003.

[127] E Ekmekci, RD Averitt, and G Turhan-Sayan. Effects of substrate parameters on the resonance frequency of double-sided srr structures under two different excitations. In PIERS Proceedings, pages 538–540, 2010.

[128] Zhongyan Sheng and Vasundara V Varadan. Tuning the effective properties of metamaterials by changing the substrate properties. Journal of applied physics, 101(1):014909, 2007.

[129] Evren Ekmekci and Gonul Turhan-Sayan. Comparative investigation of resonance characteristics and electrical size of the double-sided srr, bc-srr and conventional srr type

metamaterials for varying substrate parameters. Progress In Electromagnetics Research, 12:35–62, 2009.

[130] Evren Ekmekci, Andrew C Strikwerda, Kebin Fan, G Keiser, X Zhang, G Turhan-Sayan, and RD Averitt. Frequency tunable terahertz metamaterials using broadside coupled split-ring resonators. Physical Review B, 83(19):193103, 2011.

[131] Evren Ekmekci and Gonul Turhan-Sayan. Reducing the electrical size of magnetic metamaterial resonators by geometrical modifications: A comparative study for single-sided and double-sided multiple srr, spiral and u-spiral resonators. In Antennas and Propagation Society International Symposium, 2008. AP-S 2008. IEEE, pages 1–4. IEEE, 2008.

[132] Jiafu Wang, Shaobo Qu, Jieqiu Zhang, Hua Ma, Yiming Yang, Chao Gu, Xiang Wu, and Zhuo Xu. A tunable left-handed metamaterial based on modified broadside-coupled split-ring resonators. Progress In Electromagnetics Research Letters, 6:35–45, 2009.

[133] J Machac, J Zehentner, and M Blaha. Coupling of split ring resonators in a mu-negative volumetric metamaterial. In 2008 IEEE MTT-S International Microwave Symposium Digest, pages 327–330. IEEE, 2008.

[134] Gaurav Bisht and Usha Kiran. Csrr loaded microstrip transmission line with stopband characteristics. In 2016 International Conference on Wireless Communications, Signal Processing and Networking (WiSPNET), pages 293–296. IEEE, 2016.

[135] Raghuraman Selvaraju, Mohd H Jamaluddin, Muhammad Ramlee Kamarudin, Jamal Nasir, and Muhammad H Dahri. Complementary split ring resonator for isolation enhancement in 5g communication antenna array. 2018.

[136] Ali F Almutairi, Mohammad Shahidul Islam, Md Samsuzzaman, Md Tarikul Islam, Norbahiah Misran, and Mohammad Tariqul Islam. A complementary split ring resonator based metamaterial with effective medium ratio for c-band microwave applications. Results in Physics, 15:102675, 2019.

[137] Mohammad Arif Hussain Ansari, Abhishek Kumar Jha, and Mohammad Jaleel Akhtar. Design and application of the csrr-based planar sensor for noninvasive measurement of complex permittivity. IEEE Sensors Journal, 15(12):7181–7189, 2015.

[138] Ahmed Salim and Sungjoon Lim. Complementary split-ring resonator-loaded microfluidic ethanol chemical sensor. Sensors, 16(11):1802, 2016.

[139] Jaswinder Guide Kaur et al. Investigation ff Microstrip Patch Antenna Using Comple-

mentary Split Ring Resonators for Wireless Applications. PhD thesis, 2014.

[140] O Turkmen, E Ekmekci, and G Turhan-Sayan. A new multi-ring srr type metamaterial design with multiple magnetic resonances. In Progress in Electromagnetic Research Symposium, 2011.

[141] Filiberto Bilotti, Alessandro Toscano, and Lucio Vegni. Design of spiral and multiple split-ring resonators for the realization of miniaturized metamaterial samples. IEEE transactions on antennas and propagation, 55(8):2258–2267, 2007.

[142] M Jagadish and AS Pradeep. Design of hexagonal shaped split ring resonator for multi-resonant behaviour. onfring International Journal of Research in Communication Engineering, Vol., Special Issue, 2016.

[143] Imene Sassi, Larbi Talbi, and Khelifa Hettak. Compact multi-band filter based on multi-ring complementary split ring resonators. Progress in Electromagnetics Research, 57:127–135, 2015.

[144] W Fu, ER Lopez, WST Rowe, and K Ghorbani. A planar dual-arm equiangular spiral antenna. IEEE Transactions on Antennas and Propagation, 58(5):1775–1779, 2010.

[145] G-L Dai and M-Y Xia. An investigation of quarter-wavelength square-spiral resonator and its applications to miniaturized bandpass filters. Journal of Electromagnetic Waves and Applications, 24(10):1303–1313, 2010.

[146] Anju Pradeep, S Mridula, and P Mohanan. High security identity tags using spiral resonators. Computers, Materials & Continua, 52(3):185–195, 2016.

[147] Zunfu Jiang, PS Excell, and ZM Hejazi. Calculation of distributed capacitances of spiral resonators. IEEE Transactions on Microwave Theory and Techniques, 45(1):139–142, 1997.

[148] Behnood G Ghamsari, John Abrahams, Stephen Remillard, and Steven M Anlage. High-temperature superconducting spiral resonator for metamaterial applications. IEEE Transactions on Applied Superconductivity, 23(3):1500304–1500304, 2012.

[149] Di Wu, Bin Wei, Bo Li, Xu-Bo Guo, Xin-Xiang Lu, and Bi-Song Cao. Compact wide stopband superconducting bandpass filter using modified spiral resonators with interdigital structure. Chinese Physics B, 27(6):068502, 2018.

[150] Irfan Bulu, Humeyra Caglayan, and Ekmel Ozbay. Experimental demonstration of labyrinth-based left-handed metamaterials. Optics express, 13(25):10238–10247, 2005.

[151] Irfan Bulu, Humeyra Caglayan, and Ekmel Ozbay. Experimental demonstration of subwavelength focusing of electromagnetic waves by labyrinth-based two-dimensional metamaterials. Optics letters, 31(6):814–816, 2006.

[152] Ekmel Ozbay, Irfan Bulu, and Humeyra Caglayan. Transmission, refraction, and focusing properties of labyrinth based left-handed metamaterials. Physica Status Solidi-B-Basic Solid State Physics, 244(4):1202, 2007.

[153] Ekmel Ozbay, Irfan Bulu, and Humeyra Caglayan. Labyrinth-based left-handed metamaterials and subwavelength focusing of electromagnetic waves. In Photonic Crystal Materials and Devices IV, volume 6128, page 612813. International Society for Optics and Photonics, 2006.

[154] JS Dong, LP Yan, CJ Liu, and KM Huang. Design of a coplanar labyrinth-based left handed material and its application to horn antennas. Journal of Electromagnetic Waves and Applications, 23(17-18):2373–2384, 2009.

[155] R Marqués, JD Baena, J Martel, F Medina, F Falcone, M Sorolla, and F Martín. Novel small resonant electromagnetic particles for metamaterial and filter design. In Proc. Electromagnetics in Advanced Applications Int. Conf, pages 439–442, 2003.

[156] Hongsheng Chen, Lixin Ran, Jiangtao Huangfu, Xianmin Zhang, Kangsheng Chen, Tomasz M Grzegorczyk, and Jin Au Kong. Left-handed materials composed of only s-shaped resonators. Physical Review E, 70(5):057605, 2004.

[157] Hongsheng Chen, Lixin Ran, Jiangtao Huangfu, Xianmin Zhang, Kangsheng Chen, Tomasz M Grzegorczyk, and Jin Au Kong. Negative refraction of a combined double s-shaped metamaterial. Applied Physics Letters, 86(15):151909, 2005.

[158] MF Khan and MJ Mughal. Tuned s-shaped resonators. In Microwave, Antenna, Propagation and EMC Technologies for Wireless Communications, 2007 International Symposium on, pages 1017–1019. IEEE, 2007.

[159] MF Khan and MJ Mughal. Design of tunable metamaterials by varying the height of rings of s-shaped resonator. In Electrical Engineering, 2009. ICEE'09. Third International Conference on, pages 1–4. IEEE, 2009.

[160] Hayet Benosman and Nouredine Boukli Hacene. Design and simulation of double" s" shaped metamaterial. International Journal of Computer Science Issues (IJCSI), 9(2):534, 2012.

[161] Ali K Horestani, Miguel Durán-Sindreu, Jordi Naqui, Christophe Fumeaux, Ferran

Martı, et al. S-shaped complementary split ring resonators and their application to compact differential bandpass filters with common-mode suppression. IEEE Microwave and Wireless Components Letters, 24(3):149–151, 2014.

[162] Ali Karami Horestani, Zahra Shaterian, Jordi Naqui, Ferran Martín, and Christophe Fumeaux. Reconfigurable and tunable s-shaped split-ring resonators and application in band-notched uwb antennas. IEEE transactions on antennas and propagation, 64(9):3766–3776, 2016.

[163] Alana Mauluidy Soehartono, Aaron David Mueller, Landobasa Yosef Mario Tobing, Kok Ken Chan, Dao Hua Zhang, and Ken-Tye Yong. Ultra-small v-shaped gold split ring resonators for biosensing using fundamental magnetic resonance in the visible spectrum. Nanotechnology, 28(40):405305, 2017.

[164] C Sabah. Multi-resonant metamaterial design based on concentric v-shaped magnetic resonators. Journal of Electromagnetic Waves and Applications, 26(8-9):1105–1115, 2012.

[165] Sumer S Singhwal, Binod K Kanaujia, Ajit Singh, and Jugul Kishor. Circularly polarized v-shaped dielectric resonator antenna. International Journal of RF and Microwave Computer-Aided Engineering, page e21832.

[166] Mamdouh MI Saadoun and Nader Engheta. A reciprocal phase shifter using novel pseudochiral or ω medium. Microwave and optical technology letters, 5(4):184–188, 1992.

[167] Constantin R Simovski and Sailing He. Frequency range and explicit expressions for negative permittivity and permeability for an isotropic medium formed by a lattice of perfectly conducting ω particles. Physics letters A, 311(2-3):254–263, 2003.

[168] Jiangtao Huangfu, Lixin Ran, Hongsheng Chen, Xian-min Zhang, Kangsheng Chen, Tomasz M Grzegorczyk, and Jin Au Kong. Experimental confirmation of negative refractive index of a metamaterial composed of ω-like metallic patterns. Applied Physics Letters, 84(9):1537–1539, 2004.

[169] Vasundara V Varadan and Sravanthi Penumarthy. Negative index and reciprocal behavior using resonances of omega image pairs. URSI general assembly, New Delhi, India, 2005.

[170] Vasundara V Varadan, Ruyen Ro, and Sravanthi Penumarthy. Switching of electrical and magnetic resonances in omega structures by a reflection operation experimental

studies. Microwave and Optical Technology Letters, 48(12):2624–2629, 2006.

[171] Sergei A Tretyakov, Constantin R Simovski, and M Hudlička. Bianisotropic route to the realization and matching of backward-wave metamaterial slabs. Physical Review B, 75(15):153104, 2007.

[172] Koray Aydin, Zhaofeng Li, M Hudlička, SA Tretyakov, and Ekmel Ozbay. Transmission characteristics of bianisotropic metamaterials based on omega shaped metallic inclusions. New Journal of Physics, 9(9):326, 2007.

[173] Koray Aydin, Zhaofeng Li, Serafettin Bilge, and Ekmel Ozbay. Experimental and numerical study of omega type bianisotropic metamaterials combined with a negative permittivity medium. Photonics and Nanostructures-Fundamentals and Applications, 6(1):116–121, 2008.

[174] Michel Audrey Abaga Abessolo, Ahmed El Moussaoui, and Noura Aknin. Dual-band monopole antenna with omega particles for wireless applications. Progress In Electromagnetics Research, 24:27–34, 2011.

[175] Mondher Labidi, Ridha Salhi, and Fethi Choubani. A design of metamaterial multiband bowtie antenna based on omega-shaped resonator. Applied Physics A, 123(5):313, 2017.

[176] L La Spada, F Bilotti, and L Vegni. Metamaterial-based design of biological sensors operating at thz frequencies. In Proceedings of the Fifth International Congress on Advanced Electromagnetic Materials in Microwaves and Optics–Metamaterials, Barcelona, Spain, pages 10–15, 2011.

[177] Hairun Chen, Bin Yang, Yan Gui, Jiaqi Niu, and Jingquan Liu. Hollow complementary omega-ring-shaped metamaterial modulators with dual-band tunability. Optics letters, 43(16):3913–3916, 2018.

[178] Koray Aydin, Irfan Bulu, Kaan Guven, Maria Kafesaki, Costas M Soukoulis, and Ekmel Ozbay. Investigation of magnetic resonances for different split-ring resonator parameters and designs. New journal of physics, 7(1):168, 2005.

[179] K Aydin and E Ozbay. Identifying magnetic response of split-ring resonators at microwave frequencies. Opto-Electronics Review, 14(3):193–199, 2006.

[180] Koray Aydin and Ekmel Özbay. Experimental and numerical analyses of the resonances of split ring resonators. physica status solidi (b), 244(4):1197–1201, 2007.

[181] Philippe Gay-Balmaz and Olivier JF Martin. Efficient isotropic magnetic resonators. Applied Physics Letters, 81(5):939–941, 2002.

[182] Philippe Gay-Balmaz and Olivier JF Martin. Electromagnetic resonances in individual and coupled split-ring resonators. Journal of applied physics, 92(5):2929–2936, 2002.

[183] Yi-Jang Hsu, Yen-Chun Huang, Jiann-Shing Lih, and Jyh-Long Chern. Electromagnetic resonance in deformed split ring resonators of left-handed meta-materials. Journal of applied physics, 96(4):1979–1982, 2004.

[184] Hee-Jo Lee and Jong-Gwan Yook. Biosensing using split-ring resonators at microwave regime. Applied Physics Letters, 92(25):254103, 2008.

[185] Jingbo Sun, Lingyun Liu, Guoyan Dong, and Ji Zhou. An extremely broad band metamaterial absorber based on destructive interference. Optics Express, 19(22):21155–21162, 2011.

[186] En Li, Zai-Ping Nie, Gaofeng Guo, Qishao Zhang, Zhongping Li, and Fengmei He. Broadband measurements of dielectric properties of low-loss materials at high temperatures using circular cavity method. Progress In Electromagnetics Research, 92:103–120, 2009.

[187] Rohat Melik, Emre Unal, Nihan Kosku Perkgoz, Christian Puttlitz, and Hilmi Volkan Demir. Metamaterial based telemetric strain sensing in different materials. Optics express, 18(5):5000–5007, 2010.

[188] Yang Qiu Xu, Pei Heng Zhou, Hui Bin Zhang, Liang Chen, and Long Jiang Deng. A wide-angle planar metamaterial absorber based on split ring resonator coupling. Journal of Applied Physics, 110(4):044102, 2011.

[189] Alexandros Dimitriadis, Nikolaos Kantartzis, and Theodoros Tsiboukis. A polarization-/angle-insensitive, bandwidth-optimized, metamaterial absorber in the microwave regime. Applied Physics A, 109(4):1065–1070, 2012.

[190] Kirsty E Hannam, David A Powell, Ilya V Shadrivov, and Yuri S Kivshar. Tuning the nonlinear response of coupled split-ring resonators. Applied Physics Letters, 100(8):081111, 2012.

[191] ZX Cao, FG Yuan, and LH Li. A super-compact metamaterial absorber cell in l-band. Journal of Applied Physics, 115(18):184904, 2014.

[192] Hasanul Kairm, Diego Delfin, Mohammad Arif Ishtiaque Shuvo, Luis A Chavez, Ce-

sar R Garcia, Jay H Barton, Sara M Gaytan, Monica A Cadena, Raymond C Rumpf, Ryan B Wicker, et al. Concept and model of a metamaterial-based passive wireless temperature sensor for harsh environment applications. IEEE Sensors Journal, 15(3):1445–1452, 2014.

[193] Gabriel Galindo-Romera, Francisco Javier Herraiz-Martínez, Marta Gil, José Juan Martínez-Martínez, and Daniel Segovia-Vargas. Submersible printed split-ring resonator-based sensor for thin-film detection and permittivity characterization. IEEE Sensors journal, 16(10):3587–3596, 2016.

[194] Javier Carnerero-Cano, Gabriel Galindo-Romera, José Juan Martínez-Martínez, and Francisco Javier Herraiz-Martínez. A near-field split-ring resonator-based monopole sensor for permittivity characterization. Multidisciplinary Digital Publishing Institute Proceedings, 1(8):793, 2017.

[195] Betsy George, S Bhuvana Nair, and Sreedevi K Menon. Investigations on edge coupled metamaterial filters. In 2017 International Conference on Wireless Communications, Signal Processing and Networking (WiSPNET), pages 632–635. IEEE, 2017.

[196] Olivier Reynet and O Acher. Voltage controlled metamaterial. Applied Physics Letters, 84(7):1198–1200, 2004.

[197] I Gil, J Garcia-Garcia, J Bonache, F Martin, M Sorolla, and R Marques. Varactor-loaded split ring resonators for tunable notch filters at microwave frequencies. Electronics Letters, 40(21):1347–1348, 2004.

[198] Ignacio Gil, Jordi Bonache, Joan Garcia-Garcia, and Ferran Martin. Tunable metamaterial transmission lines based on varactor-loaded split-ring resonators. IEEE transactions on Microwave theory and techniques, 54(6):2665–2674, 2006.

[199] Adolfo Velez, Jordi Bonache, and Ferran Martín. Varactor-loaded complementary split ring resonators (vlcsrr) and their application to tunable metamaterial transmission lines. IEEE Microwave and wireless components letters, 18(1):28–30, 2008.

[200] K Aydin and E Ozbay. Capacitor-loaded split ring resonators as tunable metamaterial components. Journal of Applied Physics, 101(2):024911, 2007.

[201] Thomas H Hand and Steven A Cummer. Frequency tunable electromagnetic metamaterial using ferroelectric loaded split rings, 2008.

[202] Qian Zhao, Lei Kang, Bo Du, Bo Li, Ji Zhou, Hong Tang, Xiao Liang, and Baizhe Zhang. Electrically tunable negative permeability metamaterials based on nematic

liquid crystals. Applied physics letters, 90(1):011112, 2007.

[203] Shumin Xiao, Uday K Chettiar, Alexander V Kildishev, Vladimir Drachev, IC Khoo, and Vladimir M Shalaev. Tunable magnetic response of metamaterials. Applied Physics Letters, 95(3):033115, 2009.

[204] Lei Kang, Qian Zhao, Hongjie Zhao, and Ji Zhou. Magnetically tunable negative permeability metamaterial composed by split ring resonators and ferrite rods. Optics express, 16(12):8825–8834, 2008.

[205] Lei Kang, Qian Zhao, Hongjie Zhao, and Ji Zhou. Ferrite-based magnetically tunable left-handed metamaterial composed of srrs and wires. Optics Express, 16(22):17269–17275, 2008.

[206] Jiaguang Han and Akhlesh Lakhtakia. Semiconductor split-ring resonators for thermally tunable terahertz metamaterials. Journal of Modern Optics, 56(4):554–557, 2009.

[207] Evren Ekmekci, Kagan Topalli, Tayfun Akin, and Gonul Turhan-Sayan. A tunable multi-band metamaterial design using micro-split srr structures. Optics express, 17(18):16046–16058, 2009.

[208] Francisco Javier Falcone Lanas, Mario Sorolla Ayza, and Ferrán Martín Antolín. Synthesis and applications of microwave metamaterials in planar circuit technology: from electromagnetic bandgaps to left handed materials. Telecomunicaciones. NAFARROAKO UNIBERTSITATE PUBLIKOA IngeniaritzaElektriko eta ElektronikoSaila, 2005.

[209] Mehmet Bayindir, K Aydin, E Ozbay, P Markoš, and CM Soukoulis. Transmission properties of composite metamaterials in free space. Applied Physics Letters, 81(1):120–122, 2002.

[210] Koray Aydin, Kaan Guven, Costas M Soukoulis, and Ekmel Ozbay. Observation of negative refraction and negative phase velocity in left-handed metamaterials. Applied Physics Letters, 86(12):124102, 2005.

[211] Koray Aydin, Kaan Guven, Maria Kafesaki, Lei Zhang, Costas M Soukoulis, and Ekmel Ozbay. Experimental observation of true left-handed transmission peaks in metamaterials. Optics Letters, 29(22):2623–2625, 2004.

[212] Koray Aydin, Kaan Guven, Nikos Katsarakis, Costas M Soukoulis, and Ekmel Ozbay. Effect of disorder on magnetic resonance band gap of split-ring resonator structures. Optics Express, 12(24):5896–5901, 2004.

[213] Fumiaki Miyamaru, Mitsuo Wada Takeda, and Kazuo Taima. Characterization of terahertz metamaterials fabricated on flexible plastic films: toward fabrication of bulk metamaterials in terahertz region. Applied Physics Express, 2(4):042001, 2009.

[214] P Menon Ragi, KS Umadevi, Paul Nees, Jovia Jose, MV Keerthy, and VP Joseph. Flexible split-ring resonator metamaterial structure at microwave frequencies. Microwave and Optical Technology Letters, 54(6):1415–1416, 2012.

[215] E Ekmekci and G Turhan-Sayan. Sensitivity of the resonance characteristics of srr and dsrr (double-sided srr) type metamaterials to the changes in substrate parameters and the usefulness of dsrr structure for reduced electrical size. In PIERS Proceedings, pages 598–602, 2008.

[216] David J Griffiths. Introduction to electrodynamics. Prentice Hall New Jersey, 1962.

List of Publications

1. **K. S. Umadevi**, Sikha K. Simon, Sreedevi P. Chakyar, Jolly Andrews and V. P. Joseph, *Wide band microwave absorber using flexible broadside coupled split ring resonator metamaterial structure*, Proceedings of 2019 Thirteenth International Congress on Artificial Materials for Novel Wave Phenomena (Metamaterials), Rome, Italy, pp.X-453 - X-455, IEEE Explore, doi: 10.1109/MetaMaterials.2019.8900801

2. **K. S. Umadevi**, Sreedevi P. Chakyar, Sikha K. Simon, Jolly Andrews, and V. P. Joseph, *Split ring resonators made of conducting wires for performance enhancement*, Euro Physics Letters (IOP Science), **118**, 24002, 2017, doi: 10.1209/0295-5075/118/24002.

3. Ragi.P.Menon, **K. S. Umadevi**, Nees Paul, Jovia Jose, M.V.Keerthy and V.P.Joseph, *Flexible split ring resonator metamaterial structure at microwave frequencies*, Microwave and Optical Technology Letters (Wiley Publishers),**Vol.54, no.6**, pp.1415-1416, 2012, doi: 10.1002/mop.26814.

4. **K. S. Umadevi** and V. P. Joseph, *Experimental studies on the effect of substrate dielectric*

constant on the resonant frequency of split-ring resonator metamaterial structure , International Journal of Science and Research (IJSR), **Vol.3, no.7**, pp.132-135, 2014,

5. Nees Paul, Sreedevi P. Chakyar, **K. S. Umadevi**, Simon K. Sikha, Joe Kizhakooden, Jolly Andrews, V. P. Joseph, *Humidity sensitive flexible microwave absorbing sheet using polyaniline–Polytetrafluoroethylene composite*, Arabian Journal for Science and Engineering, 22 June 2018, doi: 10.1007/s13369-018-3402-0.

6. Joe Kizhakooden, Jovia Jose, Nees Paul, Sreedevi P. Chakyar, Anju Sebastian, Sikha K. Simon, **K. S. Umadevi**, C. Bindu, Jolly Andrews and V. P. Joseph, *Broadside coupled split ring resonator based multiband monopole patch antenna for wireless communication applications*, AIP Conference Proceedings, 020068, 2019, doi: 10.1063/1.5130278.

7. C. Bindu, Sreedevi P. Chakyar, Anju Sebastian, Sikha K. Simon, Jovia Jose, Nees Paul, **K. S. Umadevi**, Joe Kizhakooden, Jolly Andrews, and V. P. Joseph, *Enhancing the resolution in imaging using folded metamaterial split ring resonator structure at microwave frequencies*, AIP Conference Proceedings 2162, 020067, 2019, doi: 10.1063/1.5130277.

8. Jovia Jose, Sikha K. Simon, Anju Sebastian, Sreedevi P. Chakyar, Joe Kizhakooden, Nees Paul, C. Bindu, **K. S. Umadevi**, Jolly Andrews, and V. P. Joseph, *Scattering from artificial plasma cylinder using nonstandard FDTD*, AIP Conference Proceedings 2162, 020069, 2019, doi:10.1063/1.5130279.

9. Nees Paul, Janet Jimmy, Sreedevi P. Chakyar, Sikha K. Simon, Joe Kizhakooden, C. Bindu, Anju Sebastian, **K. S. Umadevi**, Jovia Jose, Jolly Andrews, and V. P. Joseph, *Microwave absorption properties of flexible zinc oxide sheet* , AIP Conference Proceedings 2162, 020070. 2019, doi: 10.1063/1.5130280.

10. **K. S. Umadevi** and V. P. Joseph, *Experimental studies on the tunable characteristics of a flexible broad side-coupled split ring resonator metamaterial structures*, Proceedings of the National conference on Emerging Vistas of Engineering and Management, Viswajyothi College of Engineering and Technology, Vazhakulam, 2014.

11. **K. S. Umadevi** and V. P. Joseph, *Resonant Properties of Wire SRR*, Andromeda, Multi Disciplinary Journal, Vol.1, no.1, pp. 55-58, 2015.

12. **K. S. Umadevi** and V. P. Joseph, *An Efficient method for finding the Resonance properties of Split Ring Resonator*, Proceedings of the National Seminar on Materials for Electromagnetic Applications, Christ College, Irinjalakuda, 2011.

Conference Presentations

1. Wide band microwave absorber using flexible broadside coupled split ring resonator metamaterial structure, **2019 Thirteenth International Congress on Artificial Materials for Novel Wave Phenomena - Metamaterials, Rome, Italy, 16th September -21st September 2019** (Presented by the Research Supervisor).

2. Experimental studies on the tunable characteristics of a flexible broad side-coupled split ring resonator metamaterial structures, **National conference on Emerging Vistas of Engineering and Management, Viswajyothi College of Engineering and Technology, Vazhakulam, 24th and 25th November 2014** (Presented by the Research Supervisor).

3. Automation of Gunn Diode for microwave frequency Scanning, **National Seminar on Electronics EIKOS 2009, Prajyoti Niketan College, Pudukad, 13th November 2009**.

4. An Efficient method for finding the Resonance properties of Split Ring Resonator, **National Seminar on Materials for Electromagnetic Applications, Christ College, Irinjalakuda, 29, 30, November 2011**.

5. Effect of substrate Dielectric constant on the resonant frequency of Broad-side coupled

Split ring resonator metamaterial structure, **National Seminar on Electroceramics, St. Aloysius College, Elthuruthu, Thrissur, 24th, 25th February 2014**.

6. A novel flexible negative permeability metamaterial structure made of conducting wires, **3rd International Conference on Competency Building Strategies in Business and Technology for Sustainable Development Sri Ganesh School of Business Management, Salem, 25th February 2014**.

7. Flexible Wire Split Ring Resonator Metamaterial Structure (WSRR) for Frequency Selective Applications, **National Seminar on Materials, Methods and Sensors for Electromagnetic Applications, 24th, 25th January 2019**.

Selected Publications

A Letters Journal Exploring the Frontiers of Physics

April 2017

EPL, **118** (2017) 24002 www.epljournal.org
doi: 10.1209/0295-5075/118/24002

Split ring resonators made of conducting wires for performance enhancement

K. S. Umadevi[1,3], Sreedevi P. Chakyar[2], Sikha K. Simon[2], Jolly Andrews[2] and V. P. Joseph[2]

[1] *Department of Physics, Newman College, Mahathma Gandhi University - Thodupuzha, Kerala, India*
[2] *Department of Physics, Christ College (Autonomous), University of Calicut - Irinjalakuda, Kerala, India*
[3] *Department Electronics, Prajyoti Niketan College, University of Calicut - Thrissur, Kerala, India*

received 28 January 2017; accepted in final form 8 June 2017
published online 26 June 2017

PACS 41.20.Jb – Electromagnetic wave propagation; radiowave propagation
PACS 42.60.Da – Resonators, cavities, amplifiers, arrays, and rings

Abstract – This paper introduces a negative permeability metamaterial structure —Wire Split Ring Resonator (WSRR)— constructed using conducting wires and experimentally investigates its tunable properties at microwave frequencies. The structure is fabricated by fixing conducting rings made of copper wires on a thin flexible polymer film. The resonance properties of a single WSRR are studied by placing it between two monopole antennas connected to a vector network analyser. For the analysis of bulk samples, two horn antennas are used. The structure shows strong magnetic response with high-quality factor and is observed to be very sensitive to parameter variations. A comparitive study with conventional SRR is made and the results are verified by simulation. The proposed WSRR structure is easy to construct and is superior to conventional SRR in frequency selective and tunable applications.

Introduction. – The emerging field of metamaterials has significantly raised the interest of researchers in various fields of science and engineering due to its unique properties and manifold applications. This new class of artificially engineered materials with negative parameters (permeability μ, permittivity ϵ and refractive index n) may be even described as the material of the millennium. The realisation of this negative refractive index material by Smith *et al.* in 2000 has triggered immense research activities in this new field [1].

The two constituents of negative-index metamaterial structures are negative permeability and permittivity counterparts. The first negative permeability structure called Split Ring Resonator (SRR) was proposed by Pendry [2]. SRR which is also called Edge Coupled SRR (ECSRR) is usually fabricated on planar dielectric substrates. As the name suggests, they consist of two concentric metallic flat rings of circular or rectangular shape with negligible thickness each having small splits situated at opposite ends. Resonance properties of such metamaterial structures entirely depend upon their structure, substrate and other dielectric environments [3–8].

In order to overcome the limitations of SRR-like bianisotropy, lower limit for resonant frequency, etc., several other designs have been proposed and analysed. Broad side Coupled SRR (BCSRR) proposed in 2002 [9] is one among the most explored structures. The two rings of the BCSRR are fabricated on either sides of the substrate coaxially with the splits at opposite ends. Studies have shown that BCSRR has smaller resonant frequency, higher Q value, smaller electrical size and higher isotropy in the plane of the structure than the ECSRR [10,11]. Another structure called Double sided SRR (DSRR), studied by different researchers, is a mixture of both ECSRR and BCSRR, where two ECSRRs are placed on the two sides of a dielectric substrate [12]. A comparative study using numerical simulation of SRR, DSRR and BCSRR structures showed that DSRR can provide better miniaturization and have wider half-power bandwidth as compared to conventional SRR (ECSRR) [5]. Effects of substrate parameters on resonant frequency of DSRR structures under magnetic and electrical excitations are also investigated [13].

Other types of SRR structures explored are Complimentary SRR (CSRR), multiple ring SRR and labyrinth-based metamaterial structures [14–17]. Some other structures of different forms like S-shaped, V-shaped, C-shaped and Ω-shaped resonators are also attempted [18–23].

In this paper we propose a new split ring resonator structure, named as Wire Split Ring Resonator (WSRR),

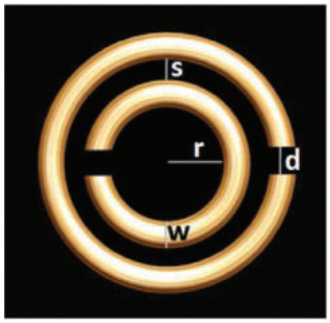

Fig. 1: (Colour online) Schematic representation of the proposed Wire Split Ring Resonator (WSRR) with structural parameters.

constructed using thin metallic wires. Even though the shape of this structure is similar to conventional SRR, its theoretical analysis and resonant properties show a marked deviation from the conventional one. The highlight of this proposed novel structure is that they are fabricated devoid of any solid substrate which makes it self-standing and thereby avoiding the constraints associated with a supporting substrate and hence the intrinsic resonant properties of the SRR can be directly obtained. The changes induced on the resonant frequency due to the interaction of the excitation field with the supportive dielectric substrate of the existing SRRs are avoided here. Any conventional SRR, if fabricated without a rigid substrate with the intention to use it in the field of sensors, is prone to sudden changes in resonant frequencies for even minor structural fluctuations because of its thin metallisation. This limitation is avoided in the case of WSRR due to the comparatively rigid nature of the wire metallisation. This may also lead to possible applications in various fields where our WSRR can be used as a movable sensor probe. Since wires are used for the fabrication of the proposed SRR, structural refinements aiming at frequency tunability can be more easily realized. Here we analyse the resonant behaviour of the proposed WSRR by varying its structural parameters and make a comparative analysis with the resonant properties of the conventional SRR along with its confirmation by simulation.

Design and fabrication of the structure. – In the presence of the magnetic-field components of an external applied electromagnetic wave, the SRR structure undergoes resonant absorption. The resonant frequency f in terms of the total capacitance C between the rings and the effective inductance L can be obtained using the equation

$$f = \frac{1}{2\pi\sqrt{LC}}. \tag{1}$$

The schematic representation of the proposed WSRR unit cell is shown in fig. 1. The structural parameters are inner radius r, diameter of wire w, spacing between rings s and split width d. The fabrication method of this negative permeability structure is quite simple compared

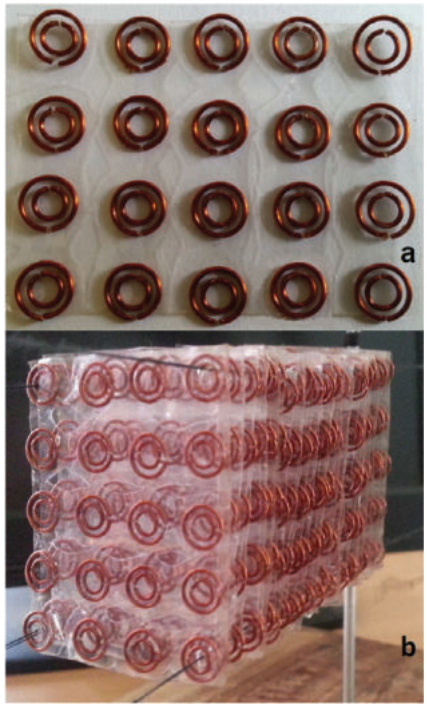

Fig. 2: (Colour online) Photograph of the WSRR constructed with structural parameters $w = 0.4\,\text{mm}$, $r = 1.68\,\text{mm}$, $s = 0.5\,\text{mm}$, $d = 0.5\,\text{mm}$. (a) Two dimensional array with periodicity of $10\,\text{mm} \times 10\,\text{mm}$; (b) bulk medium with periodicity of $10\,\text{mm} \times 10\,\text{mm} \times 10\,\text{mm}$.

to other SRR structures since no procedures like photo masking, chemical etching, etc., are involved. The WSRR unit cells are constructed using small pieces of copper wires bent into the form of split rings using a cylindrical-cavity–shaped mold and fixing them on a thin adhesive polymer film. The flexibility of the polymer film is an added advantage of the structure. WSRR unit cells having different inner radii and gap distances are constructed using copper wires of diameter 0.4 mm, 0.5 mm, 0.6 mm, 0.7 mm and 0.8 mm. The thickness of the supporting polymer film used is 18 μm. The WSRR units are fixed periodically on the polymer sheet in the form of two-dimensional array. Such layers are arranged side by side to form a two-dimensional bulk WSRR medium. The photograph of the WSRR units constructed in planar and bulk form are given in fig. 2. We can reduce the small asymmetries observed in the structure by employing any standard engineering procedures. For comparing the resonance behaviour of WSRR with conventional SRR, we fabricated a SRR structure on another piece of the same polymer film. The two flat rings of the conventional SRR are fabricated by the chemical etching process using a thin copper sheet of 20 μm thickness [7].

Measurements and results. – Two monopole antennas connected to a Vector Network Analyser (VNA) are used to study the transmission properties of the WSRR unit cell structure [4,24]. Figure 3(a) depicts a schematic representation of the experimental arrangement with the

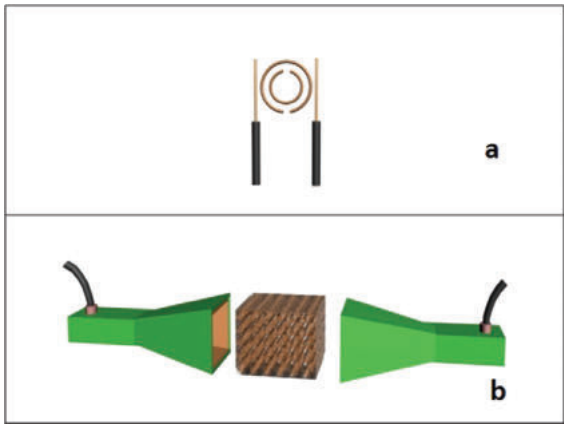

Fig. 3: (Colour online) Schematic representation of the experimental setup: (a) single WSRR between transmitting and receiving probes; (b) bulk WSRR medium placed between transmitting and receiving horn antennas.

WSRR unit cell kept between the transmitting and the receiving probes. For measuring the absorption properties of bulk WSRR medium, a sample of dimension 50 mm × 40 mm × 100 mm is placed between two horn antennas, one acts as the transmitter and the other as the receiver (fig. 3(b)).

Transmission spectra. The measured transmission spectra of a typical WSRR unit cell is shown in fig. 4(a). The geometrical parameters of the structure are $r = 2.45\,\text{mm}$, $s = 0.8\,\text{mm}$, $w = 0.7\,\text{mm}$ and $d = 0.5\,\text{mm}$. The result shows sharp resonant absorption of power at 3.64 GHz. For comparative study, a conventional SRR structure with the same values for r, s and d is fabricated. The width of the conventional SRR is taken equal to the wire diameter w of the WSRR. The resonant graph of the equivalent SRR is shown along with that of the WSRR in fig. 4(a). It is evident from the figure that the bandwidth of the WSRR is quite smaller than that of the SRR which is indicative of a high-Q resonance performance. The verification of experimental results by simulation is performed using Ansoft HFSS and both results are found quite in agreement (fig. 4(b)). Figure 5 gives transmission spectra obtained for the bulk medium which also shows strong absorption dip (5.39 GHz). Structural parameters selected for fabricating the bulk medium are $w = 0.4\,\text{mm}$, $r = 1.68\,\text{mm}$, $s = 0.5\,\text{mm}$, $d = 0.5\,\text{mm}$ and periodicity is 10 mm × 10 mm × 10 mm.

Effect of structural parameters. Absorption curves of different WSRR units with varying values for w, r and s are examined and the effects of these structural parameters on the resonance frequency are analysed.

The split width d is kept constant (0.5 mm) since its effect on resonance frequency is comparably less. The variation of resonance frequency with inner radius r for two different values of w, by keeping the spacing between the rings s constant is plotted in fig. 6. It shows that irrespectively of the value of w, as r increases the

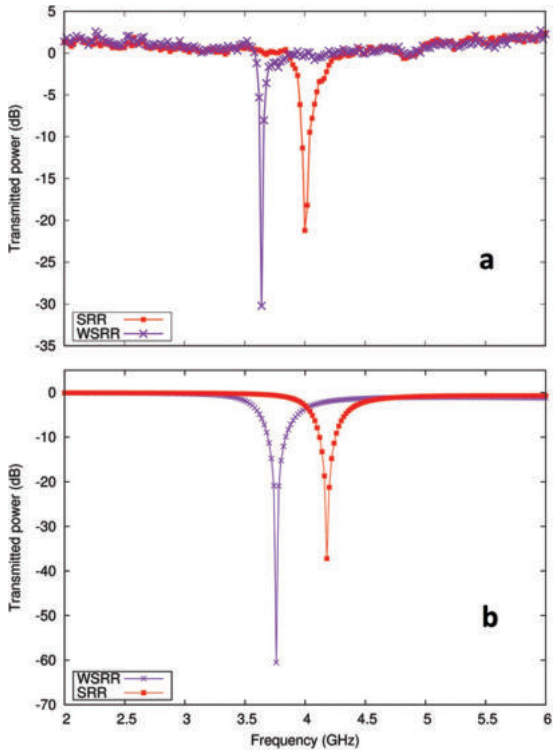

Fig. 4: (Colour online) Transmission spectra of Wire SRR (WSRR) and conventional SRR with the same structural parameters r, s, d and width w equal to the diameter of the wire: (a) experimental, (b) simulation.

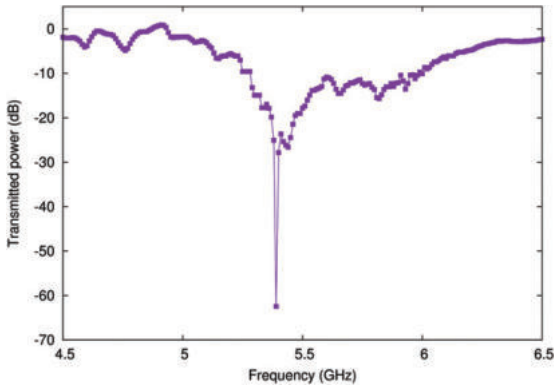

Fig. 5: (Colour online) Experimental transmission spectra of WSRR bulk medium.

resonance frequency decreases —a result similar to conventional SRR [4], but showing higher variations. Figure 7 demonstrates the effect of s on the resonance frequency for different r, when w is kept constant. As s increases, due to the decrease in effective capacitance and mutual inductance between the two rings of SRR, the resonance frequency shifts towards the high-frequency region. This result also is qualitatively similar to that of a conventional SRR. Figure 8 is a similar graph which depicts the dependence of the resonance frequency on the diameter of the wire w. As is evident from the figure, for an increase of

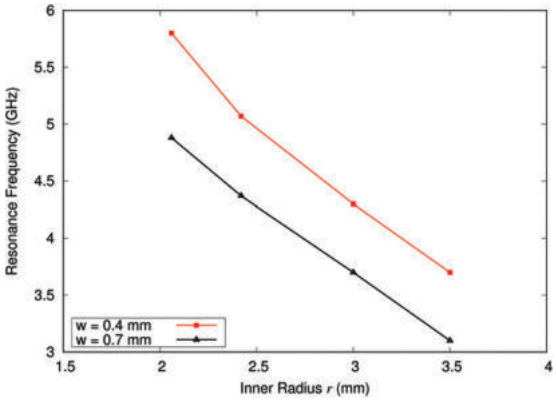

Fig. 6: (Colour online) Variation of resonance frequency of WSRR with inner radius r for two different wire diameters w keeping spacing between the rings s constant (0.97 mm).

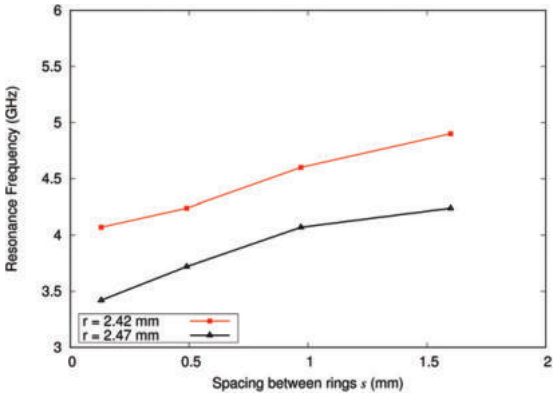

Fig. 7: (Colour online) Variation of resonance frequency of WSRR with the spacing between the rings s for two different inner radii r keeping wire diameter w constant (0.6 mm).

the wire diameter the resonant frequency is seen decreasing. In the case of SRR, the enhancement of the width of the ring results in an increase in the resonant frequency, whereas for the WSRR it behaves oppositely —*i.e.*, as the wire diameter increases the resonant frequency decreases. This may be due to the variation in effective capacitance occurred due to the structural difference between SRR and WSRR.

Significant characteristics of WSRR. – Apart from the above-mentioned variations of structural dependent resonant properties of WSRR in comparison with the conventional SRR, the following points are worth mentioning. WSRR shows a very high Q value compared to SRR of the same structural dimensions where the width is replaced with the diameter of WSRR. This may be due to the higher volume of metallisation of the WSRR leading to increased induced current flow through the rings. Since the cross-sectional area of the WSRR rings is much greater than that of the SRR, the Ohmic loss is very much reduced. Another possible reason which may lead to the enhancement of the Q value can be explained by analysing

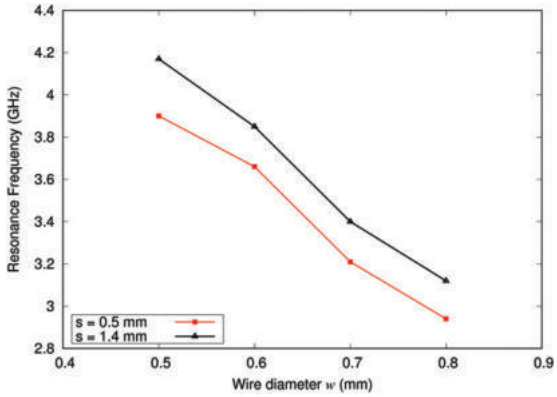

Fig. 8: (Colour online) Variation of resonance frequency of WSRR with wire diameter w for two different values of s keeping inner radius r constant (2.2 mm).

the region of field concentration between the rings of the structure. In the case of conventional SRR, due to the flat nature of the rings the supportive film is in tight contact with the metallisation and a significant portion of the electric field passes through the dielectric [24]. But the capacitance contribution in WSRR is mainly by the curved semi-spherical portions of the rings facing each other and only a minor portion of the field passes through the thin supporting polymer substrate film, which is attached at the bottom part of the SRR ring. So the dielectric loss which adversly influences the quality factor of the resonator is negligibly small for the WSRR case. This new SRR may find potential applications in fields of sensor devices, material characterization studies, frequency selective surfaces, etc. Secondly we noticed that the dependence of structural parameters on the resonant frequency of WSRR is much greater than that of a conventional SRR. This greater tunability of WSRR also finds specific applications in various fields. In addition to this, non-requirement of any solid substrate removes the loss factors and constraints associated with them and thereby enhances the sensitivity of our structure in the external excitation field. The flexibility properties of the film used for fixing the rings in order to maintain the structural parameters of individual units and periodicity of bulk samples is another added advantage in selected fields of applications.

Conclusion. – The fabrication method and resonance characteristics of a novel flexible negative permeability split ring resonator structure made of conducting wires (WSRR) for microwave frequencies are presented. The resonant properties of this proposed structure are analysed both by experiment and simulation. The frequency tunability of WSRR by structural parameter variations is also analysed. A comparative study with conventional SRR shows higher structural dependent frequency tunability for our structure. The other noticeable characteristics of the WSRR are the enhanced quality factor and the absence of any rigid supporting substrate and hence

may have potential applications in the field of sensors, material characterisation studies, etc. Fabrication of this newly proposed metamaterial element is much easier and cost effective. The design may be extended to the fabrication of bulk negative-index metamaterials.

* * *

We are thankful to Prof. K. T. Mathew, Department of Electronics, Cochin University of Science and Technology, for providing us with technical support in performing the simulation works.

REFERENCES

[1] Smith D. R., Padilla W. J., Vier D., Nemat-Nasser S. C. and Schultz S., *Phys. Rev. Lett.*, **84** (2000) 4184.
[2] Pendry J. B., Holden A. J., Robbins D. and Stewart W., *IEEE Trans. Microwave Theory Tech.*, **47** (1999) 2075.
[3] Sheng Z. and Varadan V. V., *J. Appl. Phys.*, **101** (2007) 014909.
[4] Aydin K., Bulu I., Guven K., Kafesaki M., Soukoulis C. M. and Ozbay E., *New J. Phys.*, **7** (2005) 168.
[5] Ekmekci E. and Turhan-Sayan G., *Prog. Electromagn. Res. B*, **12** (2009) 35.
[6] Chakyar S. P., Andrews J. and Joseph V. P., *World Acad. Sci. Eng. Tech. Int. J. Mech. Aerospace Ind. Mechatron. Manuf. Eng.*, **10** (2016) 1030.
[7] Ragi P. M., Umadevi K. S., Nees P., Jose J., Keerthy M. V. and Joseph V. P., *Microwave Opt. Tech. Lett.*, **54** (2012) 1415.
[8] Zhu J., Li D., Yan S., Cai Y., Liu Q. H. and Lin T., *EPL*, **112** (2015) 54002.
[9] Marqués R., Medina F. and Rafii-El-Idrissi R., *Phys. Rev. B*, **65** (2002) 144440.
[10] Lee H.-J., *J. Korean Phys. Soc.*, **55** (2009) 1596.
[11] Marqués R., Mesa F., Martel J. and Medina F., *IEEE Trans. Antennas Propag.*, **51** (2003) 2572.
[12] Sauviac B., Simovski C. and Tretyakov S., *Electromagnetics*, **24** (2004) 317.
[13] Ekmekci E., Averitt R. and Turhan-Sayan G., *Effects of substrate parameters on the resonance frequency of double-sided srr structures under two different excitations*, in *PIERS Proceedings, Cambridge, USA, 2010*, pp. 538–540.
[14] Baena J. D., Bonache J., Martin F., Sillero R. M., Falcone F., Lopetegi T., Laso M. A., Garcia-Garcia J., Gil I., Portillo M. F. *et al.*, *IEEE Trans. Microwave Theory Tech.*, **53** (2005) 1451.
[15] Bilotti F., Toscano A. and Vegni L., *IEEE Trans. Antennas Propag.*, **55** (2007) 2258.
[16] Ozbay E., Bulu I. and Caglayan H., *Phys. Status Solidi B*, **244** (2007) 1202.
[17] Bulu I., Caglayan H. and Ozbay E., *Opt. Express*, **13** (2005) 10238.
[18] Liu Z., Li H., Zhan S., Cao G., Xu H., Yang H. and Xu X., *Opt. Mater.*, **35** (2013) 948.
[19] Ekmekçi E. and Turhan-Sayan G., *Investigation of effective permittivity and permeability of novel v shaped metamaterial using simulated s parameters*, in *Proceedings of the 5th International Conference on Electrical and Electronics Engineering, Bursa, Turkey, 2007*, pp. 251–254.
[20] Saadoun M. M. and Engheta N., *Microwave Opt. Tech. Lett.*, **5** (1992) 184.
[21] Aydin K., Li Z., Hudlička M., Tretyakov S. and Ozbay E., *New J. Phys.*, **9** (2007) 326.
[22] Aydin K., Li Z., Bilge S. and Ozbay E., *Photon. Nanostruct. - Fundam. Appl.*, **6** (2008) 116.
[23] Chen H., Ran L., Huangfu J., Zhang X., Chen K., Grzegorczyk T. M. and Kong J. A., *Phys. Rev. E*, **70** (2004) 057605.
[24] Chakyar S. P., Sikha S. K., Bindu C., Andrews J. and Joseph V. P., *J. Appl. Phys.*, **121** (2017) 054101.

International Journal of Science and Research (IJSR)
ISSN (Online): 2319-7064
Impact Factor (2012): 3.358

Experimental Studies on the Effect of Substrate Dielectric Constant on the Resonant Frequency of Split-Ring Resonator Metamaterial Structure

K. S Umadevi[1, 2], V. P Joseph[3]

[1]Department of Electronics, Prajyoti Niketan College, Pudukad, Thrissur, Kerala, India
[2]PG and Research Department of Physics, Newman College, Thodupuzha, Kerala, India
[3]PG and Research Department of Physics, Christ College, Irinjalakuda, Kerala, India

Abstract: ***The results of an experimental study for tuning the resonant frequency of a split ring resonator (SRR) metamaterial structure at microwave frequencies, by changing the material and thickness of substrate are presented. The SRR structure is fabricated by photochemical etching on a copper foil glued on a thin low loss polymer film of negligible thickness. The transmission properties are studied using a unit cell of SRR between two monopole antennas. The materials used for the fabrication of substrate are the Poly Methyl Methacrylate (PMMA) and Wax. The experimental results predicts the possibility of tuning the resonant frequency of the SRR unit to any desired value by changing the material or thickness of the substrate and are in good agreement with theoretical expectations. This possibility may be used for the fabrication of wide band frequency selective and cloaking materials. This method may be extended to the design and fabrication of tunable negative index materials.***

Keywords: metamaterial, split-ring resonator (SRR), frequency tuning, negative permeability.

1. Introduction

Metamaterials are artificial materials that exhibit unusual electromagnetic properties that are not observed with natural materials. The extraordinary properties of these materials such as negative refraction, reversed Doppler effect etc. are due to its negative values of permittivity μ, permittivity ε and index of refraction n. In these negative materials, the electric field **E,** magnetic field **H,** and wave vector **k,** form a left-handed triplet and the Poynting vector **E×H** is anti-parallel to the wave vector. So these materials are also called left handed media (LHM), double negative media (DNG) and backward wave media. Focusing beyond the diffraction limit, amplification of evanescent waves, frequency selective surfaces, miniaturization of antennas, cloaking, sensing etc. are some of the promising applications of these materials.

The metamaterial concept was theoretically introduced by Victor Veselago in 1968 [1]. For several years nobody can materialize it due to the non availability of negative permeability structures. In 1999 Pendry *et.al* fabricated negative permeability structures using an array of split ring resonators (SRR) at microwave frequencies [2]. The first left handed metamaterial was materialized by Smith and colleagues in 2000 by periodically arranging negative permeability and permittivity unit structures [3], [4].

Split ring resonators are the most fundamental unit cell used for almost all microwave metamaterial applications. It has two interleaved metallic rings with two opposite gaps. Each unit cell acts as an LC oscillator in an external magnetic field causing sharp absorption of power corresponding to the resonance frequency. The resonant properties of SRR structures have been studied by different researchers [5], [6], [7]. Almost all experimental studies related to the resonant frequency are performed using structures fabricated on some rigid substrate like FR4 circuit board. To analyze the effect of ε on resonance frequency experimentally, SRR structures with certain specific geometric parameters are to be fabricated using boards of different substrate materials. An attempt in this direction using two substrate samples of the same material but of two different thicknesses is presented by Zhongyan *et. al* along with some numerical results [8]. Detailed numerical analysis of this problem is available in [9], [10] and [11] also. Recently the authors have reported a flexible SRR structure at microwave frequencies fabricated on a thin polymer film of negligible dielectric constant using photochemical etching [12]. We have used this structure for the experimental study of the effect of substrate dielectric constant on the resonant frequency of SRR. Two key factors that influence the resonant frequency of SRR are the permittivity and thickness of the substrate. In this paper we present the effect of both these parameters on the resonant frequency of SRR.

2. Resonance frequency of SRR

The schematic representation of the SRR unit is pictured in Fig. 1. The geometrical parameters that affect the resonant frequency are inner radius r, metal width w, slit width d and gap distance s.

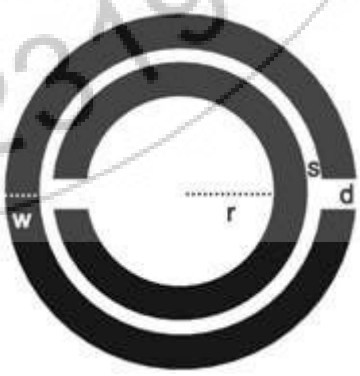

Figure 1: The schematic representation of the SRR unit cell.

SRR unit cell structures arranged in two or three dimensional pattern can be considered as a homogeneous medium if the

interacting radiation is of wavelength much greater than the array spacing (lattice constant) a. The effective permeability of this artificially engineered medium can be written as

$$\mu_{eff} = 1 - \frac{\pi r^2/a^2}{1 + \frac{i2\rho l}{\omega r \mu_0} - \frac{3l}{\mu_0 r^3 \pi^2 \omega^2 C_1}}$$

where ρ is the resistance per unit length and l is the vertical lattice parameter. The resonance frequency of the SRR unit cell depends on its intrinsic values of inductance and capacitance. The dielectric constant and thickness of the substrate material changes the capacitance of the material considerably. The capacitance of a SRR unit with a substrate of dielectric constant ε_r is given by

$$C_1 = \frac{\epsilon_0 \epsilon_r}{\pi} \ln \frac{2w}{s}$$

The resonance frequency of SRR with the dielectric becomes

$$\omega_{0m} = \sqrt{\frac{3lc_0^2}{\pi \epsilon_r r^3 \ln \frac{2w}{s}}}$$

3. Fabrication of the Structure

The SRR units are fabricated using a copper foil of thickness 20 µm. Two methods were tried for the fabrication. One method is using photolithographic etching and the other is by direct printing technique. In the first method the copper sheet after fixing on a thin polymer film is coated with liquid photo-resist and exposed to ultraviolet radiation with proper mask and subjected to chemical etching using dilute ferric chloride solution. The second method also uses chemical etching, but instead of photo masking direct printing of the SRR pattern on the copper sheet is made using a printer. For this study, the SRR structure fabricated on a thin polymer film of thickness 18 µm using photochemical etching method is used. Fig. 2 shows the photograph of the fabricated structure. The structural parameters are inner radius r = 3 mm, metal width w =1.25 mm, slit width d = 0.3 mm and gap between rings s = 0.5 mm.

The SRR is glued on substrates of PMMA and Wax having different thickness and are used to study the effect of relative permittivity on resonance frequency. PMMA is a vinyl polymer made by free radical polymerization from the monomer methyl methacrylate. Fig. 3 shows the photograph of PMMA and wax samples prepared for the study. PMMA substrates used are of thicknesses 0.15 mm, 0.24 and 0.29 mm. The thicknesses of wax samples used are 0.68 mm, 0.91 mm and 1.07 mm.

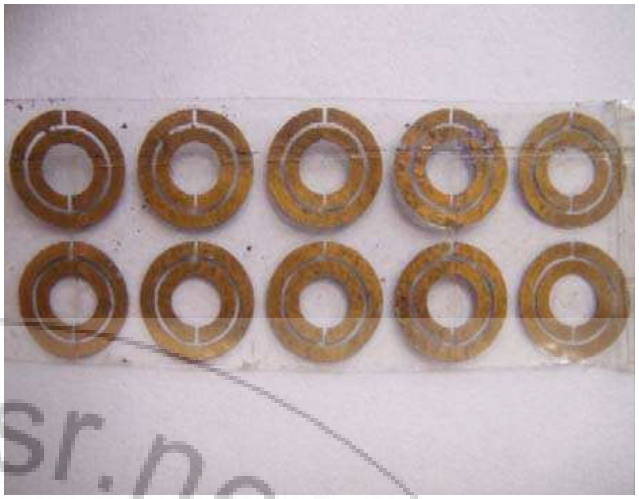

Figure 2: Photograph of the SRR structure fabricated on a low loss flexible polymer film. The dimensions are d = 0.3 mm, w = 1.25 mm, r = 3 mm, s = 0.5 mm and a = 9 mm. Thickness of metallization (copper) 20 µm.

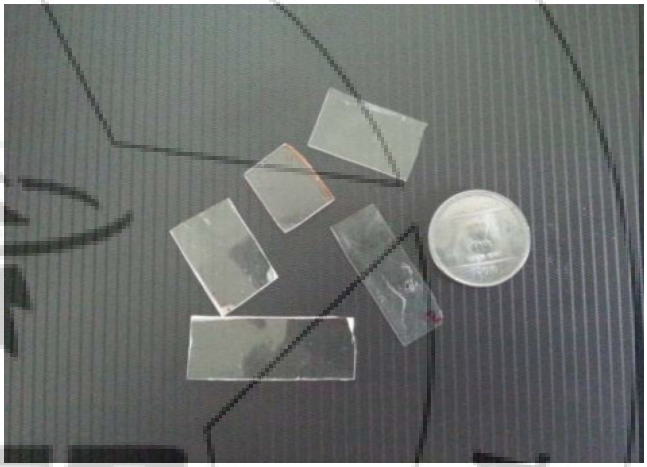

Figure 3: Photographs of the samples of PMMA and Wax prepared for using as substrates for the SRR

4. Measurements and Results

The transmission properties are studied by placing the SRR unit cell between two monopole antennas. It is schematically represented in Fig. 4. Measurements are performed using a Network Analyzer system. The effect of substrate dielectric constant on the resonant properties of SRR is studied using different PMMA and Wax sheets. The dielectric constants of samples used are measured using the waveguide method proposed by Dube *et. al* [13]. The measured values of ε_r are around 2.6 for PMMA and 2.2 for wax. When the substrate thickness increases, the capacitance between rings increases and correspondingly, resonant frequency shifts to the lower frequency region because of its inverse dependence. Fig. 5 and Fig. 6 depict the resonant frequency variation of SRR with PMMA and Wax substrates for different thicknesses. The resonant frequency obtained for PMMA substrate for thickness 0.15 mm is 6.37 GHz. It shifts to 6.32 GHz and 6.23 GHz for substrates of thickness 0.24 mm and 0.29 mm respectively. For the wax samples the resonance frequencies are at 6.41 GHz for t = 0.68 mm, 6.39 GHz for t = 0.91 GHz and 6.35 GHz for t = 1.07 mm. The study clearly shows that an increase in dielectric constant or thickness of the substrate decreases the resonance frequency considerably. These

results are in good agreement with the theoretical predictions and previous numerical studies.

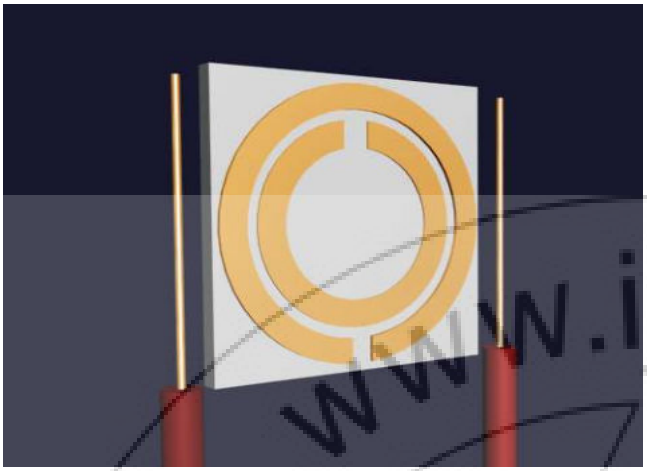

Figure 4: Schematic diagram of the experimental arrangement used for the study of transmission spectra, with the SRR unit cell between two monopole antennas.

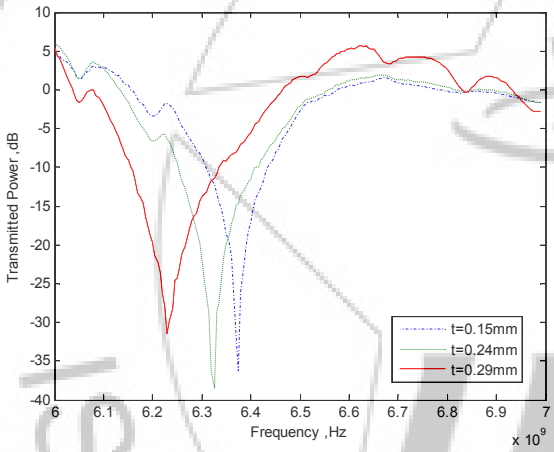

Figure 5: Measured transmission spectra of a SRR unit cell, for different values of substrate (PMMA) thickness *t*. The dimensions are $d = 0.3$ mm, $s = 0.5$ mm, $w = 1.25$ mm, $r = 3$ mm and metallization thickness 20 µm.

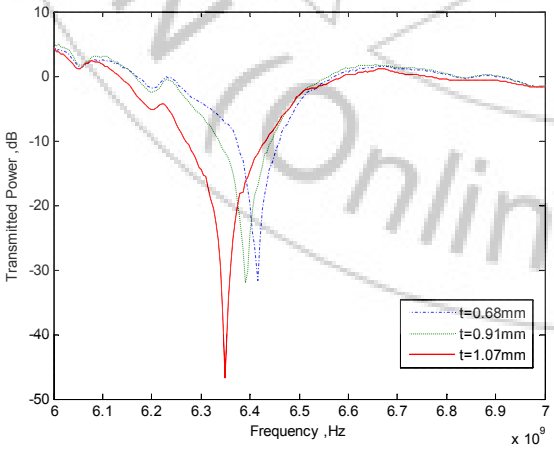

Figure 6: Measured transmission spectra of a SRR unit cell, for different values of substrate (Wax) thickness *t*. The dimensions are $d = 0.3$ mm, $s = 0.5$ mm, $w = 1.25$ mm, $r = 3$ mm and metallization thickness 20 µm.

5. Conclusions

The resonance tuning properties of SRR by changing the permittivity or thicknesses of the substrate are presented. The result of this experimental study clearly shows the possibility of tuning the resonant frequency of the structure to any desired value by changing dielectric constant or thickness of the substrate. This method of fabrication can easily be extended to the design and fabrication of flexible and tunable negative index materials. This structure may be used for realizing cloaking media and for frequency selective applications.

References

[1] V.G. Veselago, "The electrodynamics of substances with simultaneous negative values of ε and µ", Sov. Phy. Usp, vol. 47, pp. 509-514, 1968.
[2] J.B. Pendry, A.J Holden, D.J Robbins and W.J Stewart, "Magnetism from conductors and enhanced non linear phenomena", IEEE Trans Microwave Theory Tech, 47, pp. 2075-2084, 1999.
[3] D.R. Smith, W.J Padilla, D.C Vier, S.C Nemat-Naser and S. Schuz, "Composite medium with simultaneously negative permeability and permittivity", Phys. Rev. Lett., vol. 84, pp. 4184-4187, 2000.
[4] J. B. Pendry, A. J. Holden, D. J. Robbins, and W. J. Stewart, "Low frequency plasmons in thin-wire structures", J. Phys.: Condens. Matter 10, 4785, 1998.
[5] T. Weiland and R. Schuhmann, "Ab initio numerical calculation of left-handed metamaterials: Comparison of calculations and experiments", Journal of Applied Physics, vol. 90, no. 10, pp. 5419-5424, Nov 2001.
[6] M. Kafesaki, Th Koschny, R. S. Penciu, T. F. Gundogdu, E N Economu and C M Soukoulis, "Left-handed metamaterials: detailed numerical studies of the transmission properties", J. Opt. A: Pure Appl. Opt. 7 S12-S22, 2005.
[7] R. Marques, F. Mesa, J. Martel, and F. Medina, "Comparative analysis of edge- and Broadside-coupled split ring resonators for metamaterial design - theory and experiments," IEEE Trans. Antennas Propag., vol. 51, no. 10, pp. 2572–2581, 2003.
[8] Zhongyan Sheng and Vasundara V. Varadan, "Tuning the effective properties of metamaterials by changing the substrate properties", Journal of Applied Physics 101, 014909, 2007.
[9] E. Ekmekci and G. Turhan-Sayan, "Comparative investigation of resonance characteristics and electrical size of the double-sided SRR, BC-SRR and conventional SRR type metamaterials for varying substrate parameters", Progress In Electromagnetics Research B, vol. 12, 35–62, 2009.
[10] E. Ekmekci, R. D. Averitt, and G. Turhan-Sayan, "Effects of Substrate Parameters on the Resonance Frequency of Double-sided SRR Structures under Two Different Excitations", PIERS Proceedings, Cambridge, USA, July, 2010.
[11] E. Ekmekci and G. Turhan-Sayan, "Sensitivity of the resonance characteristics of SRR and DSRR (Double-Sided SRR) type metamaterials to the changes in substrate parameters and the usefulness of DSRR

structure for reduced electrical size", PIERS Proceedings, Cambridge, USA, July, 2008.
[12] P.M. Ragi, K.S. Umadevi, P. Nees, J. Jovia, M.V. Keerthy and V.P. Joseph, "Flexible split-ring resonator metamaterial structure at microwave frequencies", Microwave Opt. Technol. Lett., 54, 1415-1416, 2012.
[13] D.C Dube, and R. Natarajan, "Determination of dielectric parameters for films at microwave frequencies", J. Appl. Phys., 44, 1973.

Author Profile

K. S. Umadevi received B.Sc. in Electronics from Prajyoti Niketan College Pudukad, University of Calicut, in 2003 and M.Sc. in Electronics from Illahia College of Arts and Science, M.G University, Kottayam in 2005. Presently she is working as Assistant Professor in the Department of Electronics, Prajyoti Niketan College, Pudukad, Thrissur, Kerala, India

V.P. Joseph obtained M.Sc. in Physics from St. Thomas College Pala, M.G University, Kottayam in 1886 and Ph.D. from Cochin University of Science and Technology, Kochi in 2000. Presently he is working as Associate Professor in the Research Department of Physics, Christ College, Irinjalakuda. His main areas of research interests are microwave antennas, metamaterials and FDTD analysis.

13th International Congress on Artificial Materials for Novel Wave Phenomena - Metamaterials 2019
Rome, Italy, Sept. 16$^{\text{th}}$ - Sept. 21$^{\text{th}}$ 2019

Wide Band Microwave Absorber using Flexible Broadside Coupled Split Ring Resonator Metamaterial Structure

Umadevi K. S[2,3], Sikha K. Simon[1,4], Sreedevi P. Chakyar[1], Jolly Andrews [1] and V. P. Joseph[1]

[1]Christ College(Autonomous) Irinjalakuda, University of Calicut, Physics, Thrissur, Kerala, India
[2]Newmann College, Thodupuza, M.G. University, Physics, Kottayam, Kerala, India
[3]Prajyothi Nikethan College, Pudukkad, University of Calicut, Electronics, Thrissur, Kerala, India
[4] St. Thomas' College (Autonomous), University of Calicut, Physics, Thrissur, Kerala, India
vpj@christcollegeijk.edu.in

Abstract – **This paper proposes a wide band microwave absorber in a bulk form realized using a Broad Side Coupled Split Ring Resonator (BCSRR) metamaterial structural units fabricated in a novel way which possesses structural flexibility and wide band frequency tunability. Instead of using a conventional structure, the two conducting rings of the structure are prepared separately by photochemical etching using thin copper sheets glued on polypropylene film. The resonant property studies of the BCSRR show a noticeable tunability in resonant frequency with spacing variation, a result not observed using other conventional SRR structures. A spacing variation of 1 mm of a typical BCSRR unit shows around 3 GHz resonant tunability which makes it suitable for materializing various sensor applications. The resonant properties of BCSRR in a bulk form made with specific structural dimensions arranged in periodic manner with progressively varying spacing using layers of cotton fabric, show wide band resonant absorption. By suitably modifying the structural parameters of BCSRR rings, the range of the frequency absorption band can be specifically designed. The result of the study predicts a possibility of using this proposed BCSRR designs in various types of wide band absorbers.**

I. Introduction

There is vibrant research carried out by different groups in order to explore the potential possibilities and manifold applications of different types of Split Ring Resonators (SRRs) [1]. Broad Side Coupled Split Ring Resonator (BCSRR), one of the important candidates for negative permeability metamaterial resonating units, is widely used in different sensors, miniaturized antennas, frequency selective surfaces etc [2]. Conventionally BCSRRs are constructed by etching the rings of the structure on two sides of a single substrate and there by will have a fixed resonating frequency due to the thickness of the substrate used for selected structural parameters. By designing BCSRR in a novel way by fabricating the two rings on separate substrate of the same material, the spacing variation between the rings leading to wide band frequency tunability was easily achieved [3]. Instead of using rigid substrates for fabricating the rings, we have incorporated flexible, lossless microfilms as the substrate unit which will provide the added advantage of flexibility [4]. In this paper, such specially designed BCSRR units are periodically structured to materialize a bulk medium to achieve a noticeable wide band frequency absorption which is not possible with conventional structures.

II. Fabrication and Measurements

The rings of BCSRR are fabricated on thin copper sheets of thickness 20 μm. The substrate used is a polypropylene film of thickness 18 μm which is glued to the copper sheets. By using photochemical etching method the required BCSRR rings of specific dimensions are fabricated. Three sets of rings with inner radius r = 5.4 mm, 4.7 mm, 3.0 mm and width w= 2.7 mm, 1.8 mm, 2 mm and slit width d = 0.2 mm are precisely made. Cotton fabric strips of thickness of 0.1 mm are used for achieving the required spacing between the rings of the BCSRR. Planar array of BCSRR rings with periodicity 12 mm having five columns with varying spacing using different

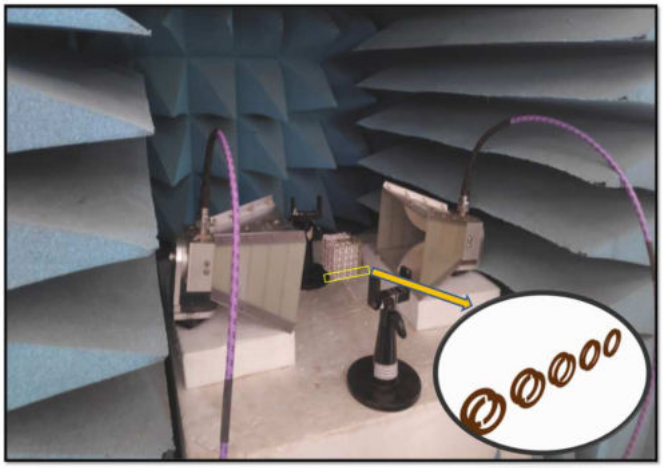

Fig. 1: Experimental setup for studying the wide band frequency absorption characteristics of the BCSRR bulk medium.

layers of cotton fabrics are made. Accordingly, the spacing between the rings of BCSRR units of five columns are progressively varying from 0.1 mm to 0.5 mm. Eight layers of such BCSRR groups are arranged with same periodicity of 12 mm in order to form three different samples of bulk media.

To find the resonant frequency of a single BCSRR unit, the measurement set up consisting of a BCSRR unit placed between the transmitting and receiving probes of a Vector Network Analyzer (VNA) is used [5]. In order to analyze the wide band absorption characteristics of the bulk medium made with BCSRR rings, a transmission-reception system using two horn antennas as shown in Fig. 1 is employed.

III. Results and Discussion

The transmission spectra of a single BCSRR ring is studied for the three selected units by varying the spacing between the rings using layers of cotton fabric. As spacing increases, the capacitance between the rings decreases and will result in the corresponding increasing in the resonant frequency. The spacing variation graph of three BCSRR units with three distinct structural parameters is given in Fig. 2. For the structure with inner radius r =

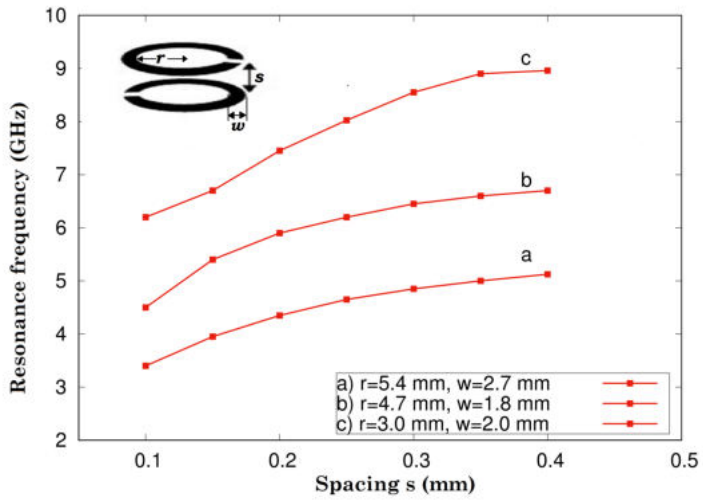

Fig. 2: The variation of resonant frequency with spacing for three different BCSRR units.

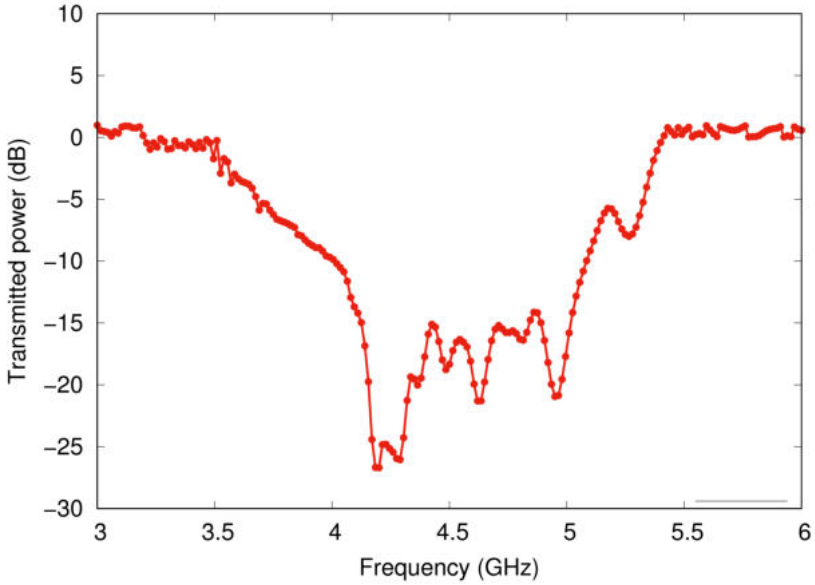

Fig. 3: The wide band absorption curve obtained for the BCSRR bulk sample .

5.4 mm given as (a), for a spacing from 0.1 mm to 0.4 mm, we observe a frequency tunability of 3.5 GHz to 5.3 G Hz. For the other two cases marked as (b) and (c), the frequency shifts observed are from 4.5 to 6.9 GHz and 6.2 to 9 GHz respectively. It is quite obvious that by properly adjusting the spacing between the rings of BCSRR, a wide range of frequency tunability can be easily achieved. By combining the units of BCSRR rings having same structural dimensions with different spacings (between 0.1 mm to 0.5 mm), a bulk medium with a wide range of resonant frequency absorption can be realized. One typical absorption graph obtained for the bulk medium fabricated with r = 5.4 mm , w = 2.7 mm is shown in Fig. 3. If we combine the three bulk forms together, we can achieve a wide band microwave absorber which works between 3 to 9 GHz.

IV. Conclusion

Fabrication methodology along with wide band frequency tunability property of a specially designed flexible metamaterial BCSRR structure is presented. By combining different BCSRR units having varying spacing and structural dimensions, a bulk medium metamaterial structure is realized which shows wide band frequency absorption from 3 GHz to 9 GHz. This study can be extended to the realization of three dimensional wide band microwave absorbers in bulk form with moderate thickness which will have the added advantage of flexibility and tunability.

References

[1] N. Engheta, R.W. Ziolkowski *Metamaterials: physics and engineering explorations,* John Wiley & Sons, 2006.
[2] R. Marqués, F. Mesa, J. Martel, F. Medina, " Comparative analysis of edge-and broadside-coupled split ring resonators for metamaterial design-theory and experiments.," *IEEE Transactions on Antennas and Propagation* , vol. 51(10), p. 2572-2581, 2003.
[3] Sikha K. Simon, Sreedevi P. Chakyar, Jolly Andrews, V.P. Joseph, " Metamaterial split ring resonator as a sensitive mechanical vibration sensor," Proceedings of *American Institute of Physics, OPTICS'17,* pp. 020021-(1-8), NIT Calicut, India, 9-10 January 2017.
[4] P.M. Ragi, K.S. Umadevi, Nees Paul, Jovia Jose , M.V. Keerthy, V.P. Joseph, " Flexible split-ring resonator metamaterial structure at microwave frequencies.," *Microwave and Optical Technology Letters* , vol. 54(6), p. 1415, 2012.
[5] K.S. Umadevi,Chakyar, Sikha K. Simon, Sreedevi P. Chakyar, Jolly Andrews, V.P. Joseph, " Split ring resonators made of conducting wires for performance enhancement," *EPL (Europhysics Letters),IOP Publishing* vol. 118(2), p. 24002, 2017.